

MONODROMY AND HÉNON MAPPINGS

A Dissertation

Presented to the Faculty of the Graduate School

of Cornell University

in Partial Fulfillment of the Requirements for the Degree of

Doctor of Philosophy

by

Christopher Lipa

August 2009

© 2009 Christopher Lipa
ALL RIGHTS RESERVED

MONODROMY AND HÉNON MAPPINGS

Christopher Lipa, Ph.D.

Cornell University 2009

We discuss the monodromy action of loops in the horseshoe locus of the Hénon map on its Julia set. We will show that for a particular class of loops there is a certain combinatorially-defined subset of the Hénon Julia set which must remain invariant under the monodromy action of loops in certain regions. We will then describe a conjecture for what the monodromy actions of these loops are as well as a possible connection between the algebraic structure of automorphisms of the full 2-shift and the existence of certain types of loops in the horseshoe locus.

BIOGRAPHICAL SKETCH

Christopher Lipa graduated from North Carolina State University in 2003 where he read mathematics and computer science. He attended graduate school at Cornell University, graduating in 2009 with a Ph. D. in mathematics.

This thesis is dedicated to my parents.

ACKNOWLEDGEMENTS

This work depends on fundamental insights from Sarah Koch, John Milnor, Adrien Douady, and John Hubbard. The programs SaddleDrop and FractalAsm written by Karl Papadantonakis were essential to the discovery of the phenomenon that this thesis describes. I'd like to express gratitude for conversations with John Smillie, Dierk Schleicher, and Laurent Bartholdi. I also wish to thank Zin Arai, William Thurston, Eric Bedford, and Ralph Oberste-Vorth.

This work also could not have been possible if not for the generous financial support of the Mathematics Department of Cornell University and the National Science Foundation's VIGRE Grant.

TABLE OF CONTENTS

Biographical Sketch	iii
Dedication	iv
Acknowledgements	v
Table of Contents	vi
List of Figures	viii
1 Introduction	1
1.1 Hénon Mappings	1
1.2 Monodromy Image Conjecture	2
1.3 Monodromy Action Conjectures	3
1.4 Structurally Stable Set	5
2 Preliminaries	7
2.1 Standard Definitions	7
2.2 Monodromy Action	10
3 Monodromy in the HOV region	11
3.1 Inverse Limit Description	11
3.2 Homotopy of HOV	11
3.3 Monodromy Action of γ_b	12
3.4 Monodromy Action of γ_c	12
4 Orbit Portraits and Puzzles	13
4.1 Formal Orbit Portraits	13
4.2 Actual Orbit Portraits	14
4.3 Puzzle Pieces	15
4.4 Fattened Puzzle Pieces	18
4.5 Itineraries Relative to Orbit Portraits	21
4.6 Kneading Sequences	21
4.6.1 Kneading Sequences of Quadratic Polynomials	21
4.6.2 Kneading Sequences of Orbit Portraits	24
4.7 Examples	26
4.7.1 The Airplane	26
4.7.2 BABB	31
5 \mathcal{X}_c^W	36
5.1 Defining \mathcal{X}_c^W	36
5.2 Multi-Itineraries	38
5.3 Adaptation to Γ	40
5.4 Relations Between Points and Itineraries	42
5.5 Continuity of \mathcal{X}_c^W	44
5.6 W -itineraries of \mathcal{X}_c^W	47

6	$\mathcal{X}_{b,c}^W$	52
6.1	Crossed Mappings	52
6.2	Horizontal Disk Contraction	55
6.3	Perturbations of One-Dimensional Orbit Portraits	57
6.4	Continuity of $\mathcal{X}_{b,c}^W$	62
6.5	Coding $\mathcal{X}_{b,c}^W$	65
6.6	Relationships Between Points and Itineraries	68
7	Monodromy Invariant	70
8	Monodromy Conjectures	72
8.1	Speculative Structure of Hénon Parameter Space	72
8.2	Monodromy Conjecture	73
9	Examples	76
9.1	$B \star BAA$	77
9.2	$BB \star BAA$ and $AB \star BAA$	86
9.3	$A \star BAA$	87
9.4	$A \star BAA, A \star BABBA$	87
9.5	$A \star BAA, A \star BABBA, B \star BAA$	91
9.6	$ABAAB \star BAA$ and $BBAAB \star BAA$	96
A	Monodromies of Inverse Limit Systems	100
A.1	Inverse Limit System Setup	100
A.2	Coding Setup	101
A.3	Monodromy Actions	102
	Bibliography	108

LIST OF FIGURES

4.1	\mathcal{M} with $3/7$ and $4/7$ parameter rays	27
4.2	Airplane polynomial with actual orbit portrait \mathcal{O}_{air}	28
4.3	\mathcal{O}_{air} and the Julia set of airplane polynomial	29
4.4	Γ_{air}	30
4.5	Mandelbrot set with $13/31$ and $18/31$ parameter rays	32
4.6	\mathcal{O}_{BABB} and the Julia set of f_{BABB}	33
4.7	Puzzle pieces for f_{BABB} associated with \mathcal{P}_{BABB}	34
4.8	Γ_{BABB}	35
9.1	Parameter slice with $b = 0$	78
9.2	Parameter slice with $b = 0.005i$	79
9.3	Parameter slice with $b = 0.01i$	80
9.4	Parameter slice with $b = 0.015i$	81
9.5	Parameter slice with $b = 0.02i$	82
9.6	Parameter slice with $b = 0.03i$	83
9.7	Parameter slice with $b = 0.05i$	84
9.8	Loop around B herd of \mathcal{W}_{air} with $b = 0.05i$	85
9.9	Loops around BB and AB herds of \mathcal{W}_{air} with $b = 0.2 + 0.3i$	86
9.10	Loop around A herd of \mathcal{W}_{BABB}	88
9.11	Parameter slice with $b = -0.03 + 0.02i$	92
9.12	Parameter slice with $b = -0.03 + 0.01i$	93
9.13	Parameter slice with $b = -0.03$	94
9.14	$ABAAB$ and $BBAAB$ herds of \mathcal{W}_{air} with $b = -0.1 + 0.9i$	97
9.15	Other herds near the $ABAAB$ and $BBAAB$ herds of \mathcal{W}_{air} with $b = -0.1 + 0.9i$	98
9.16	Other herds obstructing loops around $ABAAB$ and $BBAAB$ herds of \mathcal{W}_{air} with $b = -0.1 + 0.9i$	99

CHAPTER 1
INTRODUCTION

1.1 Hénon Mappings

In 1963, Lorenz [Lor63] introduced a three-dimensional differential equation which was an attempt at a simplified model of convection of air currents in the atmosphere. There is a particular Poincaré first-return map that Hénon [Hén76] noticed had an action that is qualitatively similar to, but not exactly equal to the two parameter polynomial diffeomorphism of the plane, now called the Hénon map:

$$H_{b,c} : \begin{pmatrix} x \\ y \end{pmatrix} \mapsto \begin{pmatrix} x^2 + c - by \\ x \end{pmatrix}$$

Over the past four decades, the Hénon map has arguably been the most-studied multi-dimensional dynamical system. This is in part due to the fact that the Hénon mapping is a perturbation of the (mostly) well-understood one-dimensional logistic family and has a relatively simple formulation, yet the dynamics of the Hénon map are fantastically complicated and the Hénon map exhibits chaotic phenomena that do not appear in one-dimensional maps.

Subsequent to the success realized in understanding logistic maps by complexifying and bringing complex analytic techniques to bear, in the 1980s, Hubbard [Hub86] had the idea to complexify the Hénon mapping and examine structures in complex dynamical and parameter space in order to try to glean insight into the real mappings.

One result revealed through the work of Hubbard and Oberste-Vorth [HOV94a] is that there is a large region of parameter space, called the *horseshoe locus*, where the dynamics on the Julia set is hyperbolic and conjugate to Smale's horseshoe map.

Arai [Ara08] has more recently exhibited loops in this horseshoe locus in addition to the “obvious” classes of loops exhibited in Hubbard and Oberste-Vorth’s work. If one has a loop in the horseshoe locus, one can continuously follow points of the Julia set around and back to some (possibly different) point in the Julia set at the basepoint. This induces an action on the Julia set at the basepoint of the loop, which is called the *monodromy action* associated with the loop. The monodromy action maps a loop to a continuous automorphism of the Julia set of the basepoint of the loop, and this automorphism must commute with the action of the Hénon map. We call the image of the monodromy action the *induced monodromy group*, and (up to conjugacy) the monodromy group is independent of the basepoint of the loop in path-connected regions of the horseshoe locus.

From the monodromy action of a loop in parameter space, one can deduce implications on what types of dynamics must occur as the loop is homotoped to a constant, and we hope that further results may use monodromy as one of many tools in developing a road map of Hénon parameter space similar to Douady, Hubbard, Schleicher, and Milnor’s combinatorial description of quadratic polynomial parameter space.

1.2 Monodromy Image Conjecture

In the complement of the Mandelbrot set, the Julia set is hyperbolic and isomorphic to the one-sided shift on sequences of two symbols. $\text{Aut}(\Sigma_2^+, \sigma)$ is generated by the automorphism that acts on sequences by exchanging A and B . The generator of the fundamental group of the complement of the Mandelbrot set induces this automorphism on the Julia set at any base point. In other words, the induced monodromy group of the shift locus of quadratic polynomials is $\text{Aut}(\Sigma_2^+, \sigma)$.

For degree d one-complex-dimensional polynomial maps, there is also a shift locus

\mathcal{L} in parameter space, where the polynomial restricted to the Julia set is hyperbolic and conjugate to the one-sided shift on d symbols. Loops in \mathcal{L} based at a specific basepoint also have a continuous monodromy action on Σ_d^+ which commutes with the shift. There is again a natural monodromy action $\pi_1(\mathcal{L}) \mapsto \text{Aut}(\Sigma_d^+, \sigma)$. The situation is here is more complicated, as whenever $d > 2$, then $\text{Aut}(\Sigma_d^+, \sigma)$ is infinitely generated. However, as Blanchard, Devaney, and Keen [BDK91] show, the induced monodromy group of the shift locus is again $\text{Aut}(\Sigma_d^+, \sigma)$, and moreover, Blanchard, Devaney, and Keen give an explicit method to realize the generators.

Based on these facts, Hubbard conjectured that the pattern continued in the two-dimensional case.

Conjecture 1.1 (Hubbard). *The induced monodromy group of the horseshoe locus together with the shift generate $\text{Aut}(\Sigma_2, \sigma)$.*

The one-sided shifts are relatively well-understood. By contrast, the group of continuous automorphisms of the two-sided shift on two symbols which commute with the shift is not [BLR88]. We know it contains as subgroups all finite groups as well as \mathbb{Z} and the product of countably many \mathbb{Z} 's. It also contains a subgroup isomorphic to the free group on infinitely many generators. It is unknown if the group is generated by involutions and the shift. No nontrivial generating set is known. Proving or refuting Conjecture 1.1 would be a significant advance for automata theory as well as dynamics.

1.3 Monodromy Action Conjectures

The Mandelbrot set lives in a complex slice of Hénon parameter space. Koch ([Koc05] and [Koc07]) experimentally found that components of the Mandelbrot set bifurcate in

Hénon parameter space into many pieces, called *herds*. All of the interesting loops in the horseshoe locus that are presently known wrap around these herds. Extensive computer experimentation has led to Conjecture 8.3, which describes what the Monodromy action is for this class of loops which wrap around Koch's herds.

Conjecturally, non-hyperbolic components in parameter space can be labeled with a finite string on two symbols, by which herd they are in and can also be followed back to a region of the Mandelbrot set. Conjecture 8.3 states that the monodromy action of a loop around such a non-hyperbolic component in parameter space is described by a natural generalization of marker automorphisms, which we call *compound marker automorphisms* (defined in Chapter 8). We postulate that the compound marker automorphism describing the monodromy action for such a loop has two parts. Our conjecture is that the prefix of the marker string comes from the labeling of which herd the looped component is in and that the suffix of the marker string comes from the kneading sequences realized by the polynomials in the region of the Mandelbrot set where the looped component can be followed back to as the Jacobian moves to 0.

An example illustrating Conjecture 8.3 is that experimentally we have found that the monodromy action of a loop around the B -herd of the region further out than the airplane polynomial in the natural ordering of the Mandelbrot set to be described by the marker automorphism $B \star BAA$. We conjecture that the B that comes before the \star corresponds to the fact the loop goes around the B herd and that the BAA coming after the \star corresponds to the fact that every polynomial that is further out than the airplane in the natural ordering on the Mandelbrot set has a kneading sequence with initial segment BAA .

It is possible to construct marker strings which do not yield automorphisms. Conjecture 8.4 states that when this occurs, there is some obstruction in parameter space to

loops going around the prescribed herds and only the prescribed herds.

1.4 Structurally Stable Set

If Conjecture 8.3 is correct, then loops around non-hyperbolic components coming from any particular region of the Mandelbrot set must have a trivial action on all points of the Julia set that lack a particular coding that relates to the symbolic dynamics present in that region. Though we don't prove Conjecture 8.3, we do prove this consequence of the conjecture in Theorem 7.5, which states that the monodromy action must be invariant on the points in the Julia set that lack a particular (finite) list of words in their symbolic coding.

To this end, we use two powerful tools. The first is Milnor's orbit portrait construction in one complex variable dynamics which is described in [Mil00] and was inspired by the works of Douady, Hubbard, and Schleicher ([DH82], [DH84], [DH85], [Sch94], [Sch00], and [Sch04]). Milnor's construction gives a puzzle decomposition of one-complex-dimensional dynamical space. With every orbit portrait, we get a Markov graph Γ that describes the allowable transitions between puzzle pieces. Most importantly, we get expansion on all of the puzzle pieces that don't include the critical point. Hence, the set of points \mathcal{X}_c^W (defined in Chapter 5 as the set of points which never visit this critical puzzle piece) is hyperbolic and stable under small perturbation. Also, we get a two-symbol coding of this set described by Corollary 5.22, which states that all possible two-symbol codings are realizable by points of \mathcal{X}_c^W , with the exception that there is a finite list of finite strings which may only appear at the beginning of a coding. This finite list of strings depends only on the abstract orbit portrait from which the puzzle pieces were generated and is closely related to the kneading sequences of

one-dimensional polynomials that satisfy the orbit portrait.

The second major tool we use is Hubbard and Oberste-Vorth's crossed mappings, as described in [HOV94b]. Roughly speaking, a crossed mapping is a map from one bi-disk over another with contraction in one direction and expansion in the other. Hubbard and Oberste-Vorth show that if we have a bi-infinite sequence of degree-one crossed maps, then there is precisely one point who visits each bi-disk in turn.

In Chapter 6, we construct two-dimensional puzzle pieces which are extensions in the y -direction of the one-dimensional puzzle pieces from Chapter 4. Then the mapping of one puzzle piece over another in one-variable dynamics implies that there is a 1-crossed mapping of the corresponding two-dimensional puzzle pieces. Any bi-infinite path in Γ then yields a point of the Hénon Julia set. This construction works in a neighborhood of any one-dimensional quadratic wake living inside Hénon parameter space, so this subset of the Julia set forms a trivial fibre-bundle, and we see in Chapter 7 that any loop in this region must have a trivial monodromy action on this subset.

This subset corresponds to precisely the points whose itinerary avoids the critical puzzle piece. The points which avoid the critical puzzle piece are those which do not have in their itineraries the initial kneading sequences of polynomials in that region of the Mandelbrot set. Theorem 7.5 expresses the fact that there must be a trivial monodromy action on this combinatorially-defined subset in a domain around the one-dimensional wake.

CHAPTER 2
PRELIMINARIES

2.1 Standard Definitions

For the relevant definitions, we follow [HOV94a], [BS06], and [Ara08]. For parameter values $b, c \in \mathbb{C}$, we define the Hénon map $H_{b,c} : \mathbb{C}^2 \rightarrow \mathbb{C}^2$ by:

$$H_{b,c} : \begin{pmatrix} x \\ y \end{pmatrix} \mapsto \begin{pmatrix} x^2 + c - by \\ x \end{pmatrix}$$

When $b = 0$, the first coordinate reduces to a quadratic polynomial on \mathbb{C} . When $b \neq 0$, the map is diffeomorphism of \mathbb{C}^2 . We define the following dynamically meaningful subsets of \mathbb{C}^2 :

$$K_{b,c}^{\pm} = \left\{ \begin{pmatrix} x \\ y \end{pmatrix} \left| \lim_{n \rightarrow \infty} \left\| H_{a,c}^{\circ \pm n} \begin{pmatrix} x \\ y \end{pmatrix} \right\| \neq \infty \right. \right\}$$

as well as:

$$U_{b,c}^{\pm} = \mathbb{C}^2 \setminus K_{b,c}^{\pm}$$

$$J_{b,c}^{\pm} = \partial K_{b,c}^{\pm} = \partial U_{b,c}^{\pm}$$

$$U_{b,c} = U_{b,c}^+ \cap U_{b,c}^-$$

$$K_{b,c} = K_{b,c}^+ \cap K_{b,c}^-$$

$$J_{b,c} = J_{b,c}^+ \cap J_{b,c}^-$$

$$K_{b,c}^{\mathbb{R}} = K_{b,c} \cap \mathbb{R}^2$$

$$J_{b,c}^{\mathbb{R}} = J_{b,c} \cap \mathbb{R}^2$$

We also define the Green's function $G_{b,c}^+ : \mathbb{C}^2 \rightarrow \mathbb{R}$ by:

$$G_{b,c}^+ \begin{pmatrix} x \\ y \end{pmatrix} = \lim_{n \rightarrow \infty} \frac{1}{2^n} \log \left(\text{pr}_1 \left(H_{b,c}^{on} \begin{pmatrix} x \\ y \end{pmatrix} \right) \right)$$

where pr_1 is projection to the first co-ordinate.

For any parameter value (b, c) , there exists an $R_{b,c} \in \mathbb{R}^+$ so that dynamical space is partitioned into three regions:

$$V_{b,c}^0 = \{(x, y) \mid |x| \leq R_{b,c} \text{ and } |y| \leq R_{b,c}\}$$

$$V_{b,c}^- = \{(x, y) \mid |y| \geq |x| \text{ and } |y| \geq R_{b,c}\}$$

$$V_{b,c}^+ = \{(x, y) \mid |x| \geq |y| \text{ and } |x| \geq R_{b,c}\}$$

with the dynamics on these sets such that $H_{b,c}(V_{b,c}^+) \subset V_{b,c}^+ \subset U_{b,c}^+$ and $H_{b,c}^{-1}(V_{b,c}^-) \subset V_{b,c}^- \subset U_{b,c}^-$.

We define the complex horseshoe locus as the following region in parameter space:

$$\mathcal{H}^{\mathbb{C}} = \left\{ (b, c) \in \mathbb{C}^2 \mid H_{b,c}|_{K_{b,c}} \text{ is hyperbolic and conjugate to the horseshoe} \right\}$$

and we define the real horseshoe locus as the following region in parameter space:

$$\mathcal{H}^{\mathbb{R}} = \left\{ (b, c) \in \mathbb{R}^2 \mid H_{b,c}|_{K_{b,c}^{\mathbb{R}}} \text{ is hyperbolic and conjugate to the horseshoe} \right\}$$

Here, the horseshoe refers to the space of bi-infinite sequences on two symbols under the action of the shift map (also referred to as the full 2-shift).

Let $\mathcal{HOV} = \left\{ (b, c) \in \mathbb{C}^2 \mid b \neq 0 \text{ and } |c| > 2(1 + |b|)^2 \right\}$, the Hubbard-Oberste-Vorth region described in [OV87], which is a connected subset of $\mathcal{H}^{\mathbb{C}}$. Let $\mathcal{H}_0^{\mathbb{C}}$ be the connected component of $\mathcal{H}^{\mathbb{C}}$ which contains \mathcal{HOV} . It is unknown if $\mathcal{H}^{\mathbb{C}} = \mathcal{H}_0^{\mathbb{C}}$.

Also define:

$$\text{Conn} = \left\{ (b, c) \in \mathbb{C}^2 \mid J_{b,c} \text{ is connected} \right\}$$

Let $f_c(z) = z^2 + c$. Let \mathcal{M} denote the Mandelbrot set. Let \mathcal{A} and \mathcal{B} be hyperbolic components of \mathcal{M} with the parameter rays with angles $\theta_{\mathcal{A}}^-$ and $\theta_{\mathcal{A}}^+$ landing at the root point of \mathcal{A} and the parameter rays with angles $\theta_{\mathcal{B}}^-$ and $\theta_{\mathcal{B}}^+$ landing at the root point of \mathcal{B} . We define a partial ordering $<$ on hyperbolic components as follows: $\mathcal{A} < \mathcal{B}$ if and only if $(\theta_{\mathcal{B}}^-, \theta_{\mathcal{B}}^+) \subset (\theta_{\mathcal{A}}^-, \theta_{\mathcal{A}}^+)$. Also define the Green's function $G : \mathbb{C} \rightarrow \mathbb{R}_0^+$ associated with f_c to be:

$$G(z) = \lim_{n \rightarrow \infty} \frac{1}{2^n} \log^+ (|f_c^{\circ n}(z)|)$$

Let Σ_2 denote the two-sided shift on two symbols. Let Σ_2^+ denote the one-sided shift on two symbols, let σ denote the shift operator on each of these spaces, and let δ denote the automorphism of each of these spaces that acts on sequences by exchanging the two symbols.

For any dynamical system $f : M \rightarrow M$ on a topological space, let $\text{Aut}(M, f)$ denote the continuous automorphisms of M that commute with f . Also let $\varprojlim(M, f)$ denote the inverse limit system:

$$\varprojlim(M, f) = \left\{ (\dots, x_{-1}, x_0, x_1, \dots) \mid x_i \in M \text{ and } f(x_i) = x_{i+1} \text{ for all } i \in \mathbb{Z} \right\}$$

Define $b_0 = \frac{1}{100}$, $c = -3$, and $p_0 = (b_0, c_0)$. Then $p_0 \in \mathcal{HOV} \cap \mathcal{H}^{\mathbb{R}}$. Also there is a canonical homeomorphism from K_{b_0, c_0} to Σ_2 which conjugates H_{b_0, c_0} with σ .

2.2 Monodromy Action

For $(b, c) \in \mathcal{H}^{\mathbb{C}}$, then $J_{b,c} = K_{b,c}$ is a Cantor set and varies continuously with respect to (b, c) . Let \mathcal{K} be the space of all points which are bounded in positive and negative time, each associated with their base points:

$$\mathcal{K} = \left\{ \left(\begin{array}{c} b \\ c \end{array} \right) \left(\begin{array}{c} x \\ y \end{array} \right) \middle| \left(\begin{array}{c} x \\ y \end{array} \right) \in K_{b,c} \right\}$$

The restriction of \mathcal{K} to the horseshoe locus is a locally trivial bundle of Cantor sets.

Given some loop $\gamma : [0, 1] \rightarrow \mathcal{H}^{\mathbb{C}}$ based at (b_0, c_0) , we can follow the points of J_{b_0, c_0} along γ back to the original base point, giving a homeomorphism on J_{b_0, c_0} which commutes with H_{b_0, c_0} , and moreover, this homeomorphism depends only on the homotopy type of γ . Because of the canonical identification of J_{b_0, c_0} with Σ_2 , this induces a natural map $\rho : \pi_1(\mathcal{H}, (b_0, c_0)) \rightarrow \text{Aut}(\Sigma_2, \sigma)$.

The facts that $\rho(1) = 1$ and $\rho(\gamma_1 \circ \gamma_2) = \rho(\gamma_2) \circ \rho(\gamma_1)$ mean that ρ is an anti-homomorphism. ρ is called the *monodromy action*.

CHAPTER 3

MONODROMY IN THE \mathcal{HOV} REGION

3.1 Inverse Limit Description

We know from [HOV94b] that if $c \notin \mathcal{M}$, then there exists some $0 < \varepsilon_c$ so that for all $b \in \mathbb{C}$ with $0 < |b| < \varepsilon_c$ we have $(J_{b,c}, H_{b,c}) \cong \varprojlim (J_c, f_c)$. Let \mathcal{L} be the subset \mathbb{C}^2 described here. Let $\pi_2 : \mathcal{L} \rightarrow (\mathbb{C} \setminus \mathcal{M})$ be the projection that takes (b, c) to c .

For $c \notin \mathcal{M}$, the removal of the two inverse images of the dynamical ray that includes c partitions dynamical space, and there is an isomorphism between J_c and Σ_2^+ , where one direction ($J_c \rightarrow \Sigma_2^+$) is given by mapping a point to its itinerary relative to this partition. This encoding gives a conjugacy between f_c and the shift operator. If $c \notin \mathbb{R}^+$, then this isomorphism can be made canonical by assigning the symbol A to the side of the partition that includes the dynamical ray of angle zero and assigning the symbol B to the side of the partition that includes c . For $(b, c) \in \mathcal{L}$, we see that the two-symbol coding on J_c induces a two-symbol coding on $J_{b,c}$ which gives a conjugacy between the maps $H_{b,c} : J_{b,c} \rightarrow J_{b,c}$ and $\sigma : \Sigma_2 \rightarrow \Sigma_2$.

For parameter values in \mathcal{L} , the Julia set of the Hénon map at $\gamma_c(t)$ is the inverse limit system of the quadratic map at $\pi_2(\gamma_c(t))$, so we precisely have the setup described in Appendix A.

3.2 Homotopy of \mathcal{HOV}

\mathcal{HOV} is homeomorphic to the space $(\mathbb{C} \setminus \{0\}) \times (\mathbb{C} \setminus \mathbb{D})$, the product of two spaces which each have homotopy group isomorphic to \mathbb{Z} , so $\Pi_1(\mathcal{HOV}) \cong \mathbb{Z} \times \mathbb{Z}$.

Define $\gamma_b : \mathbb{I} \rightarrow \mathcal{HOV}$ by $\gamma_b(t) = \left(\frac{1}{100}e^{2\pi it} - 3\right)$ and define $\gamma_c : \mathbb{I} \rightarrow \mathcal{HOV}$ by $\gamma_c(t) = \left(\frac{1}{100}, -3e^{2\pi it}\right)$.

γ_b and γ_c are both based at p_0 and lie in \mathcal{L} , and together they generate the fundamental group of \mathcal{HOV} .

3.3 Monodromy Action of γ_b

γ_b projects by π_2 down to \mathbb{C} as the trivial constant path at a base point. Trivial paths must have trivial monodromy actions, so by Theorem A.1, $\rho(\gamma_b) = 1$.

3.4 Monodromy Action of γ_c

The loop around the Mandelbrot set induces the monodromy action δ on Σ_2^+ . Hence, by Theorem A.8, $\rho(\gamma_c) = \delta$.

CHAPTER 4
ORBIT PORTRAITS AND PUZZLES

The following chapter will present several definitions which give combinatorial descriptions of one-complex-dimensional quadratic maps. The last section in this chapter is devoted to illustrating these definitions with two examples.

4.1 Formal Orbit Portraits

Let us recall a construction from [Mil00].

Definition 4.1. *A formal orbit portrait (or abstract orbit portrait) is a finite ordered p -tuple of subsets of the circle $\mathcal{P} = (A_1, A_2, \dots, A_p)$ such that the following conditions are satisfied:*

1. *Each A_j is a finite subset of \mathbb{R}/\mathbb{Z} .*
2. *For each j modulo p , the doubling map $t \mapsto 2t \pmod{\mathbb{Z}}$ takes A_j bijectively to A_{j+1} and preserves cyclic ordering of the elements.*
3. *All of the angles in $A_1 \cup \dots \cup A_p$ are periodic under angle doubling with common period rp .*
4. *The sets A_1, \dots, A_p are pairwise unlinked. This means that for $i \neq j$, the two sets A_i and A_j can be contained in disjoint, connected subsets of \mathbb{R}/\mathbb{Z} .*

Definition 4.2. *Let $\mathcal{P} = \{A_1, \dots, A_p\}$ be a formal orbit portrait. For each A_j , the connected components of $(\mathbb{R}/\mathbb{Z}) \setminus A_j$ will be called the complementary arcs of A_j .*

Theorem 4.3 (Milnor). *For each A_j in a formal orbit portrait \mathcal{P} , all but one of the complementary arcs to A_j are taken diffeomorphically to the complementary arcs of*

A_{j+1} by the angle doubling map. The remaining complementary arc of A_j has length greater than $1/2$, and its image covers one of the complementary arcs to A_{j+1} twice and every other complementary arc exactly once.

Definition 4.4. Let $\mathcal{P} = \{A_1, \dots, A_p\}$ be a formal orbit portrait. The longest complementary arc for every A_j will be called the critical arc for A_j . The complementary arc which it covers twice under the doubling map will be called the critical value arc for A_{j+1} (with the subscripts modulo p).

Theorem 4.5 (Milnor). If \mathcal{P} is a formal orbit portrait, then among the complementary arcs for the various $A_j \in \mathcal{P}$, there exists a unique arc $\mathcal{I}_{\mathcal{P}}$ of shortest length. This shortest arc is the critical value arc for its A_j and is contained within all other critical value arcs. This arc is called the characteristic arc for \mathcal{P} .

4.2 Actual Orbit Portraits

Definition 4.6. An actual orbit portrait \mathcal{O} for a one-dimensional quadratic map f_c is a repelling or periodic orbit along with the dynamical rays that land on that orbit.

Let \mathcal{O} be an actual orbit portrait for the map f_c and let (z_1, \dots, z_p) be the associated periodic orbit. Each dynamical ray in an orbit portrait has an associated angle. For $i = 1, \dots, n$, let A_p be the set of angles of the rays that land at Z_i . Then the p -tuple $\mathcal{P} = (A_1, \dots, A_p)$ satisfies the four conditions of Definition 4.1 and is hence an orbit portrait. We say that the actual orbit portrait \mathcal{O} satisfies the formal orbit portrait \mathcal{P} or that f_c satisfies the formal orbit portrait. Each actual orbit portrait satisfies exactly one formal orbit portrait, whereas each polynomial f_c may satisfy zero, finitely many, or countably many formal orbit portraits.

Moreover, Milnor showed precisely where in parameter space a given formal orbit portrait is realized.

Theorem 4.7 (Milnor). *If \mathcal{P} is a formal orbit portrait with characteristic arc $\mathcal{I}_{\mathcal{P}} = [\theta_-, \theta_+]$, then the two parameter rays R_{θ_-} and R_{θ_+} land at the same parabolic bifurcation point of \mathcal{M} .*

Definition 4.8. *The two parameter rays R_{θ_-} and R_{θ_+} corresponding to the endpoints of the characteristic arc of the abstract orbit portrait \mathcal{P} along with their common landing point partition parameter space into two sets: an open set containing 0 and a closed set containing every parameter ray with angle in $\mathcal{I}_{\mathcal{P}}$ along with a part of \mathcal{M} . The latter closed set is called the wake associated with \mathcal{P} .*

There is a 1-1 correspondence between abstract orbit portraits and parameter wakes.

Theorem 4.9 (Milnor). *f_c satisfies \mathcal{P} if and only if $c \in \mathcal{W}$, where \mathcal{W} is the wake associated with \mathcal{P} .*

4.3 Puzzle Pieces

For our purposes, it will be convenient to work with the following definitions of puzzle pieces.

Definition 4.10. *Given any actual orbit portrait O , removing the associated rays and landing points cuts up the plane into a finite number of open subsets of \mathbb{C} . We call these open sets and the finite number of landing points of these rays are called the preliminary puzzle pieces associated with the actual orbit portrait O (or equivalently, associated with the wake \mathcal{W}).*

The preliminary puzzle pieces are some number of singletons and open subsets of the plane.

Each ray in an actual orbit portrait maps to another ray in the same portrait. The boundaries of the preliminary puzzle pieces are made up entirely of rays in the portrait. The image of any preliminary puzzle piece under f_c is a union of other preliminary puzzle pieces. The mapping is a homeomorphism from each preliminary puzzle piece to a union of other preliminary puzzle pieces, with the sole exception of the preliminary puzzle piece that contains the critical point. This preliminary puzzle piece double covers the preliminary puzzle piece that contains the critical value and singly covers some other preliminary puzzle pieces.

We wish to isolate this 2-to-1 behavior. The boundary of the preliminary puzzle piece that contains the critical value is the union of the two rays whose angles are the endpoints of the characteristic arc for the corresponding abstract orbit portrait. We look at the two sets of inverse images of these two rays. One set is already in our actual orbit portrait. The other set is inside the preliminary puzzle piece that contains the critical point.

Definition 4.11. *Further subdividing the preliminary puzzle piece that contains 0 by the inverse image of the two rays from the characteristic arc gives the puzzle pieces associated with the actual orbit portrait. The two characteristic rays have a common landing point, and this landing point has two distinct inverse images. We also let both of these inverse images be puzzle pieces.*

Now, the image of each puzzle piece under f_c is a union of other puzzle pieces. These maps are all homeomorphisms, with the sole exception of the map from the puzzle piece that contains zero to the puzzle piece which contains the critical value. The puzzle piece that contains the critical point is called the *critical puzzle piece* (usually denoted Π_0)

and the puzzle piece that contains the critical value is called the *critical value puzzle piece* (usually denoted Π_1). The mapping from the critical puzzle piece to the critical value puzzle piece is a branched double cover. All of the singleton puzzle pieces are on the repelling or parabolic cycle of the actual orbit portrait, with one exception, and that exception is one of the two inverse images of the singleton puzzle piece that borders the critical value puzzle piece. Both inverse images of this singleton are on the boundary of the critical puzzle piece.

The puzzle pieces satisfy the Markov condition. That is to say that if Π_i and Π_j are puzzle pieces, then either $\Pi_i = \Pi_j$ or $\Pi_i \cap \Pi_j = \emptyset$ and either $\Pi_j \subseteq f_c(\Pi_i)$ or $f_c(\Pi_i) \cap \Pi_j = \emptyset$. In addition, it is clear that the puzzle pieces form a partition of the Julia set, since the only points of parameter space that are not in the union of the puzzle pieces are the external dynamical rays.

Definition 4.12. *We can represent the allowed dynamics with an associated directed Markov graph Γ . We define the vertices of Γ to be the puzzle pieces $\{\Pi_i\}$. We let there be an arrow $\Pi_i \rightarrow \Pi_j$ in Γ if and only if $f_c(\Pi_i) \supset \Pi_j$. We also sometimes write a double arrow $\Pi_0 \Rightarrow \Pi_1$ to signify that $f_c : \Pi_0 \rightarrow \Pi_1$ is a branched double cover.*

Lemma 4.13. *Let \mathcal{W} be a wake with associated abstract orbit portrait \mathcal{P} . If $c, c' \in \mathcal{W}$, then the two Markov graphs coming from the puzzle pieces associated with \mathcal{P} for f_c and $f_{c'}$ are isomorphic.*

Proof. The puzzles associated with \mathcal{W} at c and c' have the same sets of rays in each puzzle piece, and they also have the same sets of rays on the boundaries. f_c and $f_{c'}$ are homeomorphisms on all except for one puzzle piece. The dynamics on the rays is the doubling map on the circle. So where the rays map determines where the puzzle pieces map. □

The puzzle pieces themselves are not the same throughout the wake, because these are specific subsets of dynamical space, but they do keep the same combinatorics throughout the wake.

4.4 Fattened Puzzle Pieces

For every puzzle piece, we will define an associated bounded puzzle piece.

Definition 4.14. *The bounded puzzle piece Π_i^{bd} associated with a given puzzle piece Π_i is defined as:*

$$\Pi_i^{bd} = \Pi_i \cap G^{-1}([0, 1))$$

where G is the associated Green's function for f_c . (The use of the half-open unit interval here is arbitrary. We could have used any interval $[0, m)$ with $m > 0$ in its place.)

For every bounded puzzle, piece, we will define an associated fattened puzzle piece. There are two types of bounded puzzle pieces: singletons and open sets. We will define the associated fattened puzzle pieces for these two types of bounded puzzle pieces separately.

For $c \in \text{int}(\mathcal{W})$, because the periodic cycle associated with \mathcal{O} is repelling, we can find small disks D_1, \dots, D_p centered at the points of this repelling cycle so that D_{i+1} is relatively compact in $f_c(D_i)$. The points on this repelling cycle are on the boundaries of the puzzle pieces. We can make these disks small enough so that their closure does not contain the critical point. (For technical reasons, we also need the disks small enough so that $D_i \cup \Pi_j$ and $f_c(D_i) \cup \Pi_j$ are simply connected for every choice of i and j . We also need the images of these disks to have trivial pair-wise intersections and to be contained in the union of the closures of the open bounded puzzle pieces.)

Definition 4.15. *Define the fattened puzzle piece Δ_i associated with a bounded singleton puzzle piece $\{p_i\}$ to be the aforementioned disk D_i which contains p_i . For the unique singleton that is not in the repelling cycle, its negative is in the repelling cycle, so we use the negative of the fattened puzzle piece around its negative for the fattened puzzle piece of this singleton.*

Every ray that lands at a point p_i in the repelling periodic cycle associated with O must cross ∂D_i at some point d . The exterior of the Julia set is open, so there is some distance on either side of d in ∂D_i that is also not in the Julia set. Thus, there is also some neighborhood of the angle of the dynamical ray so that the nearby dynamical rays must also cross ∂D_i . There are finitely many rays in the actual orbit portrait so there must be some minimum angle ε that all rays can be perturbed and still intersect the same ∂D_i . Hence, if R_θ is in the orbit portrait O and lands at p_i and $|\theta - \theta'| \leq \varepsilon$ then $R_{\theta'}$ must also intersect ∂D_i .

Definition 4.16. *Define the fattened puzzle piece associated with one of the open bounded puzzle pieces as follows: We start with the corresponding bounded puzzle piece. We add on to each bounded puzzle piece the fattened puzzle piece associated with each singleton bounded puzzle piece on its boundary. We also widen each boundary ray by an angle of ε .*

Each fattened puzzle piece Δ_i is associated with one of the original puzzle pieces Π_i . Trivially, we have that $\Pi_i \subset \Delta_i$.

Theorem 4.17. *When the arrow $\Pi_i \rightarrow \Pi_j$ occurs in the Markov graph for O , then Δ_j is relatively compact in $f_c(\Delta_i)$. Additionally, if Π_i is non-critical, then the map f_c is uniformly expanding on all of the points in Δ_i that map to Δ_j , with respect to their respective Poincaré metrics.*

Proof. When f_c maps Π_i over Π_j , it is easy to see that f_c maps each part of the boundary of Δ_i outside of the closure of Δ_j . The disks around each point were constructed so that they would map over the closure of the next one. The outer boundary of Δ_i will map outside of Δ_j . The dynamics on the rays is the doubling map on angles, so perturbing a ray's angle of out by ε will perturb the angle of its image out by 2ε .

If Π_i is non-critical, then Π_j is not the critical value puzzle piece, and there are two distinct branches of the inverse of f_c on Π_j . Let f_c^{-1} be the branch of the inverse that takes Π_j inside of Π_i . Then $f_c^{-1} : \Delta_j \rightarrow f_c^{-1}(\Delta_j)$ is a holomorphic isomorphism and preserves the Poincaré metric. Because Δ_j is relatively compact in $f_c(\Delta_i)$, then $f_c^{-1}(\Delta_j)$ is relatively compact in Δ_i , and hence the inclusion map, $\iota : f_c^{-1}(\Delta_j) \rightarrow \Delta_i$ is a uniform contraction.

Thus, the composition $f_c^{-1} : \Delta_j \rightarrow \Delta_i$ uniformly contracts Poincaré metrics. Hence its inverse, $f_c : (f_c^{-1}(\Delta_j)) \rightarrow \Delta_j$, is uniformly expanding. \square

Corollary 4.18. *There exists a metric on an open set containing the closure of the union of the non-critical bounded puzzle pieces for which f_c is uniformly expanding.*

Proof. Let Δ_0 be the fattened critical puzzle piece. Let D_0 be a small disk centered at zero that does not intersect any non-critical fattened puzzle piece. We can paste together the Poincaré metrics from every non-critical fattened puzzle piece, using the Poincaré metric coming from the corresponding fattened puzzle piece when in each bounded puzzle piece. The result gives an expanding metric on the union of the non-critical bounded puzzle pieces. \square

4.5 Itineraries Relative to Orbit Portraits

Definition 4.19. *The union of the non-critical puzzle pieces has two connected components. Let $A_c^{\mathcal{W}}$ denote the connected component which contains the landing point of the dynamical ray with angle zero, and let $B_c^{\mathcal{W}}$ be the connected component that intersects the characteristic dynamical rays. When $c \in \mathcal{M}$, then $B_c^{\mathcal{W}}$ will contain the critical value.*

Definition 4.20. *If f_c satisfies an abstract orbit portrait \mathcal{P} associated with a wake \mathcal{W} and the forward orbit of z never enters the critical puzzle piece of \mathcal{P} , then we say that z has a \mathcal{W} -itinerary or has an itinerary relative to \mathcal{W} . The itinerary it has is the one-sided infinite sequence of regions (either $A_c^{\mathcal{W}}$ or $B_c^{\mathcal{W}}$) that the forward images visit. (We sometimes abbreviate these regions as A and B when c and \mathcal{W} are clear from context).*

4.6 Kneading Sequences

Let us now introduce a construction, called kneading sequences, from [Sch94], which was inspired by [DH82].

4.6.1 Kneading Sequences of Quadratic Polynomials

Choose $\theta, \varphi \in \mathbb{S}^1$. Let the θ -itinerary $I_\theta(\varphi)$ of an angle φ be a sequence of symbols defined in the following manner:

$$\text{The } n^{\text{th}} \text{ entry of } I_\theta(\varphi) = \begin{cases} A & \text{when } 2^n \varphi \in \left(\frac{\theta+1}{2}, \frac{\theta}{2}\right) \\ B & \text{when } 2^n \varphi \in \left(\frac{\theta+1}{2}, \frac{\theta}{2}\right) \\ \begin{pmatrix} B \\ A \end{pmatrix} & \text{when } 2^n \varphi = \frac{\theta}{2} \\ \begin{pmatrix} A \\ B \end{pmatrix} & \text{when } 2^n \varphi = \frac{\theta+1}{2} \end{cases}$$

Schleicher defines the kneading sequence of an angle to be $K(\theta) = I_\theta(\theta)$. Also $K^+(\theta) = \lim_{\theta' \searrow \theta} K(\theta')$ and $K^-(\theta) = \lim_{\theta' \nearrow \theta} K(\theta')$. Also, $K^+(\theta)$ is equal to $K(\theta)$ with every boundary symbol replaced with the top letter, and $K^-(\theta)$ is $K(\theta)$ with every boundary symbol replaced with the bottom letter.

If \mathcal{A} is a hyperbolic component of \mathcal{M} , then there are two external parameter rays θ^- and θ^+ landing on its root point. $K(\theta^-)$ has the same symbols as $K(\theta^+)$, with the exception that wherever one has the symbol $\begin{pmatrix} A \\ B \end{pmatrix}$ in a position, the other has the symbol $\begin{pmatrix} B \\ A \end{pmatrix}$ in the same position and vice versa. We define $K(\mathcal{A})$ to be the common symbols from $K(\theta^+)$ and $K(\theta^-)$, except we place a \star in every position where one has $\begin{pmatrix} A \\ B \end{pmatrix}$ and the other has $\begin{pmatrix} B \\ A \end{pmatrix}$. Also we define $K^-(\mathcal{A})$ to be the common sequence $K^-(\theta^-) = K^+(\theta^+)$, and we define $K^+(\mathcal{A})$ to be the common sequence $K^-(\theta^+) = K^+(\theta^-)$.

Definition 4.21. *When \mathcal{A} is a hyperbolic component of \mathcal{M} , we define the characteristic kneading sequence of \mathcal{A} to be $K^+(\mathcal{A})$.*

Theorem 4.22 (Schleicher). *Let \mathcal{A} be a hyperbolic component with angles $\theta_{\mathcal{A}}^-$ and $\theta_{\mathcal{A}}^+$ landing at its root and \mathcal{B} be a hyperbolic component with angles $\theta_{\mathcal{B}}^-$ and $\theta_{\mathcal{B}}^+$ landing at its root with $\mathcal{A} < \mathcal{B}$ (or equivalently $0 < \theta_{\mathcal{A}}^- < \theta_{\mathcal{B}}^- < \theta_{\mathcal{B}}^+ < \theta_{\mathcal{A}}^+ < 1$), and φ in either $(\theta_{\mathcal{A}}^-, \theta_{\mathcal{B}}^-)$ or $(\theta_{\mathcal{B}}^+, \theta_{\mathcal{A}}^+)$. If there is no hyperbolic component of period k or less between \mathcal{A} and \mathcal{B} , then the k^{th} term in the sequences $K^+(\mathcal{A})$, $K^-(\mathcal{B})$, $K(\varphi)$ are all identical.*

The kneading sequence of an angle can only change at the i^{th} position when moving across a point of the circle that is periodic with period i . In fact, it must change. And

when the angle is on the periodic cycle of period i , the i^{th} term must be either $\begin{pmatrix} A \\ B \end{pmatrix}$ or $\begin{pmatrix} B \\ A \end{pmatrix}$. So, the first k terms in the itineraries of points of the circle are constant on intervals of the circle where there are no periodic cycles with period less than or equal to k .

Definition 4.23. *We say a hyperbolic component \mathcal{B} is conspicuous to a hyperbolic component \mathcal{A} if $\mathcal{A} < \mathcal{B}$, \mathcal{B} has a period no greater than that of \mathcal{A} and there are no hyperbolic components of period lower than that of \mathcal{B} between the two in the $<$ ordering.*

Note that a wake is always conspicuous to itself, and for a given wake, there can only be finitely many wakes conspicuous to it. Also, as a relation, conspicuousness is not transitive or commutative. For readers familiar with the visibility relationship, conspicuousness is similar to visibility, though they are distinct. Compare with [Sch94].

The author is indebted to Dierk Schleicher for the idea behind the proof of the following theorem:

Theorem 4.24. *Let \mathcal{W} be the wake of a hyperbolic component \mathcal{A} . There are finitely many hyperbolic components conspicuous to \mathcal{A} . Let these be $\mathcal{A}_1, \dots, \mathcal{A}_r$. Choose any parameter ray R_θ inside of \mathcal{W} that is not one of the finitely many rays that land on the root points of the components conspicuous to \mathcal{A} . Then there is some \mathcal{A}_i so that $K(\theta)$ and $K^+(\mathcal{A}_i)$ have a common prefix of length m , where m is the period of \mathcal{A}_i .*

Proof. We use induction on the ordering of wakes. Let n be the period of \mathcal{A} . If the only component conspicuous to \mathcal{A} is itself then there are no periodic angles in \mathcal{W} with period less than the period of \mathcal{A} . Hence, the first n terms of the kneading sequences of angles must be constant inside of \mathcal{W} . Hence every angle in \mathcal{W} has a prefix of the characteristic kneading sequence of \mathcal{A} .

Alternately, if $r > 1$, then either R_θ is contained only in \mathcal{A} and no other conspicuous

component, or R_θ is contained in some conspicuous component other than \mathcal{A} . If the latter, we induct on this component.

If the former, then let $\theta_{\mathcal{A}}^-$ and $\theta_{\mathcal{A}}^+$ be the two parameter rays that land on the root point of \mathcal{A} . For any period $k \leq n$, there must be an even number of angles between $\theta_{\mathcal{A}}^-$ and θ of period k under doubling, for if there was an odd number, then there would have to be at least one wake of period k that contains R_θ and is contained in \mathcal{W} . And R_θ would have to be contained in some wake conspicuous to \mathcal{W} .

Since there are an even number of periodic angles of period k between $\theta_{\mathcal{A}}^-$ and θ , then the k^{th} term in the kneading sequence must flip an even number of times between these two angles, so the k^{th} terms of the sequences $K^+(\mathcal{A})$ and $K(\theta)$ must be the same. This is true for every $k \leq n$, so $K^+(\mathcal{A})$ and $K(\theta)$ have the same initial length- n string.

Note also that if θ is one of the rays that land on the root points of the components then $K(\theta)$ is not, strictly speaking, an AB coding, but both $K^+(\theta)$ and $K^-(\theta)$ satisfy the consequent of the theorem statement (except for the two rays landing on \mathcal{A} , and in this case, exactly one of $K^-(\theta)$ and $K^+(\theta)$ do). \square

4.6.2 Kneading Sequences of Orbit Portraits

We will define a characteristic kneading sequence for an orbit portrait and the associated wake.

Let \mathcal{P} be an abstract orbit portrait of period n with associated wake \mathcal{W} . Choose some $c \in \mathcal{W}$. Then f_c has an actual orbit portrait \mathcal{O} that satisfies \mathcal{P} .

Definition 4.25. *The characteristic kneading sequence, $K(\mathcal{W})$, of \mathcal{W} will be a word in A 's and B 's of length n and will be constructed as follows: Start at the point of the*

periodic orbit in \mathcal{O} that borders on Π_1 , and list off the two-symbol itinerary of this point relative to \mathcal{W} up to, but not including the point on the orbit that borders Π_0 . The n^{th} symbol will be the opposite of the two symbol coding of this point that borders Π_0 .

This definition is somewhat counter-intuitive. The intuition for this choice is that the characteristic kneading sequence is the initial segment of the kneading sequences of polynomials that are “just-beyond” the hyperbolic component at the root of \mathcal{W} . We see this in the following theorem:

Theorem 4.26. *The characteristic kneading sequence for a wake of period n with hyperbolic component \mathcal{A} at its root is precisely the first n terms in $K^+(\mathcal{A})$.*

Proof. Let \mathcal{P} be the abstract orbit portrait associated with \mathcal{W} . Let θ_1^- be the angle of the smaller of the two rays that borders the critical value puzzle piece. Let θ_0^- be the inverse image of θ_1^- that is in \mathcal{P} . Choose ε to be a small positive number. Then $K(\theta_1^- + \varepsilon)$ is the itinerary of $\theta_1^- + \varepsilon$ under the partition of the circle $\{(\theta_0^- + \frac{\varepsilon}{2}, \theta_0^- + \frac{\varepsilon}{2} + \frac{1}{2}), (\theta_0^- + \frac{\varepsilon}{2} + \frac{1}{2}, \theta_0^- + \frac{\varepsilon}{2})\}$. If ε is small enough, then the first $n-1$ terms in this itinerary will be identical to the \mathcal{W} -itinerary of the point of the periodic orbit that borders Π_1 . The difference comes at the n^{th} term. $2^{n-1}(\theta_1^- + \varepsilon) = \theta_0^- + 2^{n-1}\varepsilon$, which (when ε is small enough) is on the opposite side of the partition as θ_0^- , which is the angle of the external parameter ray that lands on the point of the orbit bordering Π_0 . Hence the n^{th} term of $K^+(\mathcal{A})$ is the opposite of the \mathcal{W} -coding of the point of the periodic orbit that borders Π_0 . □

It is worth noting that if \mathcal{A} is the hyperbolic component at the root of the wake \mathcal{W} , then $K^+(\mathcal{A})$ is not the same as $K(\mathcal{W})$. $K^+(\mathcal{A})$ is a one-sided infinite sequence on two symbols. $K(\mathcal{W})$ is a finite string of n symbols (where n is the period of \mathcal{A} and \mathcal{W}) and is just the first n symbols of $K^+(\mathcal{A})$.

Corollary 4.27. *Let R_θ be a parameter ray that lands in the interior of a wake \mathcal{W} . Then either there is some wake \mathcal{W}' conspicuous to \mathcal{W} so that $K(\theta)$ begins with $K(\mathcal{W}')$ or R_θ is one of the boundary rays of a wake conspicuous to \mathcal{W} . If the latter, then both $K^-(\theta)$ and $K^+(\theta)$ begin with the characteristic kneading sequences of (different) wakes.*

Proof. Consequence of Theorems 4.24 and 4.26. □

Thus, we see that the characteristic kneading sequence for a wake describes the initial segments of the kneading sequences for the group of polynomials that come after the hyperbolic region at the base of the wake, but before smaller wakes of lower period. Sometimes we know the initial segments of the kneading sequence for all the subsequent polynomials (when there are no smaller conspicuous wakes). Other times we only know the initial segments of kneading sequences of polynomials in a wake that are not in one of the wakes conspicuous to that wake.

4.7 Examples

The following two examples will illustrate the definitions in this chapter.

4.7.1 The Airplane

The following ordered triple of two-element sets is a formal orbit portrait:

$$\mathcal{P}_{\text{air}} = (\{3/7, 4/7\}, \{6/7, 1/7\}, \{2/7, 5/7\})$$

Here, $A_1 = \{3/7, 4/7\}$, $A_2 = \{6/7, 1/7\}$, $A_3 = \{2/7, 5/7\}$, and it is easily verified that \mathcal{P}_{air} satisfies the four conditions of Definition 4.1.

The complementary arcs of $\{3/7, 4/7\}$ are $(3/7, 4/7)$ and $(4/7, 3/7)$. The complementary arcs of $\{6/7, 1/7\}$ are $(6/7, 1/7)$ and $(1/7, 6/7)$. The complementary arcs of $\{2/7, 5/7\}$ are $(2/7, 5/7)$ and $(5/7, 2/7)$. Among these, the critical arcs are $(4/7, 3/7)$, $(1/7, 6/7)$, and $(5/7, 2/7)$. The critical value arcs are $(3/7, 4/7)$, $(1/7, 6/7)$, and $(2/7, 5/7)$. The characteristic arc of \mathcal{P}_{air} is $(3/7, 4/7)$.

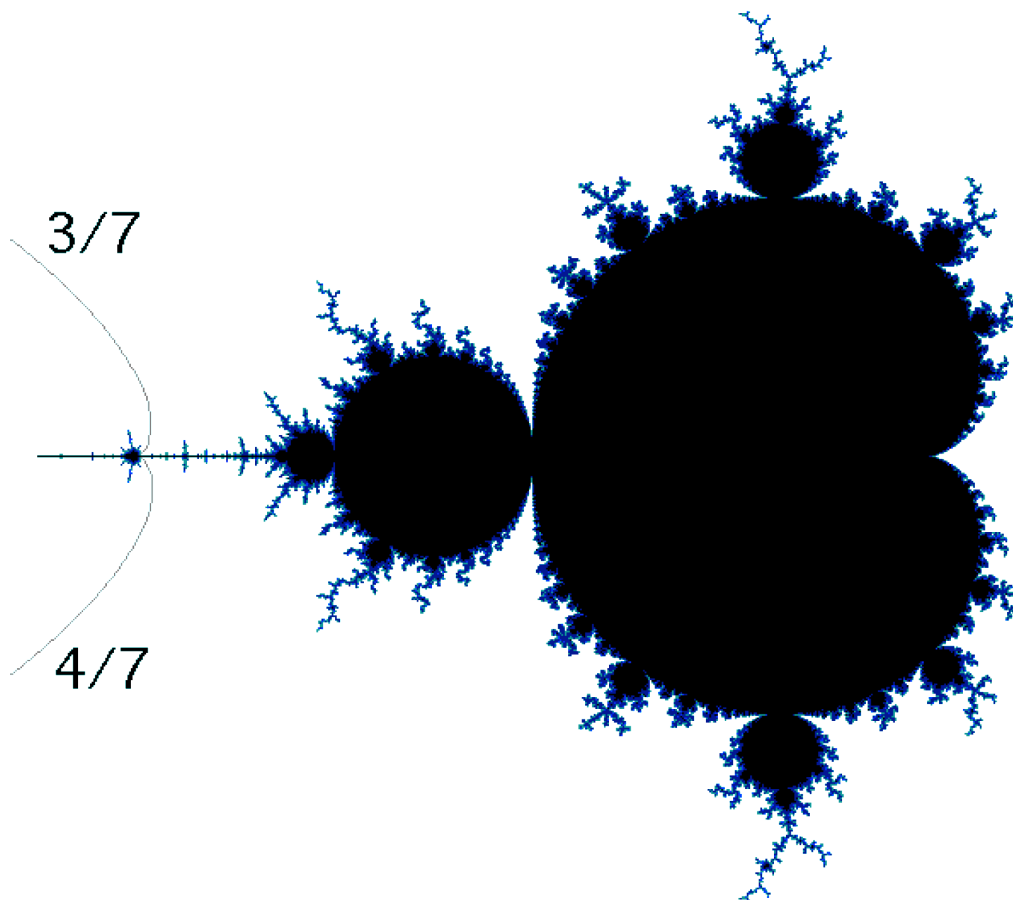


Figure 4.1: \mathcal{M} with $3/7$ and $4/7$ parameter rays.

As shown in Figure 4.1, the two rays of angles $3/7$ and $4/7$ land at the same point of the Mandelbrot set. Let \mathcal{W}_{air} be the wake associated with \mathcal{P}_{air} . The two parameter rays $3/7$ and $4/7$ form the boundary of \mathcal{W}_{air} . \mathcal{W}_{air} is the region of parameter space to

the left of these two boundary rays in Figure 4.1.

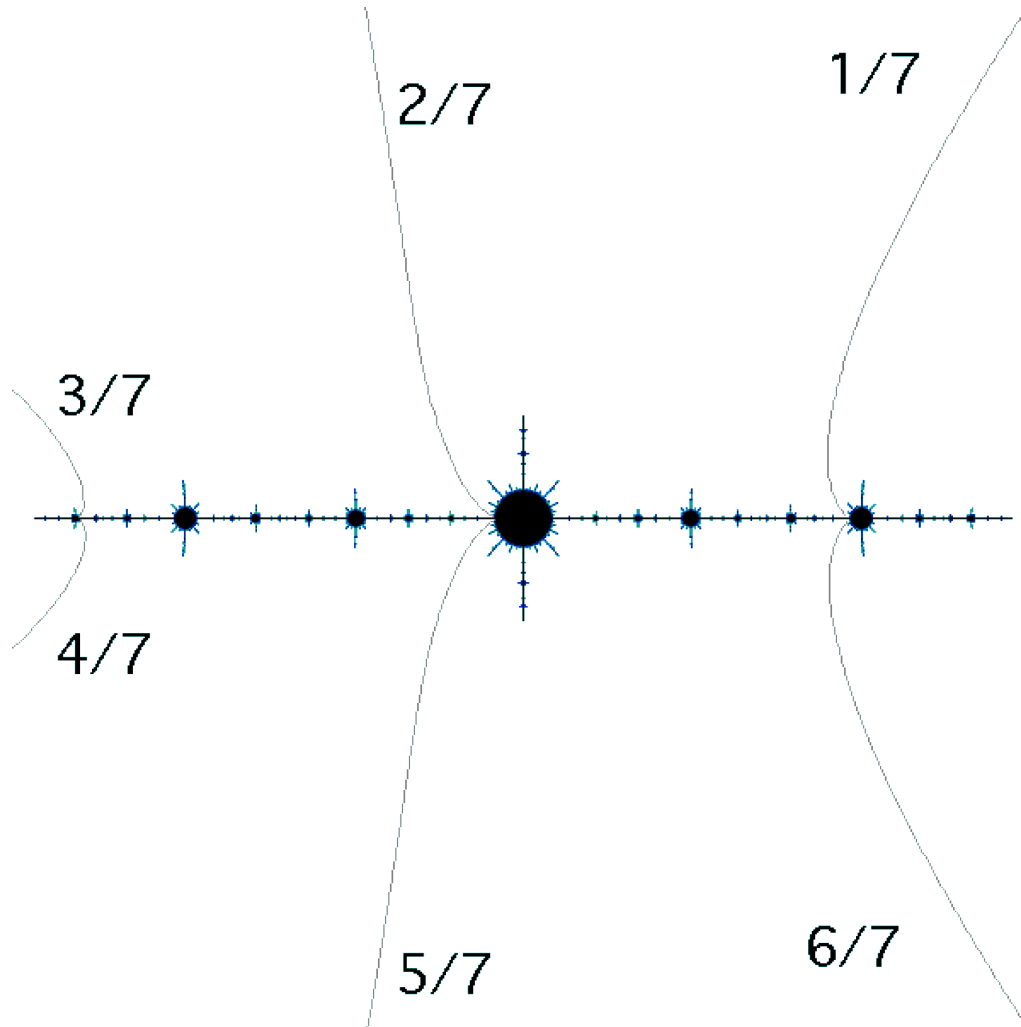


Figure 4.2: Airplane polynomial with actual orbit portrait O_{air}

Every polynomial in \mathcal{W}_{air} satisfies the formal orbit portrait \mathcal{P}_{air} . There is one such polynomial at approximately $c \approx -1.75$ called the airplane polynomial. The airplane polynomial is characterized as the unique real quadratic polynomial with a super-attracting period-three cycle. There is an actual orbit portrait O_{air} for the airplane polynomial which satisfies \mathcal{P}_{air} . Figure 4.2 shows the Julia set of the airplane along with O_{air} .

Figure 4.3 shows the nine puzzle pieces associated with \mathcal{P}_{air} . The five open puzzle

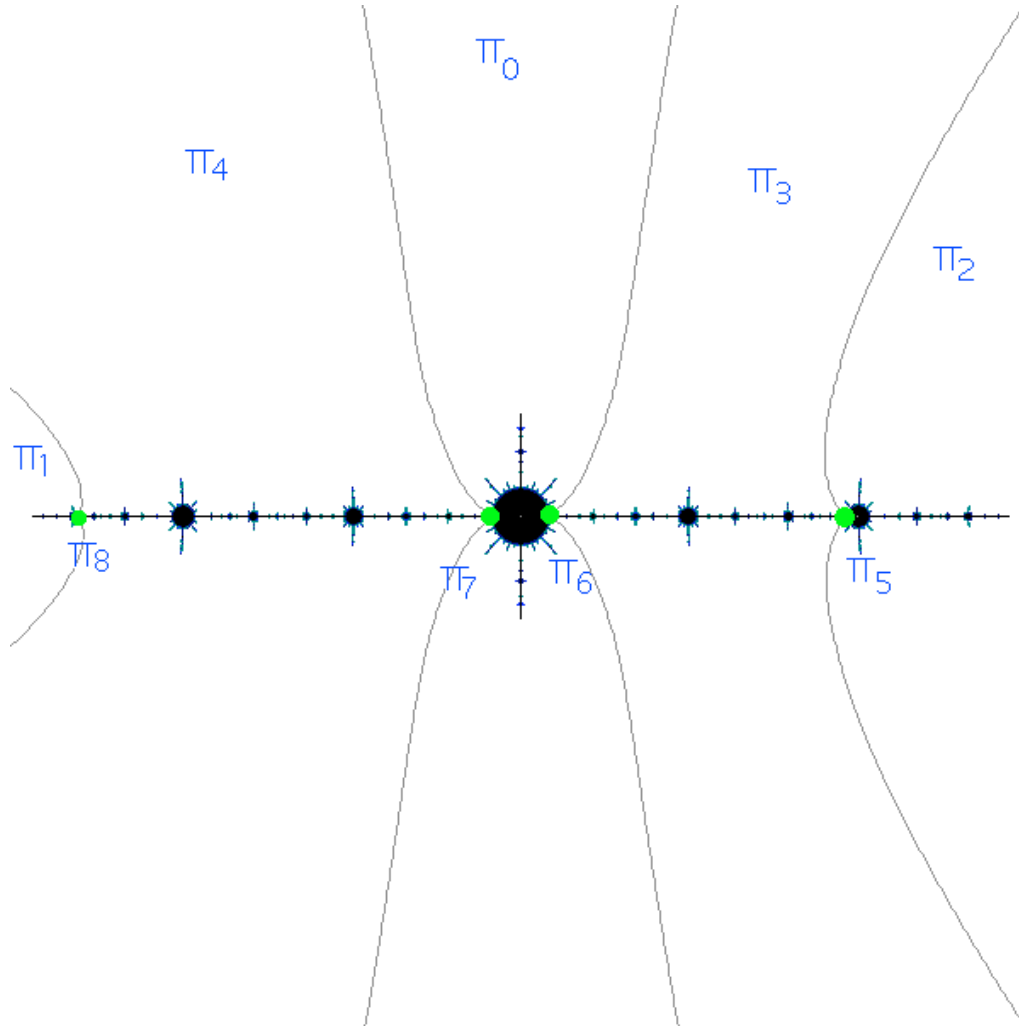


Figure 4.3: O_{air} and the Julia set of airplane polynomial

pieces are $\Pi_0, \Pi_1, \Pi_2, \Pi_3,$ and Π_4 . The four singleton puzzle pieces are $\Pi_5, \Pi_6, \Pi_7,$ and Π_8 , and are represented in Figure 4.3 by green dots along the real axis.

Let Γ_{air} be the Markov graph of the allowable transitions between puzzle pieces of \mathcal{P}_{air} . Γ_{air} is illustrated in Figure 4.4.

Let \mathcal{A}_{air} be the hyperbolic component of \mathcal{M} which contains the airplane polynomial. Then for \mathcal{A}_{air} , $\theta^- = 3/7$ and $\theta^+ = 4/7$.

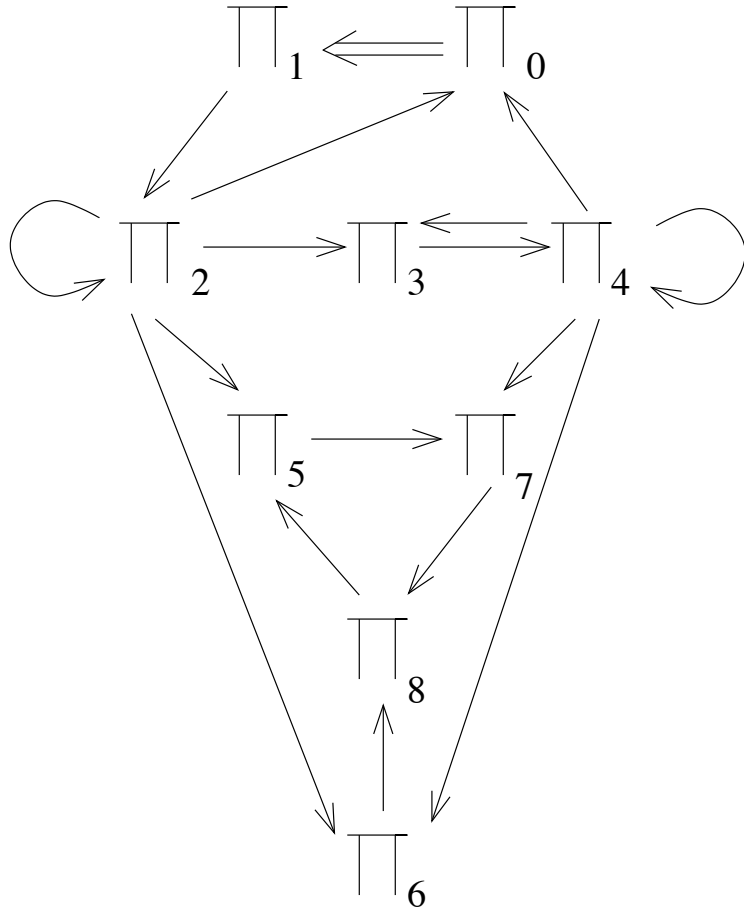


Figure 4.4: Γ_{air}

$$K(\theta^-) = \overline{BA \begin{pmatrix} A \\ B \end{pmatrix}}$$

$$K^+(\theta^-) = \overline{BAA}$$

$$K^-(\theta^-) = \overline{BAB}$$

$$K(\theta^+) = \overline{BA \begin{pmatrix} B \\ A \end{pmatrix}}$$

$$K^+(\theta^+) = \overline{BAB}$$

$$K^-(\theta^+) = \overline{BAA}$$

$$K(\mathcal{A}_{\text{air}}) = \overline{BA\star}$$

$$K^+(\mathcal{A}_{\text{air}}) = \overline{BAA}$$

$$K^-(\mathcal{A}_{\text{air}}) = \overline{BAB}$$

$$K(\mathcal{W}_{\text{air}}) = BAA$$

The period of \mathcal{W}_{air} is 3. There are no wakes contained within \mathcal{W}_{air} of lower period. Thus, the only wake conspicuous to \mathcal{W}_{air} is itself.

The fact that no other wakes are conspicuous to \mathcal{W}_{air} implies that every angle between $3/7$ and $4/7$ has a kneading sequence which begins with the three symbols BAA . Also implied is the fact that the kneading sequence of every hyperbolic component C for which $A_{\text{air}} < C$ begins with the string BAA . Additionally, every wake contained in \mathcal{W}_{air} has a characteristic kneading sequence which begins with BAA .

4.7.2 BABB

The following ordered quintuple of two-element sets is a formal orbit portrait:

$$\mathcal{P}_{BABB} = \left(\left\{ \frac{13}{31}, \frac{18}{31} \right\}, \left\{ \frac{26}{31}, \frac{5}{31} \right\}, \left\{ \frac{10}{31}, \frac{21}{31} \right\}, \left\{ \frac{20}{31}, \frac{11}{31} \right\}, \left\{ \frac{22}{31}, \frac{9}{31} \right\} \right)$$

The characteristic arc of \mathcal{P}_{BABB} is $(13/31, 18/31)$. The two parameter rays at angles $13/31$ and $18/31$ land on the same point of the Mandelbrot set, as is illustrated in Figure 4.5.

Let \mathcal{W}_{BABB} be the wake associated with \mathcal{P}_{BABB} and illustrated in Figure 4.5. Every polynomial in \mathcal{W}_{BABB} satisfies \mathcal{P}_{BABB} . Define \mathcal{A}_{BABB} to be the hyperbolic component of \mathcal{M} at the base of \mathcal{W}_{BABB} . Let f_{BABB} be the polynomial at the center of \mathcal{A}_{BABB} . f_{BABB} has a super-attracting cycle of period 5 and satisfies \mathcal{P}_{BABB} . There is an actual orbit portrait \mathcal{O}_{BABB} for f_{BABB} associated with \mathcal{P}_{BABB} . Figure 4.6 illustrates \mathcal{O}_{BABB} along with the Julia set of f_{BABB} .

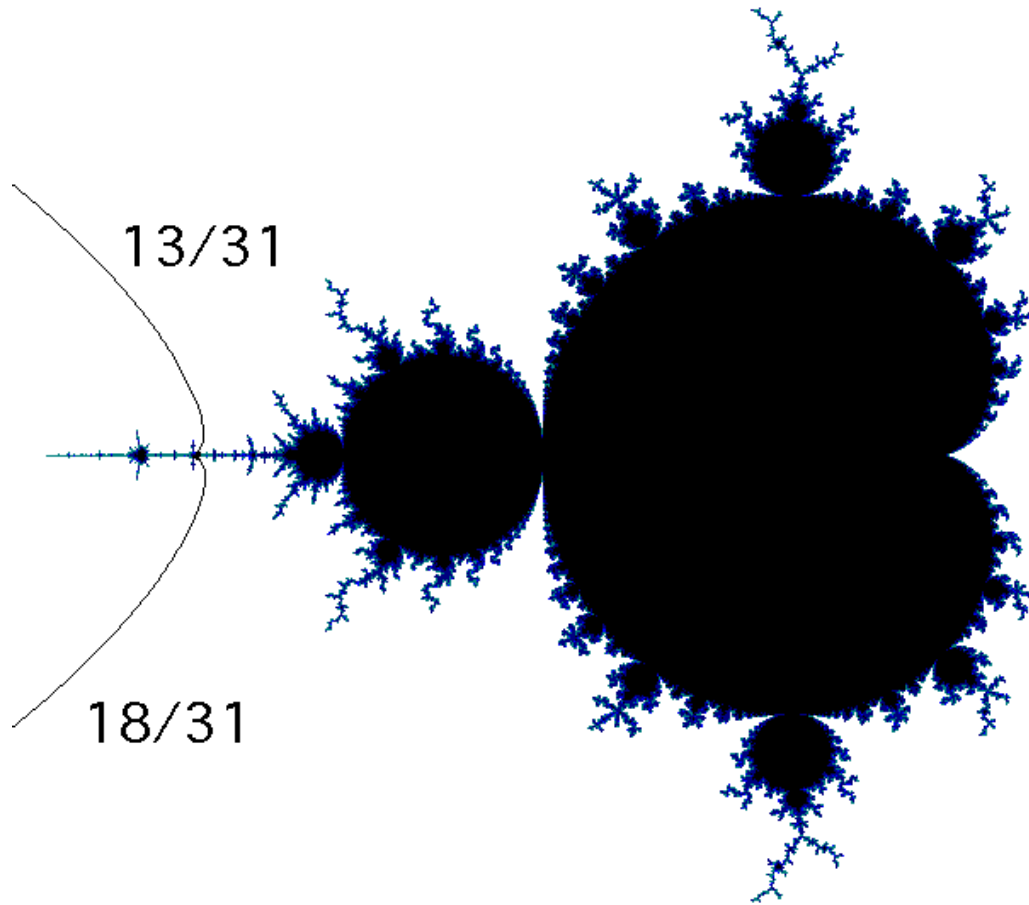


Figure 4.5: Mandelbrot set with 13/31 and 18/31 parameter rays

Figure 4.7 illustrates the puzzle piece decomposition of dynamical space associated with \mathcal{P}_{BABB} for the polynomial f_{BABB} . The open puzzle pieces are $\Pi_0, \Pi_1, \Pi_2, \Pi_3, \Pi_4, \Pi_5,$ and Π_6 . The singleton puzzle pieces are all on the real axis and are marked with green dots. These are $\Pi_7, \Pi_8, \Pi_9, \Pi_{10}, \Pi_{11},$ and Π_{12} .

Let Γ_{BABB} be the Markov graph describing the possible transitions between these puzzle pieces. Figure 4.8 shows Γ_{BABB} .

For the hyperbolic component \mathcal{A}_{BABB} , $\theta^- = 13/31$ and $\theta^+ = 18/31$. The following

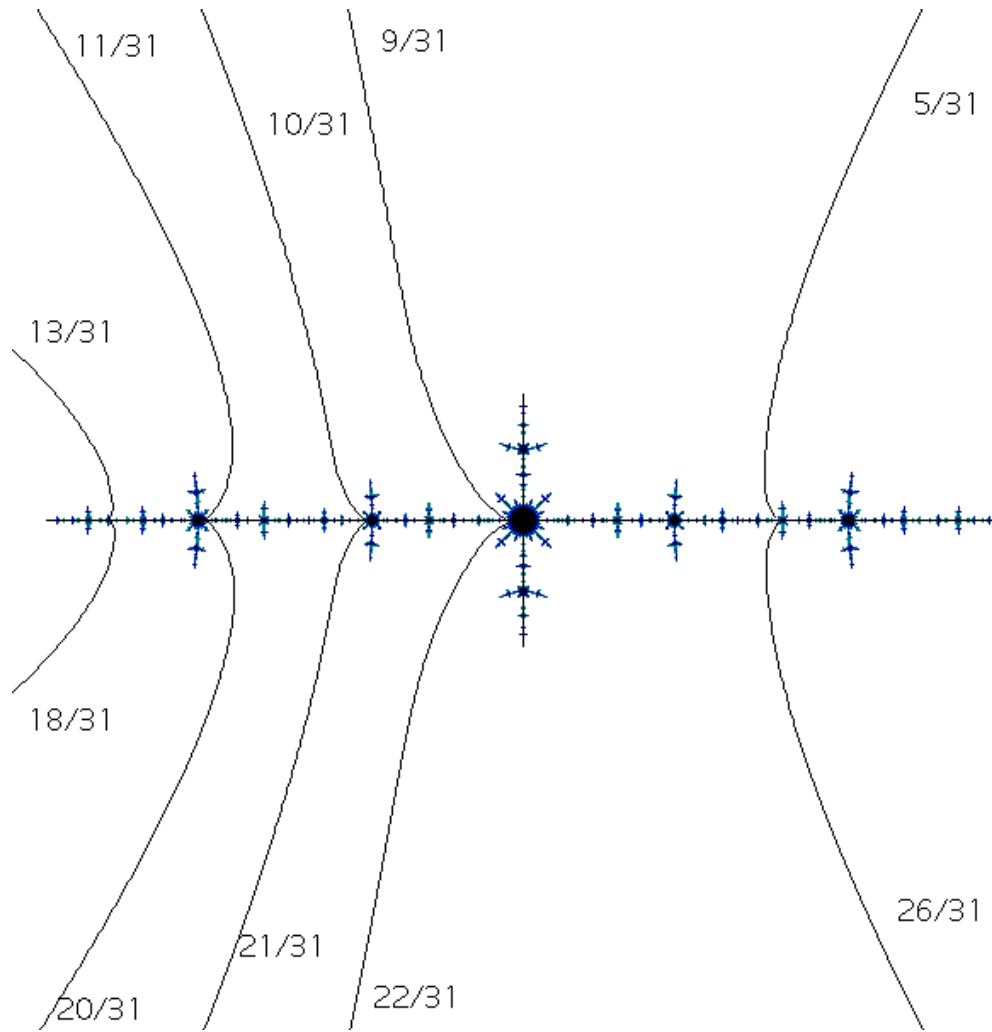


Figure 4.6: O_{BABB} and the Julia set of f_{BABB}

may be computed:

$$K(\theta^-) = \overline{BABB \begin{pmatrix} A \\ B \end{pmatrix}}$$

$$K^+(\theta^-) = \overline{BABBA}$$

$$K^-(\theta^-) = \overline{BABBB}$$

$$K(\theta^+) = \overline{BABB \begin{pmatrix} B \\ A \end{pmatrix}}$$

$$K^+(\theta^+) = \overline{BABBB}$$

$$K^-(\theta^+) = \overline{BABBA}$$

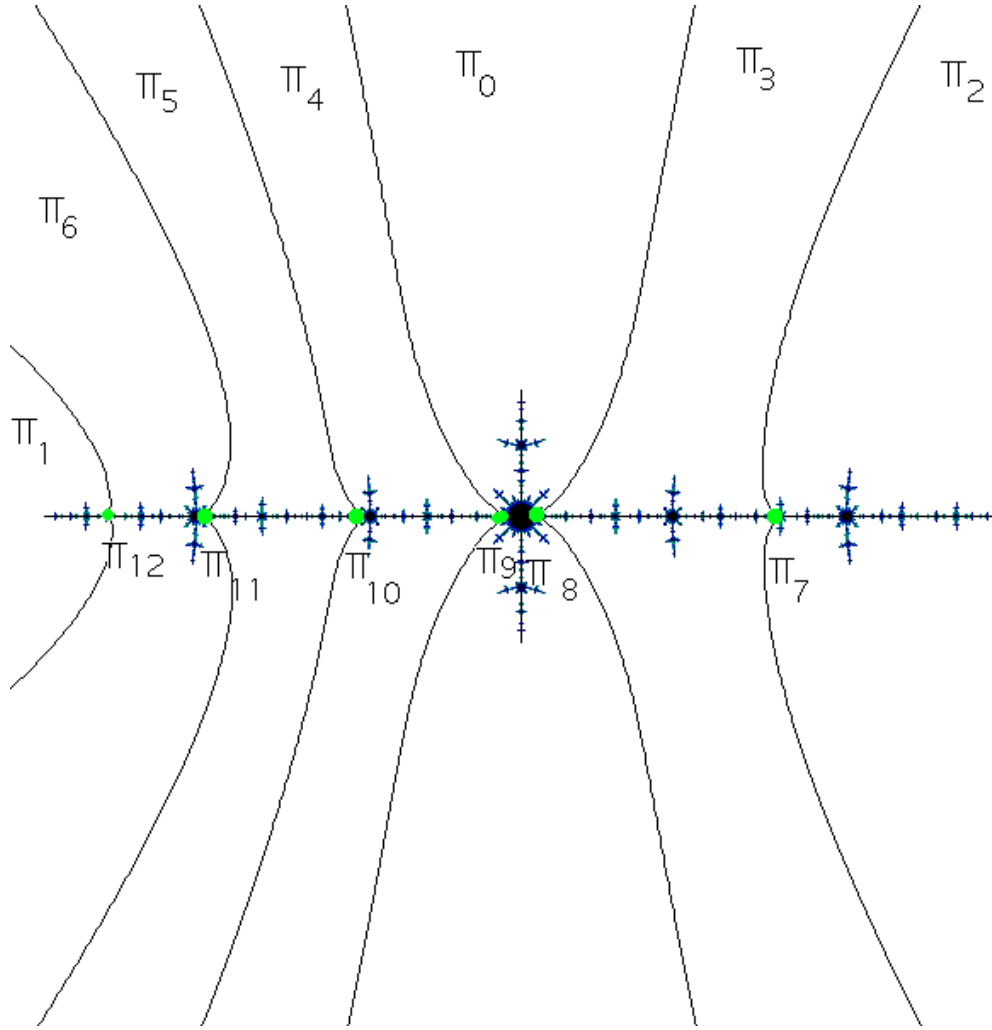


Figure 4.7: Puzzle pieces for f_{BABB} associated with \mathcal{P}_{BABB}

$$K(\mathcal{A}_{BABB}) = \overline{BABB\star}$$

$$K^+(\mathcal{A}_{BABB}) = \overline{BABBA}$$

$$K^-(\mathcal{A}_{BABB}) = \overline{BABBB}$$

$$K(\mathcal{W}_{BABB}) = BABBA$$

\mathcal{W}_{air} is contained in \mathcal{W}_{BABB} and there are no other wakes \mathcal{W}' of period lower than 3 (the period of \mathcal{W}_{air}) for which $\mathcal{W}_{BABB} < \mathcal{W}' < \mathcal{W}_{\text{air}}$. Also, the period of \mathcal{W}_{air} is less than the period of \mathcal{W}_{BABB} . Thus, \mathcal{W}_{air} is conspicuous to \mathcal{W}_{BABB} .

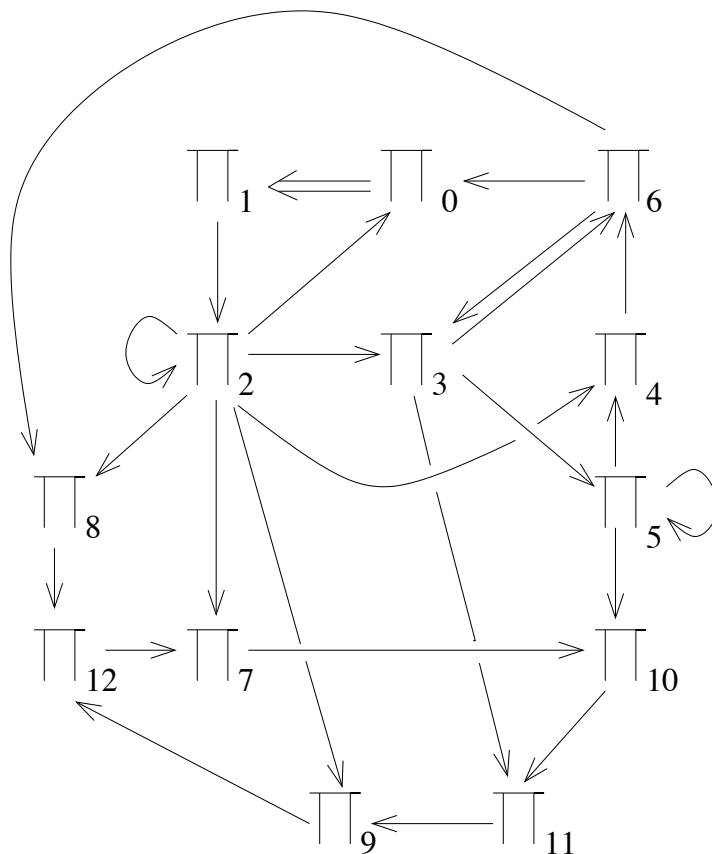


Figure 4.8: Γ_{BABB}

Let \mathcal{W}_{BAA} be the period 4 wake whose boundary is the union of the two parameter rays at angles $7/15$ and $8/15$. \mathcal{W}_{BAA} is contained in \mathcal{W}_{BABB} . Also, the period of \mathcal{W}_{BAA} is 4, which is less than the period of \mathcal{W}_{BABB} , which is 5. However, \mathcal{W}_{BAA} is not conspicuous to \mathcal{W}_{BABB} , because $\mathcal{W}_{BABB} < \mathcal{W}_{\text{air}} < \mathcal{W}_{BAA}$, and \mathcal{W}_{air} has a smaller period than \mathcal{W}_{BAA} .

Every wake is conspicuous to itself, so the only two wakes conspicuous to \mathcal{W}_{BABB} are itself and \mathcal{W}_{air} .

CHAPTER 5

$$\mathcal{X}_c^{\mathcal{W}}$$

5.1 Defining $\mathcal{X}_c^{\mathcal{W}}$

Definition 5.1. Choose any parameter wake \mathcal{W} with associated abstract orbit portrait \mathcal{P} . Choose any $c \in \text{int}(\mathcal{W})$. Then f_c has an actual orbit portrait \mathcal{O} with a repelling periodic cycle that satisfies \mathcal{P} . \mathcal{O} has a critical puzzle piece Π_0 . Let

$$\mathcal{X}_c^{\mathcal{W}} = \{x \in J_c \mid (\forall n \in \mathbb{N}_0) \quad f_c^{\circ n}(x) \notin \Pi_0\}$$

$\mathcal{X}_c^{\mathcal{W}}$ is the set of all points in the Julia set that do not visit the critical puzzle piece.

It is clear that $\mathcal{X}_c^{\mathcal{W}}$ is forward-invariant under f_c . $\mathcal{X}_c^{\mathcal{W}}$ is not backwards-invariant, because points in the critical value puzzle piece have inverse images in the critical puzzle piece. These are the only points of $\mathcal{X}_c^{\mathcal{W}}$ that do not have two inverse images in $\mathcal{X}_c^{\mathcal{W}}$. It is also clear that points in $\mathcal{X}_c^{\mathcal{W}}$ have a well defined two symbol \mathcal{W} -itinerary.

Lemma 5.2. If $\mathcal{W}' \subseteq \mathcal{W}$ are wakes and $c \in \text{int}(\mathcal{W}')$, then $\mathcal{X}_c^{\mathcal{W}'} \subseteq \mathcal{X}_c^{\mathcal{W}}$

Proof. The critical value puzzle piece of \mathcal{W}' is contained in the critical value puzzle piece of \mathcal{W} , so we also have containment of their respective critical puzzle pieces. \square

Theorem 5.3. f_c is uniformly expanding on $\mathcal{X}_c^{\mathcal{W}}$.

Proof. $\mathcal{X}_c^{\mathcal{W}}$ is contained in the union of the non-critical bounded puzzle pieces. \square

Corollary 5.4. $\mathcal{X}_c^{\mathcal{W}} \subset J_c$ and every point of $\mathcal{X}_c^{\mathcal{W}}$ is accessible.

Proof. The statement is trivial for the singleton puzzle pieces since they are the landing points of rays of the orbit portrait. We have expansion on a neighborhood of every other point in $\mathcal{X}_c^{\mathcal{W}}$. \square

Corollary 5.5. *A point of $\mathcal{X}_c^{\mathcal{W}}$ is determined by its one-sided two-symbol coding relative to \mathcal{W} .*

Proof. We have expansion on the union of all of the non-critical puzzle pieces. f_c restricted to the union of the puzzle pieces on either side of the critical puzzle piece is a homeomorphism. So if two points are distinct, then they must eventually map to different sides of the critical puzzle piece. \square

Theorem 5.6. *If $c, c' \in \text{int}(\mathcal{W})$, then the \mathcal{W} -itineraries realized by points in (respectively) $\mathcal{X}_c^{\mathcal{W}}$ and $\mathcal{X}_{c'}^{\mathcal{W}}$ are identical subsets of Σ_2^+ .*

Proof. Suppose that the itinerary ε is realized at $\mathcal{X}_c^{\mathcal{W}}$ by a point x , which is the landing point of a ray R_θ . Note that $\varepsilon = K(\theta)$. Under the doubling map, θ never enters the inverse image under the doubling map of the characteristic arc of the wake \mathcal{W} . Hence, because of the expansion on the non-critical puzzle pieces for $f_{c'}$, the dynamical ray of angle θ for the map $f_{c'}$ must land at some point $x' \in \mathcal{X}_{c'}^{\mathcal{W}}$. The \mathcal{W} -itinerary of x' under the action of $f_{c'}$ must be $K(\theta)$, the same as for x . \square

Corollary 5.7. *There exists some $\Sigma_{\mathcal{W}}^+ \subset \Sigma_2^+$, depending only on \mathcal{W} , so that for every $c \in \text{int}(\mathcal{W})$, taking the \mathcal{W} -itinerary gives an isomorphism from $(\mathcal{X}_c^{\mathcal{W}}, f_c)$ to $(\Sigma_{\mathcal{W}}^+, \sigma)$.*

Proof. If two points in $\mathcal{X}_c^{\mathcal{W}}$ have the same \mathcal{W} -itinerary, then by the expansion on $A_c^{\mathcal{W}}$ and $B_c^{\mathcal{W}}$, they must be the same point. Thus we have an injective map from $\mathcal{X}_c^{\mathcal{W}}$ to Σ_2^+ . Let $\Sigma_{\mathcal{W}}^+$ be the image of this map. By Theorem 5.6, $\Sigma_{\mathcal{W}}^+$ is independent of our choice of c . We have a bijection from $\mathcal{X}_c^{\mathcal{W}}$ to $\Sigma_{\mathcal{W}}^+$ that conjugates f_c with the shift. \square

5.2 Multi-Itineraries

The fattened puzzle pieces cover \mathcal{X}_c^W , but they do not partition it. The fattened puzzle pieces have non-trivial intersections.

Definition 5.8. *A multi-itinerary of a point x in dynamical space with respect to a map f relative to a cover $C = \{\Delta_i\}$ is sequence of elements of the power set of C , (C_0, C_1, C_2, \dots) such that $f^n(x) \in \Delta_i$ if and only if $\Delta_i \in C_n$.*

A multi-itinerary is a natural extension of the concept of an itinerary to situations where we do not have an explicit partition of dynamical space.¹

The multi-itinerary simply keeps track of all of the regions that the point lands in under iteration, even when it lands in more than one.

The puzzle pieces have the property that the image of each puzzle piece contains all of the other puzzle pieces to which there is an arrow from that puzzle piece in Γ . This property is not stable under a small C^1 perturbation, which is why we must use fattened puzzle pieces. The disadvantage of using fattened puzzle pieces is that we lose the partition of dynamical space. This introduces some difficulties which we will have to carefully deal with.

The non-critical fattened puzzle pieces cover \mathcal{X}_c^W , so points in \mathcal{X}_c^W have a multi-itinerary relative to the non-critical fattened puzzle pieces.

Theorem 5.9. *The multi-itinerary of a point $x \in \mathcal{X}_c^W$ relative to the fattened puzzle pieces determines that point's itinerary relative to the non-fattened puzzle pieces.*

¹Given sets C_α , indexed by $\alpha \in \mathfrak{N}$, the multi-itinerary is the itinerary relative to the partition:

$$\left\{ \bigcap_{\alpha \in \mathfrak{N}} \left\{ \begin{array}{ll} C_\alpha & \text{if } I(\alpha) = 1 \\ (C_\alpha)^c & \text{if } I(\alpha) = 0 \end{array} \right\} \middle| I \in 2^{\mathfrak{N}} \right\}$$

Proof. Given a multi-itinerary (C_0, C_1, \dots) of x , we will give an algorithm for how to construct x 's itinerary with respect to unfattened puzzle pieces which uses only the multi-itinerary.

Let $x_n = f_c^{o_n}(x)$. Let C_i be the first term in the itinerary that contains more than one fat puzzle piece. Then the point is inside one of the small disk-like puzzle pieces around a singleton puzzle piece. Then one of two situations occurs. Either every term in the itinerary subsequent to C_i includes multiple puzzle pieces or there is some minimum $j > i$ so that C_j does not include any small disk puzzle piece.

If the former, then by the expansion, we know that x_i is a point in the periodic cycle, and C_i and every subsequent term can be replaced with the unfattened singleton puzzle piece that the corresponding disks contain.

If the latter, then because the small disk puzzle pieces are small enough, we know that when a point leaves the region where it has a multi-itinerary, then on the next iterate, it must be in one of the unfattened puzzle pieces adjacent to the next small disk puzzle piece. Because the map is a local homeomorphism near the points of the periodic cycle, then this lets us resolve which unfattened puzzle piece from C_{j-1} that x_{j-1} is in. Note that we do not have to worry about x_j landing in multiple fattened puzzle pieces that are not small disks, because these regions lie entirely outside of the Julia set.

This procedure can be applied iteratively to resolve all of the terms between C_i and C_j , and then this process can be iteratively applied (possibly infinitely many times) to resolve the rest of the terms. Thus, we can determine the coding of x with respect to the puzzle pieces (which do form a Markov partition) from the coding of x with respect to the fattened puzzle pieces (which do not). \square

Moreover, everything in the proof of Theorem 5.9 holds for bi-itineraries of points

in the inverse limit system of (X_c^W, f_c) as well as for small enough C^1 perturbations of f_c or its inverse limit.

5.3 Adaptation to Γ

Definition 5.10. *Let U be a simply connected Riemann surface homeomorphic to the disk, and U' a relatively compact open subset. Define the size of U' in U to be $1/M$, where M is the largest modulus of an annulus separating U' from the boundary of U .*

Definition 5.11. *Sullivan defines a p -telescope to be a sequence of topological disks (W_0, W_1, \dots) such that W_{i+1} is relatively compact in $p(W_i)$.*

Theorem 5.12 (Sullivan). *If (W_0, W_1, \dots) is a p -telescope, and W_{i+1} is of uniformly bounded size in $p(W_i)$, then the intersection $\bigcap_{i=0}^{\infty} p^{\circ-i}(W_i)$ is a single point.*

Proof. Standard application of Schwarz-Pick lemma along with properties of moduli show that the Poincaré metrics in these disks are uniformly expanding under f_c . \square

We wish to have an isomorphism between points of \mathcal{X}_c^W and paths in the graph Γ . The obvious map from \mathcal{X}_c^W to paths in Γ takes a point to its itinerary relative to the bounded puzzle pieces. This map is well-defined and is injective. The obvious map going the other direction takes an itinerary of non-critical puzzle pieces, fattens them, and then uses telescopes to identify a unique point of \mathcal{X}_c^W . This action is well-defined, but unfortunately, it is not always injective.

In the case of primitive orbit portraits, there are always two itineraries that map to any pre-image of the periodic cycle. The reason for this is that when \mathcal{W} is primitive, there is a path in Γ of non-critical open puzzle pieces where successive pieces neighbor

the successive points on the repelling periodic cycle associated with \mathcal{W} . Thus, the fattened puzzle pieces will include the successive points of the periodic cycle, and the telescope will identify that point on the periodic cycle.

To get our desired isomorphism, we must exclude such paths.

Definition 5.13. *Call a path $(\Pi_{i_0}, \Pi_{i_1}, \Pi_{i_2}, \dots)$ in Γ degenerate if every Π_{i_n} is an open puzzle piece and there exists some x in the periodic cycle of the orbit portrait so that $f_c^n(x) \in \partial\Pi_{i_n}$ for every $n \in \mathbb{N}_0$.*

We call such paths degenerate because the point they identify in $\mathcal{X}_c^{\mathcal{W}}$ using telescopes is not in the first puzzle piece of the itinerary. If \mathcal{W} is satellite, there are no degenerate paths. If \mathcal{W} is primitive, there is a single cycle of degenerate paths with the same period as \mathcal{W} .

Definition 5.14. *We say that a one-sided or two-sided infinite path in Γ is adapted to Γ if it does not include the critical puzzle piece and no right-infinite tail of the path is degenerate.*

Theorem 5.15. *There is an isomorphism between $\mathcal{X}_c^{\mathcal{W}}$ and paths adapted to Γ .*

Proof. The map from $\mathcal{X}_c^{\mathcal{W}}$ to paths is given by itineraries. An itinerary of a point can never be degenerate. Because of expansion on $\mathcal{X}_c^{\mathcal{W}}$, this map is injective.

The map from paths to $\mathcal{X}_c^{\mathcal{W}}$ is given by first fattening the puzzle pieces and then taking a telescope. The strong expansion on the puzzle pieces ensure that this construction is well-defined. Now we will show that this procedure is injective.

Suppose that $(\Pi_{i_0}, \Pi_{i_1}, \Pi_{i_2}, \dots)$ and $(\Pi_{j_0}, \Pi_{j_1}, \Pi_{j_2}, \dots)$ are two different non-critical paths in Γ yield the same point x under the action of fattening and taking telescopes. Let

$x_k = f_c^{\circ k}(x)$. $x_k \in \Delta_{i_k} \cap \Delta_{j_k}$ for all k . There is some $\Pi_{i_n} \neq \Pi_{j_n}$. Fattened puzzle pieces overlap on the disks around the points in the orbit portrait, so at least one of Π_{i_n} and Π_{j_n} is an open puzzle piece that borders some point z_n on the periodic orbit. Without loss of generality, let Π_{i_n} be the open puzzle piece. Let $z_{k+n} = f_c^{\circ k}(z_n)$. Because f_c is a homeomorphism when restricted to either side of the critical puzzle piece, then $\Pi_{i_m} \neq \Pi_{j_m}$, Π_{i_m} is open, and $z_m \in \Delta_{i_m} \cap \Delta_{j_m}$ for all $m \geq n$. Hence, we see that $(\Pi_{i_0}, \Pi_{i_1}, \Pi_{i_2}, \dots)$ has a degenerate tail. So whenever two itineraries are associated with the same point in \mathcal{X}_c^W , then one must have a degenerate tail. Thus the map that associates itineraries adapted to Γ with points is also injective.

It is also clear that these two actions are inverses of each other. □

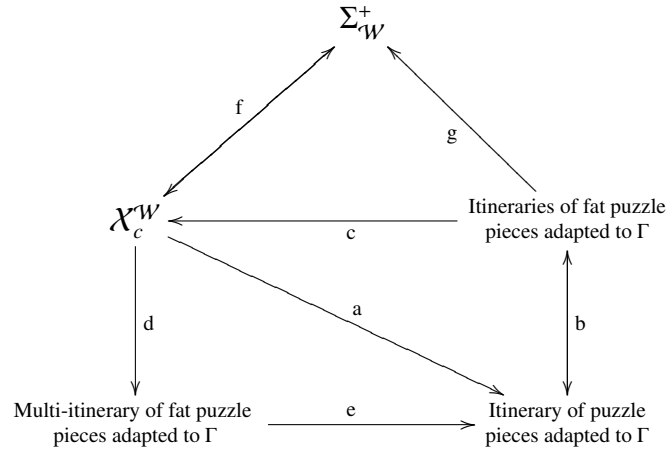
Definition 5.16. *We say that a one-sided multi-itinerary is adapted to Γ if it is the multi-itinerary of some point of \mathcal{X}_c^W relative to the fattened puzzle pieces.*

The action that takes a point of \mathcal{X}_c^W to its multi-itinerary adapted to Γ is surjective because of how adaptation to Γ is defined for multi-itineraries and is injective because of expansion on \mathcal{X}_c^W .

Definition 5.17. *We say that a two-sided multi-itinerary is adapted to Γ if every right-infinite tail of it is adapted to Γ .*

5.4 Relations Between Points and Itineraries

The following commutative diagram illustrates isomorphisms between points in dynamical space, itineraries relative to various partitions, and multi-itineraries. All of these maps commute with the shift operator or f_c (whichever is the appropriate operator on that space).



- a) The puzzle pieces partition $\mathcal{X}_c^{\mathcal{W}}$, so every point has an itinerary adapted to Γ .
- b) The correspondence between puzzle pieces and their fattened counterparts gives a trivial correspondence between bi-infinite sequences adapted to Γ .
- c) An itinerary of fattened puzzle pieces adapted to Γ gives a unique point using telescopes.
- d) Points of $\mathcal{X}_c^{\mathcal{W}}$ have multi-itineraries with respect to the fattened puzzle pieces.
- e) Theorem 5.9 gives an algorithm for determining a point's itinerary given only its multi-itinerary relative to the fattened puzzle pieces.
- f) $\mathcal{X}_c^{\mathcal{W}} \rightarrow \Sigma_{\mathcal{W}}^+$ is given by the definition of a \mathcal{W} -itinerary. $\Sigma_{\mathcal{W}}^+ \rightarrow \mathcal{X}_c^{\mathcal{W}}$ is Corollary 5.5.
- g) Non-critical puzzle pieces are always on one side or the other of the critical puzzle piece.

5.5 Continuity of $\mathcal{X}_c^{\mathcal{W}}$

Theorem 5.18. $\mathcal{X}_c^{\mathcal{W}}$ varies continuously with c .

Proof. By Corollary 5.7, every point of $\mathcal{X}_c^{\mathcal{W}}$ is identified with a unique \mathcal{W} -itinerary and the set of realizable \mathcal{W} -itineraries is independent of the choice of $c \in \text{int}(\mathcal{W})$. Define $\Phi_{c,c'}^{\mathcal{W}}(x)$ to be the point whose \mathcal{W} -itinerary under $f_{c'}$ is the same as that of x under f_c .

What we need to show that the function $\Phi_{c,c'}^{\mathcal{W}}(x) : \mathcal{W} \rightarrow \mathbb{C}$ is a continuous function of c' as x , c , and \mathcal{W} are held constant. Also note that $\Phi_{c,c}^{\mathcal{W}} : \mathcal{X}_c^{\mathcal{W}} \rightarrow \mathcal{X}_c^{\mathcal{W}}$ is the identity.

We will show that $\Phi_{c,c'}^{\mathcal{W}}(x)$ is continuous on a small open domain around c .

$x \in \mathcal{X}_c^{\mathcal{W}}$ has a \mathcal{W} -itinerary: $(\mathcal{P}_0, \mathcal{P}_1, \dots)$. Let f_{c',\mathcal{P}_i} be the restriction of $f_{c'}$ to the union of either the A - or B -side fattened puzzle pieces, depending on the symbol \mathcal{P}_i . Then

$$\Phi_{c,c'}^{\mathcal{W}}(x) = \bigcap_{n=1}^{\infty} f_{c',\mathcal{P}_0}^{-1} \left(\dots \left(f_{c',\mathcal{P}_n}^{-1}(\mathbb{C}) \right) \right)$$

For $i, j \in \mathbb{N}_0$ with $i \geq j$, define:

$$z_{i,j} = f_{c',\mathcal{P}_{i-j}}^{-1} \left(\dots \left(f_{c',\mathcal{P}_{i-1}}^{-1} \left(f_c^i(x) \right) \right) \right)$$

$z_{i,j}$ is the point you get when you map x forward i times by f_c , and then pull back j times by $f_{c'}$, each time taking the appropriate branch of the inverse. Once we fix c , x , and \mathcal{W} (as we have), then $z_{i,j}$ is a function of c' . If $\lim_{n \rightarrow \infty} z_{n,n}$ exists, then this limit must equal $\Phi_{c,c'}^{\mathcal{W}}(x)$, because it has the appropriate \mathcal{W} -itinerary under $f_{c'}$. We will prove convergence by showing that successive distances between points on the sequence $(z_{0,0}, z_{1,1}, z_{2,2}, \dots)$ are bounded geometrically with a uniform contraction constant on a small neighborhood of c . In addition, we will show that $\Phi_{c,c'}^{\mathcal{W}}(x)$ is continuous by showing that the initial

constant of the geometric series is bounded by a constant multiple of $|c - c'|$ in another open set around c .

For any $z_{i,0} \in A_c^{\mathcal{W}} \cup B_c^{\mathcal{W}}$, then the mean-value theorem applied to the square-root function gives:

$$\begin{aligned}
|z_{i+1,1} - z_{i,0}| &= |f_{c',p_i}^{-1}(f_c(z_{i,0})) - z_{i,0}| \\
&= \left| \pm \sqrt{z_{i,0}^2 + c - c'} - \pm \sqrt{z_{i,0}^2} \right| \\
&\leq \max_{x \in \{z_{i,0}^2 + t(c-c') \mid t \in \mathbb{I}\}} \left| \frac{1}{2\sqrt{x}} \right| \cdot |c' - c| \\
&\leq \frac{1}{2\sqrt{|z_{i,0}^2| - |c' - c|}} |c' - c| \\
&\leq k_0 |c' - c|
\end{aligned}$$

Obviously here, we must restrict c' to a domain U around c such that $\bar{U} \subset \text{int}(\mathcal{W})$ and small enough so that even for $w \in \bar{U}$, then $|w - c|$ is smaller in absolute value than the square of any point in either the $A_c^{\mathcal{W}}$ or $B_c^{\mathcal{W}}$ regions. And we let

$$k_0 = \sup_{\substack{y \in A_c^{\mathcal{W}} \cup B_c^{\mathcal{W}} \\ c' \in U}} \left(\frac{1}{2\sqrt{|y^2| - |c' - c|}} \right)$$

Hence $|z_{i,0} - z_{i+1,1}| \leq k_0 |c' - c|$ for all $i \in \mathbb{N}_0$ and $c' \in U$.

Let Δ_{m_i} be the fattened puzzle piece for $f_{c'}$ whose corresponding non-fattened piece for f_c contains $z_{i,0}$, and let $d_i(\cdot, \cdot)$ be the Poincaré metric on this piece.

The periodic cycle of the orbit portrait associated with \mathcal{W} is well-defined and repelling in $\text{int}(\mathcal{W})$, so it and the rays that land on it move continuously. Hence, the non-fattened and fattened puzzle pieces associated with \mathcal{W} move continuously for $c \in \mathcal{W}$. Let V be an open region in parameter space around c whose closure is in $\text{int}(\mathcal{W})$ and

such that whenever $c' \in V$, then the closures of the bounded puzzle pieces for f_c are contained in the fattened puzzle pieces for $f_{c'}$ and the closures of the bounded puzzle pieces for $f_{c'}$ are contained in the fattened puzzle pieces for f_c .

Associate with every puzzle piece Π_i at every parameter value $c' \in V$ an open set S_i that moves continuously with c' , contains the closure of the i^{th} puzzle pieces for f_c and $f_{c'}$, and is contained within the corresponding fattened puzzle pieces for both f_c and $f_{c'}$.

We apply a constant multiple to the Poincaré metrics on each fattened puzzle piece so that the resulting metrics are strictly greater than the Euclidean metrics.

For every $c' \in V$, on every S_i , the Poincaré metrics on the corresponding fattened puzzle pieces are equivalent to the Euclidian metric. There is some some $k_2 > 1$ so that for all $c' \in V$, all S_i at c' , and all $x, y \in S_i$, then

$$|x - y| < d_i(x, y) < k_2 |x - y|$$

We have uniform expansion on the map $f_{c'} : \Delta_i \rightarrow \Delta_j$ whenever $\Pi_i \rightarrow \Pi_j$ is in Γ . There are finitely many arrows in Γ , and this expansion depends continuously on c' , so there must be some $k_1 < 1$ so that $k_1 \cdot d_{n+1}(x, y) > d_n(f_{c', \mathcal{P}_n}^{-1}(x), f_{c', \mathcal{P}_n}^{-1}(y))$ whenever $c' \in W$ and $x, y \in \Delta_{m_{n+1}}$.

Fix $c' \in V$ for the following discussion.

$$d_i(z_{i,0}, z_{i+1,1}) \leq k_2 |z_{i,0} - z_{i+1,1}| \leq k_2 k_0 |c' - c|$$

By induction on the contraction of $f_{c', \mathcal{P}_n}^{-1}$,

$$d_{i-j}(z_{i,j}, z_{i+1,j+1}) \leq k_1^j k_2 k_0 |c' - c|$$

Setting $i = j$ yields

$$d_0(z_{i,i}, z_{i+1,i+1}) \leq k_1^i k_2 k_0 |c' - c|$$

We see that the sequence $(z_{0,0}, z_{1,1}, z_{2,2}, \dots)$ is Cauchy and converges. By geometric summation and repeated application of the triangle inequality,

$$|x - \Phi_{c,c'}^{\mathcal{W}}(x)| = \left| z_{0,0} - \lim_{n \rightarrow \infty} z_{n,n} \right| \leq d_0 \left(z_{0,0}, \lim_{i \rightarrow \infty} z_{i,i} \right) \leq \frac{k_2 k_0}{1 - k_1} |c' - c|$$

Since this is true in an open neighborhood W around every $c \in \text{int}(\mathcal{W})$, then $\Phi_{c,c'}^{\mathcal{W}}(x)$ is locally Lipschitz and hence continuous in c' . \square

5.6 \mathcal{W} -itineraries of $\mathcal{X}_c^{\mathcal{W}}$

Theorem 5.19. *Points in $\mathcal{X}_c^{\mathcal{W}}$ whose \mathcal{W} -itinerary contains $K(\mathcal{W})$ must lie in Π_1 . Also, $K(\mathcal{W})$ can only appear as the initial segment of \mathcal{W} -itineraries of points in $\mathcal{X}_c^{\mathcal{W}}$.*

Proof. Let $[\theta_-, \theta_+]$ be the characteristic arc of \mathcal{W} . Let n be the period of \mathcal{W} . Suppose that $z \in \mathcal{X}_c^{\mathcal{W}}$ contains the characteristic kneading sequence of \mathcal{W} , $K(\mathcal{W}) = (\chi_0, \dots, \chi_{n-1})$ as a substring. Then let z_0 be the iterate of z such that $K(\mathcal{W})$ is the initial segment of the itinerary of z_0 . Label the further iterates of z_0 by $z_{i+1} = f_c(z_i)$.

Let p_0 through p_{n-1} be the points of the repelling or parabolic cycle of \mathcal{W} with the labeling such that p_0 is the landing point of R_{θ_-} and R_{θ_+} . (There are not necessarily n distinct points in this cycle, but we only need their cyclical order for the following, not their distinctness.) For any particular p_j , the k dynamical rays that land on it partition the dynamical plane into *sectors* based at p_j . The essential fact is that sectors based at p_j map to sectors based at p_{j+1} . All but one of these sectors maps homeomorphically to the next. The critical sector (the sector that contains the critical puzzle piece) is the odd one out. The critical puzzle piece maps in a branched 2-to-1 fashion to the critical

value puzzle piece. Removal of the critical puzzle piece sometimes splits the critical sector into two parts, sometimes not. In either case, the connected components of the remainder map homeomorphically to their images.

The dynamical rays R_{θ_-} and R_{θ_+} together land on p_0 and cut off the critical value puzzle piece of \mathcal{W} . Then $R_{2^{n-1}\theta_-}$ and $R_{2^{n-1}\theta_+}$ land on p_{n-1} , and together make up one edge of the boundary of the critical value puzzle piece. Also notice that $2^n\theta_- = \theta_-$ and $2^n\theta_+ = \theta_+$.

The sector based at p_{n-1} bounded by $R_{2^{n-1}\theta_-}$ and $R_{2^{n-1}\theta_+}$ contains the critical puzzle piece as well as the other half of dynamical space which is across the critical puzzle piece from p_n . This sector must therefore contain all of either $A_c^{\mathcal{W}}$ or $B_c^{\mathcal{W}}$, whichever has the opposite coding as p_{n-1} itself. Our supposition that the point z_0 has a kneading sequence which is the characteristic kneading sequence of the wake \mathcal{W} therefore ensures that z_{n-1} is in the sector based at p_n bounded by $R_{2^{n-1}\theta_-}$ and $R_{2^{n-1}\theta_+}$.

Now, assume that z_{i+1} is in the sector bounded by $R_{2^{i+1}\theta_-}$ and $R_{2^{i+1}\theta_+}$ based at p_{i+1} . If that sector does not contain the critical point, then its inverse image has two connected components, each of which maps homeomorphically to the sector. One of these connected components is in $A_c^{\mathcal{W}}$ and the other is in $B_c^{\mathcal{W}}$. If that sector does contain the critical point, then it contains Π_1 , and its inverse image is connected and contains the critical puzzle piece. After removal of the critical puzzle piece, there are two remaining connected regions, each of which mapping homeomorphically to the original sector minus the critical value puzzle piece. Again, one of these connected components is in $A_c^{\mathcal{W}}$ and one of them is in $B_c^{\mathcal{W}}$. As mentioned earlier, points of $X_c^{\mathcal{W}}$ can never have any iterate (including themselves) in Π_0 , so z_{i+1} has two distinct inverse images, one in $A_c^{\mathcal{W}}$ and one in $B_c^{\mathcal{W}}$. One of these is z_i . Which one is z_i depends on the i^{th} entry in the itinerary of z_0 , and hence on the i^{th} entry of the characteristic kneading sequence of \mathcal{W} . Thus, z_i and p_i

are in the same one of $A_c^{\mathcal{W}}$ and $B_c^{\mathcal{W}}$.

The map $f_c|_{A_c^{\mathcal{W}}} : A_c^{\mathcal{W}} \rightarrow \mathbb{C}$ and $f_c|_{B_c^{\mathcal{W}}} : B_c^{\mathcal{W}} \rightarrow \mathbb{C}$ are both homeomorphisms onto their images. So pulling back $R_{2^{i+1}\theta_-}$, $R_{2^{i+1}\theta_+}$, p_{i+1} and z_{i+1} by the appropriate one of $f|_A$ or $f|_B$ (whichever one p_i and z_i are in) must give the appropriate containment relationship: that z_i is contained in the sector based at p_i bounded by $R_{2^i\theta_-}$ and $R_{2^i\theta_+}$. By induction, z_0 is contained in the critical value puzzle piece. Since points in the critical value puzzle piece cannot have inverse images, then we see that $z = z_0$. Hence, z lies in the critical value puzzle piece and $K(\mathcal{W})$ is the initial segment of the \mathcal{W} -itinerary of z . \square

Theorem 5.20. *Points in $X_c^{\mathcal{W}}$ whose \mathcal{W} -itinerary contains the substring $K(\mathcal{W})$ for any \mathcal{W}' conspicuous to \mathcal{W} must lie in Π_1 . Also, these substrings can only appear as the initial segment of itineraries of points in $X_c^{\mathcal{W}}$.*

Proof. Suppose the itinerary of x contains the characteristic kneading sequence of some $\mathcal{W}' \subset \mathcal{W}$. Choose some $c' \in \text{int}(\mathcal{W}') \subseteq \mathcal{W}$. $X_c^{\mathcal{W}}$ can be followed continuously to $X_{c'}^{\mathcal{W}}$, where $x \in X_c^{\mathcal{W}}$ is followed to some $x' \in X_{c'}^{\mathcal{W}}$. Because the two external rays and the point of the periodic orbit that together bound the critical value puzzle piece move continuously, then either both x and x' are in their respective critical value puzzle pieces associated with the wake \mathcal{W} for f_c and $f_{c'}$ or neither are. Similarly, the rays that bound the critical puzzle piece move continuously, so x and x' have the same \mathcal{W} -itinerary.

x' contains in its \mathcal{W}' -itinerary the characteristic kneading sequence of \mathcal{W}' , so by Theorem 5.19, then x' is in the critical value puzzle piece associated with \mathcal{W}' , and $K(\mathcal{W}')$ may only appear at the beginning of the \mathcal{W}' -itinerary of x' . Since $\mathcal{W}' \subseteq \mathcal{W}$, then we have containment of their respective critical value puzzle pieces, and we see that x' must be in the critical value puzzle piece of \mathcal{W} for $f_{c'}$. Also, whenever both are defined, then the \mathcal{W} -itinerary of a point is equal to the \mathcal{W}' -itinerary of the point. Hence

x is in the critical value puzzle piece for \mathcal{W} for the polynomial f_c and $K(\mathcal{W}')$ can only appear at the beginning of its \mathcal{W} -itinerary. \square

Theorem 5.21. *Choose $x \in \mathcal{X}_c^{\mathcal{W}}$. If x is in the critical value puzzle piece, then some initial string of the two-symbol itinerary of x relative to \mathcal{W} is equal to the characteristic kneading sequence of some conspicuous wake $\mathcal{W}' \subseteq \mathcal{W}$.*

Proof. Suppose $x \in \mathcal{X}_c^{\mathcal{W}}$ and $x \in \Pi_1$. x is accessible, so there is some dynamical ray R_θ that lands on x . The two inverse images $R_{\theta/2}$ and $R_{\theta/2+1/2}$ both lie in the critical puzzle piece. The forward images of x never enter the critical puzzle piece, so the \mathcal{W} -itinerary of x must be the same as $K(\theta)$. Since x never again enters the critical value puzzle piece, then x and θ cannot be periodic. Thus, the parameter ray R_θ cannot lie on the boundary of some wake smaller than \mathcal{W} . By Corollary 4.27, the \mathcal{W} -itinerary of x must begin with $K(\mathcal{W}')$ for some conspicuous wake \mathcal{W}' of \mathcal{W} . \square

Corollary 5.22. *Choose $x \in \mathcal{X}_c^{\mathcal{W}}$. The \mathcal{W} -itinerary of x contains the characteristic kneading sequence of some wake conspicuous to \mathcal{W} if and only if x is in the critical value puzzle piece. Additionally, the characteristic kneading sequence of the wake conspicuous to \mathcal{W} may only appear as the initial segment of the itinerary of any point of $\mathcal{X}_c^{\mathcal{W}}$.*

Proof. The “if” direction is given by Theorem 5.21. The “only if” direction is given by Theorem 5.20. \square

Corollary 5.23. *The set of one-sided two-symbol \mathcal{W} -itineraries of points in $f_c(\mathcal{X}_c^{\mathcal{W}})$ is a one-sided subshift of finite type where the disallowed words are the characteristic kneading sequences of wakes conspicuous to \mathcal{W} .*

Proof. $f_c(\mathcal{X}_c^{\mathcal{W}})$ can be characterized as the set of points which do not enter the critical value puzzle piece under iteration. Then by Corollary 5.22, the \mathcal{W} -itineraries realized

by $f_c(\mathcal{X}_c^{\mathcal{W}})$ are all of the one-sided sequences on two symbols that do not have any characteristic kneading sequence for any wake conspicuous to \mathcal{W} . \square

$\varprojlim(\mathcal{X}_c^{\mathcal{W}}, f_c)$ naturally inherits a two-sided \mathcal{W} -itinerary from the one-dimensional system.

Corollary 5.24. *The set of two-sided two-symbol \mathcal{W} -itineraries realized by $\varprojlim(\mathcal{X}_c^{\mathcal{W}}, f_c)$ is a two-sided subshift of finite type where the disallowed words are the characteristic kneading sequences of wakes conspicuous to \mathcal{W} .*

Proof. Note that every point in $\mathcal{X}_c^{\mathcal{W}}$ has two inverse images in $\mathcal{X}_c^{\mathcal{W}}$ with the exception of points in the critical value puzzle piece. The inverse images of these points are in the critical puzzle piece and hence not in $\mathcal{X}_c^{\mathcal{W}}$. Hence $\varprojlim(\mathcal{X}_c^{\mathcal{W}}, f_c)$ is made up of orbits which never visit the critical value puzzle piece, or equivalently, those that do not have any characteristic kneading sequence of any wake conspicuous to \mathcal{W} . \square

CHAPTER 6

$$\mathcal{X}_{B,C}^W$$

6.1 Crossed Mappings

Let us recall from [HOV94b] the definition of a crossed mapping:

Definition 6.1. *Let $B_1 = U_1 \times V_1$ and $B_2 = U_2 \times V_2$. Let $pr_1 : B_i \rightarrow U_i$ be the projection to the first co-ordinate and let $pr_2 : B_i \rightarrow V_i$ be projection to the second co-ordinate. A crossed mapping from B_1 to B_2 is a triple (W_1, W_2, f) , where*

1. $W_1 \subseteq U_1' \times V_1$ where $U_1' \subset U_1$ is a relatively compact open subset,
2. $W_2 \subseteq U_2 \times V_2'$ where $V_2' \subset V_2$ is a relatively compact open subset,
3. $f : W_1 \rightarrow W_2$ is a holomorphic isomorphism, such that for all $y \in V_1$, the mapping

$$pr_1 \circ f|_{W_1 \cap (U_1 \times \{y\})} : W_1 \cap (U_1 \times \{y\}) \rightarrow U_2$$

is proper, and the mapping

$$pr_2 \circ f^{-1}|_{W_2 \cap (\{x\} \times V_2)} : W_2 \cap (\{x\} \times V_2) \rightarrow V_1$$

is proper.

When W_1 and W_2 can be determined from context, we write $f : B_1 \xrightarrow[\times]{} B_2$.

Each B_i has a Kobayashi metric, and when U_i and V_i are disks, the Kobayashi metric on B_i has the simple form of the product of the Poincaré metrics on U_i and V_i , which will be denoted $|\cdot|_{U_i}$ and $|\cdot|_{V_i}$, respectively.

Definition 6.2. *An analytic curve in $B = U \times V$ is called horizontal-like if at every point $(x, y) \in U \times V$, the tangent vector at that point $(\eta, \nu) \in T_{(x,y)}B$ satisfies $|(x, \eta)|_U \geq |(y, \nu)|_V$.*

Definition 6.3. *An analytic curve in $B = U \times V$ is called vertical-like if at every point $(x, y) \in U \times V$, the tangent vector at that point $(\eta, \nu) \in T_{(x,y)}B$ satisfies $|(x, \eta)|_U \leq |(y, \nu)|_V$.*

We should note that the intersection of a horizontal-like disk with a vertical-like disk in the same bi-disk is not necessarily a singleton. However, if the absolute values of the slopes of each are never unity, then their intersection must be a singleton.

Hubbard and Oberste-Vorth go on to show the following theorems:

Theorem 6.4 (Hubbard-Oberste-Vorth). *$pr_1 \circ f|_{W_1 \cap (U_1 \times y)}$ and $pr_2 \circ f^{-1}|_{W_2 \cap \{x\} \times V_2}$ must have the same topological degree which is called the degree of the crossed mapping.*

Theorem 6.5 (Hubbard-Oberste-Vorth). *Let*

$$\dots, B_{-1} = U_{-1} \times V_{-1}, B_0 = U_0 \times V_0, B_1 = U_1 \times V_1, \dots$$

be a bi-infinite sequence of bi-disks, and $f_i : B_i \xrightarrow{\times} B_{i+1}$ be crossed mappings of degree 1 with U_i' of uniformly bounded size in U_i and V_i' of uniformly bounded size in V_i . Then for all $m \in \mathbb{Z}$,

1. *The set*

$$W_m^S = \{(x_m, y_m) | \exists (x_n, y_n) \in B_n \text{ for all } n > m \text{ such that } f_n(x_n, y_n) = (x_{n+1}, y_{n+1})\}$$

is a closed vertical-like Riemann surface in B_m , and $pr_2|_{W_m^S} : W_m^S \rightarrow V_m$ is an isomorphism.

2. *The set*

$$W_m^U = \{(x_m, y_m) | \exists (x_n, y_n) \in B_n \text{ for all } n < m \text{ such that } f_n(x_n, y_n) = (x_{n+1}, y_{n+1})\}$$

is a closed horizontal-like Riemann surface in B_m , and $pr_1|_{W_m^U} : W_m^U \rightarrow U_m$ is an isomorphism.

3. Moreover, the sequence

$$(x_m, y_m) := W_m^S \cap W_m^U \quad \text{for } m \in \mathbb{Z}$$

is the unique bi-infinite sequence with $(x_m, y_m) \in B_m$ for all $m \in \mathbb{Z}$, and $f_m(x_m, y_m) = (x_{m+1}, y_{m+1})$.

Additionally, the map $f_n|_{W_n^S} : W_n^S \rightarrow W_{n+1}^S$ is a strong contraction of Poincaré metrics and $f_n|_{f^{-1}(W_{n+1}^U)} : f^{-1}(W_{n+1}^U) \rightarrow W_{n+1}^U$ is a strong expansion of Poincaré metrics. The strong contraction and expansion is due to the fact that U_i' and V_i' are relatively compact in U and V , respectively. Moreover, the expansions and contractions are uniform for all n because of the uniform sizes of the U_i' 's and V_i' 's.

[HOV94b] guarantees that the tangent spaces of stable and unstable manifolds are respectively in the vertical-like and horizontal-like cone fields. We will need a mild extension of this result, which was already known to Hubbard and Oberste-Vorth:

Theorem 6.6. *Given the same setup as Theorem 6.5, the slopes of the stable and unstable manifolds are uniformly bounded in absolute value away from 1. Moreover, this bound depends only on the sizes of the V_n' 's in the V_n 's and the sizes of the U_n' 's in the U_n 's, and this dependency is continuous.*

Proof. Any unstable manifold W_n^U is the forward image of $W_{n-1}^U \cap W_{n-1}$ by f_{n-1} . Therefore it is completely contained in $U_n \times V_n'$. Pick any point $(x, y) \in W_n^U$ with $(\zeta, \eta) \in T_{(x,y)}(W_n^U)$. W_n^U is the graph of a conformal map from U_n to V_n' , and so by Schwarz's lemma, $|(\zeta, x)|_{U_n} \geq |(\eta, y)|_{V_n'}$. Because the V_n' 's are of uniformly bounded size in V_n , then there exists some $\kappa > 1$ so that the inclusion map $\iota : V_n' \rightarrow V_n$ contracts the Poincaré metric by at least a factor of κ . Hence $|(\zeta, x)|_{U_n} \geq \kappa \cdot |(\eta, y)|_{V_n}$. The uniform bound guarantees that κ does not depend on n , but note that κ depends continuously on the maximum of the sizes of the V_n' 's in the V_n 's.

The proof for stable manifolds is analogous. □

6.2 Horizontal Disk Contraction

We need to show that horizontal disks get closer to each other under iteration of crossed mappings, but in order to do this we will need a definition of distance for horizontal disks that is adapted to this particular situation.

Definition 6.7. *In a bi-disk, the distance between two horizontal-like disks D_1 and D_2 whose slopes never have absolute value 1 relative to a vertical-like disk V is defined as:*

$$d_V(D_1, D_2) = d(\text{pr}_2(D_1 \cap V), \text{pr}_2(D_2 \cap V))$$

where d in the previous equation refers to Poincaré distance in the disk.

Definition 6.8. *The distance between two horizontal-like disks D_1 and D_2 whose slopes never have absolute value 1 is defined as:*

$$d(D_1, D_2) = \sup_{\substack{V \text{ is a vertical-} \\ \text{like disk}}} d_V(D_1, D_2)$$

This definition of a metric on horizontal disks satisfies the triangle inequality and the equivalence $d(D_1, D_2) = 0 \iff D_1 = D_2$.

Theorem 6.9. *The distances between horizontal-like disks are uniformly contracted by a 1-crossed mapping.*

Proof. Let $f : B_1 \xrightarrow{\times} B_2$ be a 1-crossed mapping. Let D_1' and D_1'' be any two horizontal like disks in B_1 . Then their images are, respectively, D_2' and D_2'' , which are two horizontal-like disks in B_2 . Choose any $\varepsilon > 0$. Let Z_2 be any vertical-like disk in

B_2 with $|d_{Z_2}(D_2', D_2'') - d(D_2', D_2'')| < \varepsilon$. Let $Z_1 = f^{-1}(Z_2)$, which must be a vertical-like disk in B_1 . Because of the strong expansion for f^{-1} on vertical-like disks, then $d_{Z_1}(D_1', D_1'') \geq \kappa d_{Z_2}(D_2', D_2'')$ for some $\kappa > 1$. So,

$$d(D_1', D_1'') \geq d_{Z_1}(D_1', D_1'') \geq \kappa d_{Z_2}(D_2', D_2'') \geq \kappa(d(D_2', D_2'') - \varepsilon)$$

Since this is true for every $\varepsilon > 0$, then $d(D_2', D_2'') \leq \frac{1}{\kappa}d(D_1', D_1'')$. □

Theorem 6.10. *The metric d on the space of horizontal-like disks is equivalent to the metric d' defined as:*

$$d'(D_1, D_2) = \sup_{x \in \mathbb{D}} d_{\{x\} \times \mathbb{D}}(D_1, D_2)$$

Proof. $d'(D_1, D_2) \leq d(D_1, D_2)$ is clear because d' considers only a subset of the vertical-like disks that d does.

Choose any $x_1 \in \mathbb{D}$. Suppose a vertical-like disk Z intersects D_1 at (x_1, y_1) and D_2 at (x_2, y_2) . Because Z is vertical-like, then $d(x_1, x_2) \leq d(y_1, y_2)$. There is another point (x_1, y_3) on D_2 and because D_2 is horizontal-like, then $d(y_2, y_3) \leq d(x_1, x_2)$. The triangle inequality gives that $d(y_1, y_3) \leq d(y_1, y_2) + d(y_2, y_3) \leq d(y_1, y_2) + d(x_1, x_2) \leq 2d(y_1, y_2) = 2 \cdot d_Z(D_1, D_2)$. If we take the supremum over all Z that intersect D_1 at a point with x -coordinate x_1 and then take the supremum over all $x_1 \in \mathbb{D}$, then we get that $d'(D_1, D_2) \leq 2 \cdot d(D_1, D_2)$. □

Theorem 6.10 tells us that convergence of horizontal disks under our metric is equivalent to uniform convergence in vertical slices.

6.3 Perturbations of One-Dimensional Orbit Portraits

Fix any one-dimensional quadratic wake \mathcal{W} , and choose any $c \in \text{int}(\mathcal{W})$. We have an actual orbit portrait \mathcal{O} of f_c associated with \mathcal{W} . We have the non-fattened puzzle pieces $\{\Pi_i\}$ with their associated Markov graph Γ . We also have the fattened puzzle pieces $\{\Delta_i\}$ associated with \mathcal{O} , along with the relations that Δ_j is relatively compact in $f_c(\Delta_i)$ when we have containment of the corresponding non-fattened puzzle pieces: $\Pi_j \subset f_c(\Pi_i)$. If f'_c is a small enough perturbation of f_c in the C^1 -topology, then it is clear that Δ_j is relatively compact in $f'_c(\Delta_i)$.

We will define puzzle pieces in two dimensions that will code some, but not all of the points in the Julia set. This coding will be valid throughout an open region of parameter space, which we will describe.

The one-dimensional fattened puzzle pieces are bounded. Let $D(0, R_c)$ be an open disk centered at zero that is large enough to contain the closures of all of the fattened puzzle pieces.

Definition 6.11. *For every fattened puzzle piece Δ_i , define $B_i = \Delta_i \times D(0, R_c)$. The B_i 's will be called the two-dimensional (fattened) puzzle pieces.*

Theorem 6.12. *There exists some positive constant $\varepsilon_c^{\mathcal{W}}$, depending only on c and \mathcal{W} (and continuously on c), such that whenever $0 < |b| < \varepsilon_c^{\mathcal{W}}$ and $\Pi_i \rightarrow \Pi_j$ is in Γ (and Π_i is non-critical), then $H_{b,c} : B_i \xrightarrow{\times} B_j$ is a one-crossed mapping.*

Proof. Suppose $\Pi_i \rightarrow \Pi_j$ is in Γ . Because there are finitely many arrows in Γ , it suffices to prove the statement for a single pair of fattened puzzle pieces.

The degenerate Hénon mapping $H_{0,c}$ maps all of \mathbb{C}^2 to the co-dimension 1 complex parabola $x = y^2 + c$ and reduces to the one-dimensional dynamical system $x \mapsto x^2 + c$ in

the first co-ordinate. Thus $\text{pr}_1(B_j) = \Delta_j$ is relatively compact in $\text{pr}_1 \circ H_{0,c}(B_i) = f_c(\Delta_i)$. $H_{0,c}^{-1}(B_j)$ is the union of two infinitely tall open cylinders. They each have the form $f_c^{-1}(\Delta_j) \times \mathbb{C}$, where one cylinder has one branch of the inverse image f_c^{-1} and the other cylinder has the other branch. Exactly one of these cylinders intersects B_i , and in fact, the projection to the first coordinate of this cylinder is the appropriate branch of $f_c^{-1}(\Delta_j)$ and is relatively compact in $\Delta_i = \text{pr}_1(B_i)$.

Also the disk $D(0, R_c)$ was chosen precisely so that $\text{pr}_2 \circ H_{0,c}(B_i) = \Delta_i$ is relatively compact in $\text{pr}_2(B_j) = D(0, R_c)$.

$\text{pr}_2 \circ H_{b,c}$ is uniformly continuous in the C^1 topology in b and c inside a bounded region of dynamical space. Note that $\text{pr}_1 \circ H_{b,c}^{-1}(x, y) = y$, and does not depend on the parameters at all.

We have shown that these relations of relative compactness are preserved under small perturbations of parameters. Thus, there is some small open domain around $(0, c)$ so that (b', c') in this domain implies that $\text{pr}_1(H_{b',c'}^{-1}(B_j) \cap B_i)$ is relatively compact in $\text{pr}_1(B_i)$, $\text{pr}_2(H_{b',c'}(B_i) \cap B_j)$ is relatively compact in $\text{pr}_2(B_j)$, $H_{b',c'}$ maps the vertical boundary of B_i outside the closure of B_j , and $H_{b',c'}^{-1}$ maps the horizontal boundary of B_j outside the closure of B_i .

For any (b', c') in this region, we will show explicitly how $H_{b',c'} : B_i \xrightarrow{\times} B_j$ is realized as a crossed mapping. Let $W_1 = B_i \cap H_{b',c'}^{-1}(B_j)$. Let $W_2 = H_{b',c'}(W_1) = H_{b',c'}(B_i) \cap B_j$. Let $U_1' = \pi_1(W_1) = \pi_1(B_i \cap H_{b',c'}^{-1}(B_j))$. Let $V_2' = \pi_2(W_2) = \pi_2(H_{b',c'}(B_i) \cap B_j)$. We've already shown that U_1' is relatively compact in Δ_i and V_2' is relatively compact in $D(0, R_c)$. $H_{b',c'} : W_1 \rightarrow W_2$ is a holomorphic isomorphism.

Pick any $y \in D(0, R_c)$. Take any compact set $K_1 \subset \Delta_j$. Then K_1 is closed and there is some annulus A_1 that separates K_1 from the boundary of Δ_j . Because $H_{b',c'}$

maps the vertical boundary of B_1 outside B_2 , then $\text{pr}_1(H_{b',c'}(W_1 \cap (\Delta_i \times \{y\}))) = \Delta_j$. Call the projection from $H_{b',c'}(W_1 \cap (\Delta_i \times \{y\}))$ to its first coordinate ρ_1 . ρ_1^{-1} maps K_1 and A_1 to the disk $H_{b',c'}(W_1 \cap (\Delta_i \times \{y\}))$, with $\rho_1^{-1}(A_1)$ separating $\rho_1^{-1}(K_1)$ from the boundary. Then $H_{b',c'}^{-1}(\rho_1^{-1}(A_1))$ separates $H_{b',c'}^{-1}(\rho_1^{-1}(K_1))$ from the boundary of $W_1 \cap (\Delta_i \times \{y\})$. $H_{b',c'}^{-1}(\rho_1^{-1}(K_1))$ is closed because it is the inverse image of a closed set under a continuous map. Hence $H_{b',c'}^{-1}(\rho_1^{-1}(K_1))$ is compact in $W_1 \cap (\Delta_i \times \{y\})$. This implies that $\text{pr}_1 \circ H_{b',c'}|_{W_1 \cap (\Delta_i \times \{y\})} : W_1 \cap (\Delta_i \times \{y\}) \rightarrow \Delta_j$ is proper. This map is, in fact, an isomorphism.

Pick any $x \in \Delta_j$. Take any compact set $K_2 \subset D(0, R_c)$. Then K_2 is closed and there is some annulus A_2 that separates K_2 from the boundary of $D(0, R_c)$. Because $H_{b',c'}^{-1}$ maps the horizontal boundary of B_2 outside B_1 , then $\text{pr}_2(H_{b',c'}^{-1}(W_2 \cap (\{x\} \times D(0, R_c)))) = D(0, R_c)$. Call the projection from $H_{b',c'}^{-1}(W_2 \cap (\{x\} \times D(0, R_c)))$ to its second coordinate ρ_2 . ρ_2^{-1} maps K_2 and A_2 to the disk $H_{b',c'}^{-1}(W_2 \cap (\{x\} \times D(0, R_c)))$, with $\rho_2^{-1}(A_2)$ separating $\rho_2^{-1}(K_2)$ from the boundary. Then $H_{b',c'}(\rho_2^{-1}(A_2))$ separates $H_{b',c'}(\rho_2^{-1}(K_2))$ from the boundary of $W_2 \cap (\{x\} \times D(0, R_c))$. $H_{b',c'}(\rho_2^{-1}(K_2))$ is closed because it is the inverse image of a closed set under a continuous map ($H_{b',c'}^{-1}$ is continuous). Hence $H_{b',c'}(\rho_2^{-1}(K_2))$ is compact in $W_2 \cap (\{x\} \times D(0, R_c))$. This implies that $\text{pr}_2 \circ H_{b',c'}^{-1}|_{W_2 \cap (\{x\} \times D(0, R_c))} : W_2 \cap (\{x\} \times D(0, R_c)) \rightarrow D(0, R_c)$ is proper. This map is, in fact, an isomorphism.

Hence $(W_1, W_2, H_{b',c'})$ is a degree one crossed mapping from $B_1 = \Delta_i \times D(0, R_c)$ to $B_2 = \Delta_j \times D(0, R_c)$. We have shown that $H_{b,c} : B_i \xrightarrow{\times} B_j$ is a one-crossed mapping in a small neighborhood around each $(0, c)$ with $c \in \text{int}(\mathcal{W})$, and the statement of the theorem follows. \square

Definition 6.13. Let $\mathcal{R}^{\mathcal{W}} = \left\{ (b, c) \mid c \in \mathcal{W} \text{ and } 0 < |b| < \varepsilon_c^{\mathcal{W}} \right\}$.

Lemma 6.14. Given any bi-itinerary \mathcal{I} adapted to Γ and any $(b, c) \in \mathcal{R}^{\mathcal{W}}$, there is exactly one point which has this itinerary under $H_{b,c}$ relative to the two-dimensional

puzzle pieces.

Proof. There is a one-crossed mapping between any two consecutive pairs of puzzle pieces in an itinerary adapted to Γ , so a bi-itinerary adapted to Γ gives a bi-infinite sequence of 1-crossed mappings. By [HOV94b], there is exactly one point which satisfies this bi-itinerary. \square

Definition 6.15. Let \mathcal{I} be a bi-itinerary adapted to Γ . Then for $(b, c) \in \mathcal{R}^W$, define $\Psi_{b,c}^W(\mathcal{I})$ to be the unique point with this bi-itinerary for the map $H_{b,c}$.

Definition 6.16. Define $\mathcal{X}_{b,c}^W = \Psi_{b,c}^W(\{\mathcal{I} \mid \mathcal{I} \text{ is a bi-itinerary adapted to } \Gamma\})$.

Theorem 6.17. For $(b, c) \in \mathcal{R}_{b,c}^W$, then $\mathcal{X}_{b,c}^W \subset J_{b,c}$.

Proof. It is clear that $\mathcal{X}_{b,c}^W \subset K_{b,c}$. We will show that arbitrarily close to any point of $\mathcal{X}_{b,c}^W$, there are points which escape to infinity in forwards and backwards time.

Fix $(b, c) \in \mathcal{R}_{b,c}^W$. Define

$$S^+ = \left\{ (x, y) \mid |x| \geq R_{b,c} \text{ and } |y| \leq \frac{|x|^2 - |c| - |x|}{|b|} \right\}$$

$$S^- = \left\{ (x, y) \mid |y| \geq R_{b,c} \text{ and } |x| \leq |y| \right\}$$

Some algebraic manipulation gives us that if $(x, y) \in H_{b,c}(S^+)$, then $|x| \geq |y| \geq R_{b,c}$ and hence $H_{b,c}(S^+) \subset V_{b,c}^+ \subset U_{b,c}^+$. Thus $S^+ \subset U_{b,c}^+$. It is also clear that $S^- = V_{b,c}^- \subset U_{b,c}^-$.

Choose $y_0 \in \mathbb{R}^+$. Let

$$r_+ = \frac{1 + \sqrt{1 + 4(|c| + |b|y_0)}}{2}$$

$$r_- = y_0$$

For large enough y_0 , then $S^+ \cap (\mathbb{C} \times \{y_0\})$ is a plane with a disk of radius r_+ cut out of it and $S^- \cap (\mathbb{C} \times \{y_0\})$ is a disk of radius r_- . Also for large enough y_0 , then $r_- > r_+$, and in fact the ratio r_-/r_+ goes to infinity as y_0 increases. For large enough y_0 , we see that $S^+ \cap S^- \cap (\mathbb{C} \times \{y_0\})$ is an annulus entirely in $U_{b,c}$ with a modulus as large as we please.

f_c is conjugate near infinity to $x \mapsto x^2$ with a conjugating Böttcher map that is tangent to the identity at infinity. Let C_g be the level curve where the Green's function is equal to g . Because of the tangency of the Böttcher map at infinity, then C_g approximates a circle as $g \rightarrow \infty$ and there must exist some $y_0 > R_{b,c}$ and g so that $C_g \subset \text{int}(\pi_1(S^+ \cap S^- \cap (\mathbb{C} \times \{y_0\})))$, where π_1 is projection to the first coordinate.

The choice to make the one-dimensional fattened puzzle pieces of f_c have an outer boundary where the Green's function is 1 was arbitrary. We can choose for the outer boundary the level curve C_g . The choice for the vertical component of the two-dimensional fattened puzzle pieces to have radius R_c was also arbitrary. We could have chosen any disk that contains all of the one-dimensional fattened puzzle pieces. Let us choose for the vertical component of the two-dimensional fattened puzzle pieces the disk $D(0, y_0)$. Notice that we ensured that C_g is relatively compact in $D(0, y_0)$.

The entire vertical portion of the boundary of each two-dimensional puzzle piece is contained in the closed set S^+ . Because for any $y \in \overline{\mathbb{D}(0, y_0)}$, $C_g \subset \text{int}(\pi_1(S^+ \cap (\mathbb{C} \times \{y\})))$ and C_g is compact, then there exists a finite distance T_h so that the Poincaré distance in any unstable manifold in any two-dimensional puzzle piece between any point of $\mathcal{X}_{b,c}^W$ and S^+ is less than T_h .¹

¹This depends on the fact that the set all points of $\mathcal{X}_{b,c}^W$ whose itinerary at the 0th index is the fattened puzzle piece B_i is relatively compact in B_i . This property is due to the fact that whenever $\Pi_i \rightarrow \Pi_j$ is in Γ , then we have a 1-crossed mapping $H_{b,c} : B_i \rightarrow B_j$, and the corresponding V_2' (see Definition 6.1) for this crossed mapping is relatively compact in the corresponding V_2 . Also there are finitely many arrows. We also depends on the fact that the space of vertically-bounded horizontal-like disks is compact, and we know that the unstable manifolds occupy a relatively compact subset of the disk when projected to their second coordinate (see the proof of Theorem 6.6 for details).

Choose any $\varepsilon > 0$. There is a uniform expansion $\lambda_h > 1$ on the unstable manifolds. Let n be an integer larger than $\log_{\lambda_h}(T_h/\varepsilon)$. To realize a point of $U_{b,c}^+$ which is ε -close to any $x \in \mathcal{X}_{b,c}^W$, we need only to look in the two-dimensional puzzle piece B_i which is at index n in the itinerary of x . B_i contains a point $u \in U_{b,c}^+$ which is in the unstable manifold of $H_{b,c}^{on}(x)$ and is at distance at most T_h from $H_{b,c}^{on}(x)$. Hence x is at most a distance of ε from $H_{b,c}^{o-n}(u) \in U_{b,c}^+$.

The entire horizontal portion of the boundary of every two-dimensional puzzle piece is entirely contained within S^- , and in fact, there is some finite distance T_v so that for every x in the closure of any of the one-dimensional fattened puzzle pieces, then the Poincaré distance in any stable manifold in any two-dimensional puzzle piece between any point of $\mathcal{X}_{b,c}^W$ and S^- is less than T_v .

As we did for $U_{b,c}^+$, using the uniform contraction on stable manifolds, one can show that points of $U_{b,c}^-$ are arbitrarily close to every point of $\mathcal{X}_{b,c}^W$.

Hence we see that $\mathcal{X}_{b,c}^W \subset K_{b,c} \cap \overline{U_{b,c}^-} \cap \overline{U_{b,c}^+}$. □

6.4 Continuity of $\mathcal{X}_{b,c}^W$

Lemma 6.18. *If \mathcal{I}_1 and \mathcal{I}_2 are distinct bi-itineraries adapted to Γ , then $\Psi_{b,c}^W(\mathcal{I}_1) \neq \Psi_{b,c}^W(\mathcal{I}_2)$.*

Proof. We will give a proof by contradiction. Let $x_0 = \Psi_{b,c}^W(\mathcal{I}_1) = \Psi_{b,c}^W(\mathcal{I}_2)$ with $\mathcal{I}_1 \neq \mathcal{I}_2$. Let $x_i = H_{b,c}^{oi}(x_0)$. \mathcal{I}_1 and \mathcal{I}_2 differ at some index n . Thus x_n is in the intersection of two distinct two-dimensional fattened puzzle pieces which must be of the form $D_j \times D(0, R_c)$, where D_j is one of the small one-dimensional disks around a point of the

repelling cycle of f_c associated with the wake \mathcal{W} and $D(0, R_c)$ is a disk as defined earlier.

So \mathcal{I}_1 and \mathcal{I}_2 must differ for every index $m > n$. For indexes after n , one of these must consist of only open puzzle pieces, and these puzzle pieces must be adjacent to the successive points in the periodic orbit. Hence, one of \mathcal{I}_1 and \mathcal{I}_2 has a degenerate tail and is not adapted to Γ . \square

Corollary 6.19. $\mathcal{X}_{b,c}^{\mathcal{W}}$ is isomorphic to the space of bi-itineraries adapted to Γ .

Proof. Since $\mathcal{X}_{b,c}^{\mathcal{W}}$ is the image under $\Psi_{b,c}^{\mathcal{W}}$ of all bi-itineraries adapted to Γ , and we know this map is injective. \square

Theorem 6.20. $\mathcal{X}_{b,c}^{\mathcal{W}}$ is continuous in b and c for $(b, c) \in \mathcal{R}^{\mathcal{W}}$.

Proof. Every point of $\mathcal{X}_{b,c}^{\mathcal{W}}$ corresponds to a bi-itinerary \mathcal{I} of puzzle pieces adapted to Γ . We will show that $\Psi_{b,c}^{\mathcal{W}}(\mathcal{I})$ is continuous in b and c .

Choose some point $(x, y) \in \mathcal{X}_{b,c}^{\mathcal{W}}$ with an itinerary of two-dimensional puzzle pieces $(\dots, B_{i-1}, B_{i_0}, B_{i_1}, \dots)$ adapted to Γ (where every B_{i_n} is a two-dimensional fattened puzzle piece for the map $H_{b,c}$). Let V be an open subset of $\mathcal{R}^{\mathcal{W}}$ that contains (b, c) such that all of the 1-crossed mappings between the puzzle pieces for the parameters (b, c) are still 1-crossed mappings under $H_{b',c'}$. Let V' be a relatively compact open subset of V which contains (b, c) and is also bounded. It is clear that such an open sets exist. Choose $(b', c') \in V'$.

We have a bi-infinite sequence of 1-crossed mappings for $H_{b',c'}$. Thus, there is vertical-like topological disk $W_{b',c'}^S \subset B_{i_0}$ of points which have a forward itinerary $(B_{i_0}, B_{i_1}, \dots)$ under the dynamics of $H_{b',c'}$. There is also a horizontal-like topological disk $W_{b',c'}^U \subset B_{i_0}$ of points which have a backwards itinerary $(\dots, B_{i-1}, B_{i_0})$ under $H_{b',c'}$.

There is a unique point $(x', y') \in W_{b',c'}^S \cap W_{b',c'}^U$ with the same bi-itinerary under $H_{b',c'}$ as (x, y) has under $H_{b,c}$. We will show that these disks and their intersection cannot be far away from (x, y) .

Let $W_{b,c,j}^U$ be the unstable manifold in B_j for the map $H_{b,c}$. Similarly let $W_{b',c',j}^U$ be the unstable manifold in B_j for the map $H_{b',c'}$. Define $D_{j,k} = H_{b',c'}^{\circ k}(W_{b,c,-j}^U)$, which is the forward image under $H_{b',c'}$ of an unstable manifold of $H_{b,c}$. This is analogous to mapping backwards by $H_{b,c}^{-1}$ and then forwards by $H_{b',c'}$ as if we were attempting to conjugate the two maps by invoking the standard limit construction of the conjugating map.

Every $D_{j,k}$ is a horizontal-like disk in $B_{i_{k-j}}$. Also $W_{b',c',0}^U = \lim_{j \rightarrow \infty} D_{j,j}$ in the metric we defined for horizontal disks. Because $H_{b,c}$ is a Lipschitz function of b and c on compact subsets of parameter space and because the Euclidean metric is equivalent to the Poincaré metric on B_{i_j} on compact subsets of the latter, then the distances between $D_{j,0}$ and $D_{j+1,1}$ are uniformly bounded by some $q_0 \cdot \|(b, c) - (b', c')\|$ for all $(b', c') \in V'$. Mapping forward contracts distances between horizontal-like disks (uniformly so on V'), so there is some $q_1 < 1$ so that $d(D_{j,k+1}, D_{j+1,k+2}) < q_1 \cdot d(D_{j,k}, D_{j+1,k+1})$. Hence $d(D_{j,j}, D_{j+1,j+1}) < q_1^j q_0 \cdot \|(b, c) - (b', c')\|$ and so

$$d(W_{b,c,0}^U, W_{b',c',0}^U) < q_0 / (1 - q_1) \cdot \|(b, c) - (b', c')\|$$

An analogous argument for stable manifolds gives:

$$d(W_{b,c,0}^S, W_{b',c',0}^S) < q_0' / (1 - q_1') \cdot \|(b, c) - (b', c')\|$$

The two disks $W_{b',c',0}^U$ and $W_{b',c',0}^S$ have a single intersection point (x', y') which is the unique point with bi-itinerary $(\dots, B_{i_{-1}}, B_{i_0}, B_{i_1}, \dots)$ under the map $H_{b',c'}$. So $\Psi_{b',c'}(\mathcal{I}) = (x', y')$. Let $d_{B_{i_0}}$ be the Kobayashi metric in B_{i_0} . The geometry of the situation forces:

$$d_{B_{i_0}}((x, y), (x', y')) \leq \sqrt{2} \cdot d(W_{b,c,0}^U, W_{b',c',0}^U) + \sqrt{2} \cdot d(W_{b,c,0}^S, W_{b',c',0}^S)$$

Let $q_0'' = \max\{q_0, q_0'\}$ and $q_1'' = \max\{q_1, q_1'\}$. q_0'' and q_1'' do not depend on (b', c') . We get for all $(b', c') \in V'$ the inequality:

$$d_{B_{i_0}}((x, y), (x', y')) \leq \frac{2\sqrt{2} \cdot q_0''}{1 - q_1''} \|(b, c) - (b', c')\|$$

Because the Kobayashi metric is equivalent to the Euclidean metric on compact subsets, this shows that $\Psi_{b,c}(\mathcal{I})$ is locally Lipschitz and hence a continuous function of $(b, c) \in \mathcal{R}^W$. \square

6.5 Coding $\mathcal{X}_{b,c}^W$

Theorem 6.21.

$$\lim_{b \rightarrow 0} \mathcal{X}_{b,c}^W = \left\{ (x, y) \mid y \in f_c(\mathcal{X}_c^W) \text{ and } f_c(y) = x \right\}$$

In particular:

$$\text{pr}_1\left(\lim_{b \rightarrow 0} \mathcal{X}_{b,c}^W\right) = \text{pr}_2\left(\lim_{b \rightarrow 0} \mathcal{X}_{b,c}^W\right) = f_c(\mathcal{X}_c^W)$$

And points with bi-itineraries adapted to $\Gamma (\dots, B_{i-1}, B_{i_0}, B_{i_1}, \dots)$ in $X_{b,c}^W$ will limit as $b \rightarrow 0$ and then project to a point of \mathcal{X}_c^W with itinerary $(\Pi_{i_0}, \Pi_{i_1}, \dots)$.

Proof. Take any bi-itinerary $\mathcal{I} = (\dots, B_{i-1}, B_{i_0}, B_{i_1}, \dots)$. We will show that $\Psi_{b,c}^W(\mathcal{I})$ has a continuous extension to $\{0\} \times \text{int}(\mathcal{W})$, which is essentially a one-dimensional wake living inside of parameter space for Hénon mappings.

Choose $c \in \text{int}(\mathcal{W})$. Let M be larger than the radius of the Julia sets in some neighborhood of $(0, c)$. The first coordinate of orbits of $\mathcal{X}_{b,c}^W$ by $H_{b,c}$ in this neighborhood are $(M \cdot b)$ -pseudo-orbits of f_c . Hence, because the one-dimensional fattened puzzle pieces are open (and f_c 's derivative is bounded on compact subsets), then the smaller b is, the longer that $\Psi_{b,c}^W(\mathcal{I})$ and $\text{pr}_1(\Psi_{b,c}^W(\mathcal{I}))$ will have corresponding forward itineraries under

the actions of $H_{b,c}$ and f_c , respectively. Hence $\text{pr}_1(\lim_{b \rightarrow 0} \Psi_{b,c}^W(\mathcal{I}))$ will have an itinerary of $(\Pi_{i_0}, \Pi_{i_1}, \dots)$. Therefore, it must be the unique point of \mathcal{X}_c^W with this itinerary. The rest of the statement of the theorem follows easily. \square

Theorem 6.22. $(\mathcal{X}_{b,c}^W, H_{b,c}) \cong \varprojlim (\mathcal{X}_c^W, f_c)$

Proof. (\mathcal{X}_c^W, f_c) is isomorphic to one-sided itineraries adapted to Γ . $(\mathcal{X}_{b,c}^W, H_{b,c})$ is isomorphic to bi-itineraries adapted to Γ . \square

The union of the non-critical one-dimensional puzzle pieces has two connected components. Non-critical one dimensional puzzle pieces can be coded by which side of the critical puzzle piece they lie on. The two-dimensional puzzle pieces inherit this coding, so points in $\mathcal{X}_{b,c}^W$ have two-symbol codings coming from their two-dimensional puzzle piece itineraries.

In one dimension, Julia sets taken from the exterior of the Mandelbrot set have a two-symbol coding derived from cutting up the plane along the inverse image of the dynamical ray that hits the critical value. If, additionally, we remove from our consideration \mathbb{R}^+ , then we can unambiguously label the side of this cutting which contains the β -fixed point with an A and the side with the α -fixed point with a B .

Points in $J_{b,c}$ for $(b,c) \in \mathcal{HOV}$ also have a two-symbol coding arising from their realization as the inverse limit system of a one-dimensional Julia set taken from the exterior of the Mandelbrot set. If we remove the hypersurface $\mathbb{C} \times \mathbb{R}^+$, then on the negative real axis we can unambiguously label the region where x is positive with A and where x is negative with B and extend this coding unambiguously to $\mathcal{HOV} \setminus \mathbb{R}^+ \times \mathbb{C}$ continuously.

Inside of $\mathcal{HOV} \cap \mathcal{R}^W$, these two codings agree on \mathcal{X}_c^W . To see this, note that the dynamical ray that hits the critical value must lie inside the critical value puzzle piece.

Therefore, its inverse image must lie inside the critical puzzle piece, so for points in $\mathcal{X}_c^{\mathcal{W}}$, the two codings are identical, because $\mathcal{X}_c^{\mathcal{W}}$ has no points in the critical puzzle piece.

Theorem 6.23. *A point of $\mathcal{X}_{b,c}^{\mathcal{W}}$ is determined by its two-sided \mathcal{W} -itinerary.*

Proof. A bi-infinite itinerary on two symbols gives a point in the inverse limit system of $\mathcal{X}_c^{\mathcal{W}}$, which is isomorphic to $\mathcal{X}_{b,c}^{\mathcal{W}}$. □

We see here that the itinerary relative to puzzle pieces has much redundant information. It is possible to identify points using a far more coarse partition of space.

While it is true that there is not a well-defined two-symbol encoding on the whole Julia set throughout $\mathcal{R}^{\mathcal{W}}$, we can give a two-symbol coding to the points of $\mathcal{X}_{b,c}^{\mathcal{W}}$ throughout $\mathcal{R}^{\mathcal{W}}$. Theorems 6.22 and 5.6 together guarantee that the same set of two-symbol codings is realized by $\mathcal{X}_{b,c}^{\mathcal{W}}$ everywhere throughout $\mathcal{R}^{\mathcal{W}}$. Hence everywhere inside $\mathcal{R}^{\mathcal{W}}$, $\mathcal{X}_{b,c}^{\mathcal{W}}$ has exactly one point with a particular bi-infinite AB -coding if and only if that coding has no substring equal to the characteristic kneading sequence of a wake conspicuous to \mathcal{W} .

The reason we need multiple codings is that \mathcal{W} -itineraries are valid in \mathcal{HOV} , but not in $\mathcal{R}^{\mathcal{W}}$, but paths adapted to Γ give a coding in $\mathcal{R}^{\mathcal{W}}$, but not in \mathcal{HOV} .

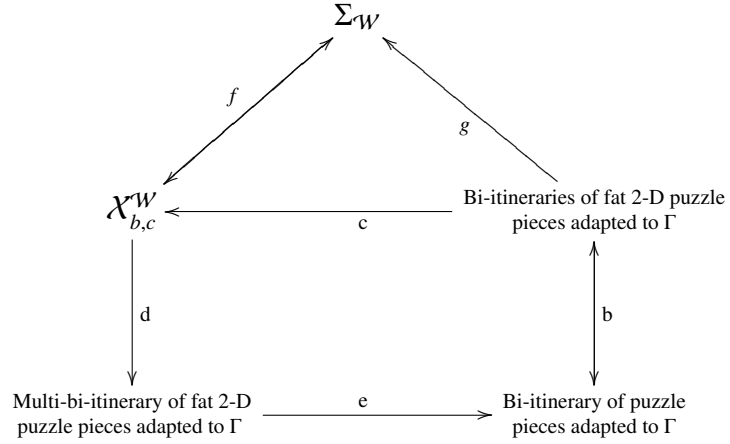
Definition 6.24. *Let $\Sigma_{\mathcal{W}}$ be the set of two-symbol \mathcal{W} -bi-itineraries realized by points of $\mathcal{X}_{b,c}^{\mathcal{W}}$.*

Theorem 6.25. *$\Sigma_{\mathcal{W}}$ is a subshift of finite type where the forbidden strings are the characteristic kneading sequences for the wakes conspicuous to \mathcal{W} .*

Proof. Theorem 6.22 and Corollary 5.24. □

6.6 Relationships Between Points and Itineraries

The following commutative diagram illustrates relationships between points of $\mathcal{X}_{b,c}^W$, \mathcal{W} -itineraries, and itineraries and multi-itineraries relative to the fattened puzzle pieces.



We describe these maps:

- b) The correspondence between puzzle pieces and their 2-D counterparts gives a trivial correspondence between bi-infinite sequences adapted to Γ .
- c) An itinerary of 2-D puzzle pieces gives a unique point of $\mathcal{X}_{b,c}^W$ using crossed mappings.
- d) Points of $\mathcal{X}_{b,c}^W$ have multi-itineraries with respect to the 2-D puzzle pieces.
- e) Theorem 5.9.
- f) $\mathcal{X}_{b,c}^W \rightarrow \Sigma_W$ is given by itineraries relative to the unions of the two-dimensional puzzle pieces on each side of the critical puzzle piece. $\Sigma_W \rightarrow \mathcal{X}_{b,c}^W$ is given by Theorem 6.23.
- g) Two-dimensional puzzle pieces are on one side or the other of the critical puzzle piece.

CHAPTER 7

MONODROMY INVARIANT

Definition 7.1. Let $\mathcal{U}^W = \mathcal{HOV} \cup \mathcal{R}^W \setminus (\mathbb{C} \times \mathbb{R}^+)$.

We are defining \mathcal{U}^W to be the region where we either know we have a horseshoe by [HOV94a] or we know that we have the structurally stable sparse set $\mathcal{X}_{b,c}^W$, but we are disallowing the class of loops homotopic to γ_c by removing the hypersurface $\mathbb{C} \times \mathbb{R}^+$. The reason for disallowing this is that γ_c has the nontrivial action on the Julia set in \mathcal{HOV} of permuting the two symbols. We wish to isolate a region of parameter space where there is a trivial monodromy action on a particular subset of the Julia set.

Points of the Julia set can be followed continuously through \mathcal{HOV} . $\mathcal{X}_{b,c}^W$ is a subset of the Julia set for $(b, c) \in \mathcal{R}_{b,c}^W \cap \mathcal{HOV}$. These points can be followed smoothly throughout \mathcal{U}^W .

Definition 7.2. Define $\mathcal{Y}_{b,c}^W = \mathcal{X}_{b,c}^W$ for $(b, c) \in \mathcal{R}^W$ and continuously extend $\mathcal{Y}_{b,c}^W \subset J_{b,c}$ for $(b, c) \in \mathcal{U}^W$.

We can extend $\mathcal{Y}_{b,c}^W$ because it is part of the Julia set, and the Julia set can be followed continuously inside of \mathcal{HOV} . Also this extension is well-defined because $\mathcal{Y}_{b,c}^W$ has a trivial monodromy around γ_b , the loop that generates the fundamental group of \mathcal{U}^W .

Lemma 7.3. If we fix a wake \mathcal{W} , the \mathcal{W} -itineraries realized by $\mathcal{Y}_{b,c}^W$ are constant for $(b, c) \in \mathcal{U}^W$.

Proof. They are constant in \mathcal{R}^W because the \mathcal{W} -itineraries of points in $\mathcal{X}_{b,c}^W$ are constant in this region. In \mathcal{HOV} , points of J are identified with their itinerary and move continuously with respect to the parameters, and the A and B regions do not interchange in \mathcal{U}^W . □

Choose any class of loops $\gamma \in \Pi_1(\mathcal{U}^W \cap \mathcal{H}^C, p_0)$, where $p_0 = (b_0, c_0) \in \mathcal{H}^{\mathbb{R}}$ is a parameter value for a real horseshoe map.

Lemma 7.4. γ has a trivial monodromy action on \mathcal{Y}_{b_0, c_0}^W .

Proof. $\mathcal{Y}_{b,c}^W$ is structurally stable in \mathcal{U}^W . The fundamental group of \mathcal{U}^W is generated by γ_b , which has a trivial monodromy action. \square

The monodromy action $\rho(\gamma)$ gives a continuous automorphism $\rho(\gamma)$ of the full 2-shift.

Theorem 7.5. If $\alpha \in \Sigma_2$ does not contain as a substring the characteristic kneading sequence of any of the finitely many wakes conspicuous to \mathcal{W} , then $\rho(\gamma)$ acts trivially on α .

Proof. For any $(b, c) \in \mathcal{U}^W$, the set $\mathcal{Y}_{b,c}^W$ is precisely the set of points of $J_{b,c}$ whose itinerary does not include the characteristic kneading sequence of any wake conspicuous to \mathcal{W} as a substring. Since γ has a trivial monodromy action on \mathcal{Y}_{b_0, c_0}^W , then $\rho(\gamma)$ must act trivially on any point which does not contain as a substring the characteristic kneading sequence of any wake conspicuous to \mathcal{W} . \square

A somewhat stronger statement than theorem 7.5 is actually true. The points in $\mathcal{Y}_{b,c}^W$ exist and are a subset of J throughout U^W whether or not the parameter values are inside the horseshoe locus. We can thus follow some points of J as we pass through non-hyperbolic parameter values.

CHAPTER 8

MONODROMY CONJECTURES

In order to describe our conjectures for the monodromy action, we will need some background and vocabulary arising from Koch’s computer-assisted investigation of Hénon parameter space ([Koc05] and [Koc07]).

8.1 Speculative Structure of Hénon Parameter Space

When the Jacobian of a quadratic Hénon mapping is zero, the first co-ordinate of the mapping reduces to the one-dimensional quadratic mapping. Koch discovered using Karl Papadantonakis’ program SaddleDrop that when taking c -plane slices of complex Hénon parameter space, as one moves away from the degenerate $b = 0$ case, then different renormalized Mandelbrot sets strictly contained in the Mandelbrot set break off and move in different directions. Moreover, she found that the direction they move in is tied to the kneading sequence of the polynomials whence they originated in the Mandelbrot set. Specifically, the direction depends most on the digits immediately preceding \star , or in other words at the end of the finite representation of kneading sequences. Renormalized Mandelbrot sets with a kneading sequence ending in an A generally move in the direction in the c -plane that the parameter value b is perturbed in, and those with a kneading sequence ending in B generally move in the opposite direction as b does.

As one perturbs b away from 0, then in c -plane slices, the Mandelbrot set seems to split into two different “herds”. One contains all renormalized Mandelbrot sets that have a kneading sequence ending in A and the other those that end in B . As one perturbs b even farther away from zero, then each of these herds split up based on the digit in the kneading sequences second from the end. Then these split by the third to last

digit in the kneading sequences. This dyadic splitting phenomenon has been witnessed experimentally using SaddleDrop to a depth of 5 splits. Misiurewicz points split into a Cantor set worth of points and appear in every herd. This is in direct contrast to the hyperbolic components, which follow only one herd. This is because in parameter space, the boundary of the region where there is an attracting periodic point is the solution of an algebraic curve and thus can only intersect a plane in finitely many points.

As noted earlier, the herd of Mandelbrot sets with a kneading sequence ending in A moves in the general direction that b does, and the herd of Mandelbrot sets with a kneading sequences ending in B moves in essentially the opposite direction. The herd of Mandelbrot sets with kneading sequence ending in AA moves a bit farther in the direction of b than does the herd with sequences ending in BA . Additionally, the two herds associated with AB and BB also move differentially, but the presence of the first B in the kneading sequence flips the direction that the hierarchically lower-level herds move in, so the BB herd is perturbed slightly more in the direction of a than is the AB herd. If one perturbs b slightly in the positive real direction, reading from left to right, one would expect to see the eight herds obtained after three splittings associated with kneading sequences in the following order: AAB , BAB , BBB , ABB , ABA , BBA , BAA , AAA .

8.2 Monodromy Conjecture

In order to describe our conjecture for the monodromy action, we will need to develop a language for conveniently describing a class of continuous automorphisms of the full 2-shift that commutes with the shift operator.

Definition 8.1. *A compound marker endomorphism is a mapping on Σ_2 described by a*

finite collection of finite strings on two symbols as well as a \star . Each string has a single \star . We use this finite collection of strings to define a mapping on Σ_2 by the following algorithm: If the sequence matches any of the strings at any location (where the \star can match anything), then the image of this sequence will have the opposite letter in the position that matched \star . If a letter at a position does not match any string at the \star position, it is left unchanged.

A compound marker endomorphism is always a continuous endomorphism of Σ_2 that commutes with the shift. It is not always bijective, though.

Definition 8.2. *If a compound marker endomorphism is an automorphism, we call it a compound marker automorphism.*

Compound marker automorphisms are a generalization of marker automorphisms. Interestingly enough, there are compound marker automorphisms whose component strings are not individually compound marker automorphisms themselves. The author knows of no automorphism of the full 2-shift that is not a composition of compound marker automorphisms and the shift. It would be of great interest to either prove or disprove that these generate the automorphisms of the full two-shift.

We conjecture the following on the basis of computer experimentation:

Conjecture 8.3. *Suppose that $\gamma \in \Pi_1(\mathcal{H}_0^{\mathbb{C}}, (b_0, c_0))$ is such that γ winds around a herd corresponding to a given string x , and this herd comes from a wake \mathcal{W}_1 with conspicuous sub-wakes $\mathcal{W}_2, \dots, \mathcal{W}_n$. Let $y_i = K(\mathcal{W}_i)$. Then $\rho(\gamma)$ is the following compound marker endomorphism:*

$$x \star y_1, \dots, x \star y_n$$

Note that in this conjecture, another way to view the y_i 's is as the initial segments of

the kneading sequences of polynomials in the region of the Mandelbrot set whence the herds originated.

If Conjecture 8.3 were true, then no point of J could be permuted by a loop in $\mathcal{U}^{\mathcal{W}}$ unless that point had in its itinerary the characteristic kneading sequence of \mathcal{W} or that of some wake contained in \mathcal{W} . That is what we proved in Chapter 7.

As the herds split and move away from each other, hyperbolic components from the Mandelbrot set will follow one herd, and create a gap in the herd that they do not follow. These gaps give rise to loops in the Horseshoe locus. It is unknown if all loops in the horseshoe locus are generated by going through these gaps (along with the two generators from \mathcal{HOV}).

We have another conjecture, which we also make on the basis of computer experimentation:

Conjecture 8.4. *If the compound marker endomorphism predicted by Conjecture 8.3 is not an automorphism, then no loop could wind around the herds in question and only those herds while staying inside the horseshoe locus.*

We are conjecturing a connection between the algebraic structure of automorphisms of the full 2-shift and the topological structure of the horseshoe locus in parameter space of Hénon mappings.

CHAPTER 9

EXAMPLES

We will conclude with a few examples which demonstrate various aspects of Theorem 7.5, Conjecture 8.3, and Conjecture 8.4. All of the following pictures of parameter space were created using the computer program SaddleDrop, written by Karl Papadantonakis. The program is available at the website <http://www.math.cornell.edu/dynamics/> and is an accompaniment to [HP00].

Generically for quadratic Hénon mappings, there are two fixed points, and the map has a larger eigenvalue (in absolute value) at one of these fixed points. SaddleDrop displays a parameterization of the unstable manifold at this fixed point, and allows the user to select critical points of G^+ restricted to this unstable manifold. SaddleDrop then smoothly follows these points throughout parameter space wherever it is possible to continue them. SaddleDrop draws planar slices of parameter space and colors points according to the value of G^+ at the identified critical points. In the following pictures, we follow the 16 most prominent critical points. There is no good way to chromatically represent the 16 rates of escape in one picture, but SaddleDrop gives us three ways to combine this information to color points. In the following pictures, the rate of escape of the slowest escaping critical point is represented as a color at that pixel. This “slowest escaping” way of coloring parameter space colors non-hyperbolic parameter values in darker hues. We do not catch all non-hyperbolic points with our 16 test critical points, but at this resolution, the pictures do not change significantly with the addition of more critical points.

Definition 9.1. *We say that a marker string matches a bi-infinite sequence if some shift of the marker string is such that in each position where the marker string has an A or a B, then the symbol in the marker string matches the symbol in the bi-infinite sequence.*

We say that the marker string matches the sequence at the position where the \star symbol is.

Definition 9.2. *We say that a marker string matches another marker string at a given position if a shift of the first string is such that in each position where both marker strings have either an A or a B, then the two marker strings have the same symbol. We say that the first marker string matches the second marker string at the position on the second marker string where the \star symbol is.*

9.1 $B \star BAA$

In the following pictures of c -plane slices of Hénon parameter space, we will perturb the Jacobian in the positive imaginary direction, and we will see that the “tail” of the Mandelbrot set splits into two parts and that the airplane follows the top part (Figures 9.1 to 9.7). The Jacobian in this sequence of pictures goes from 0 to $.05i$.

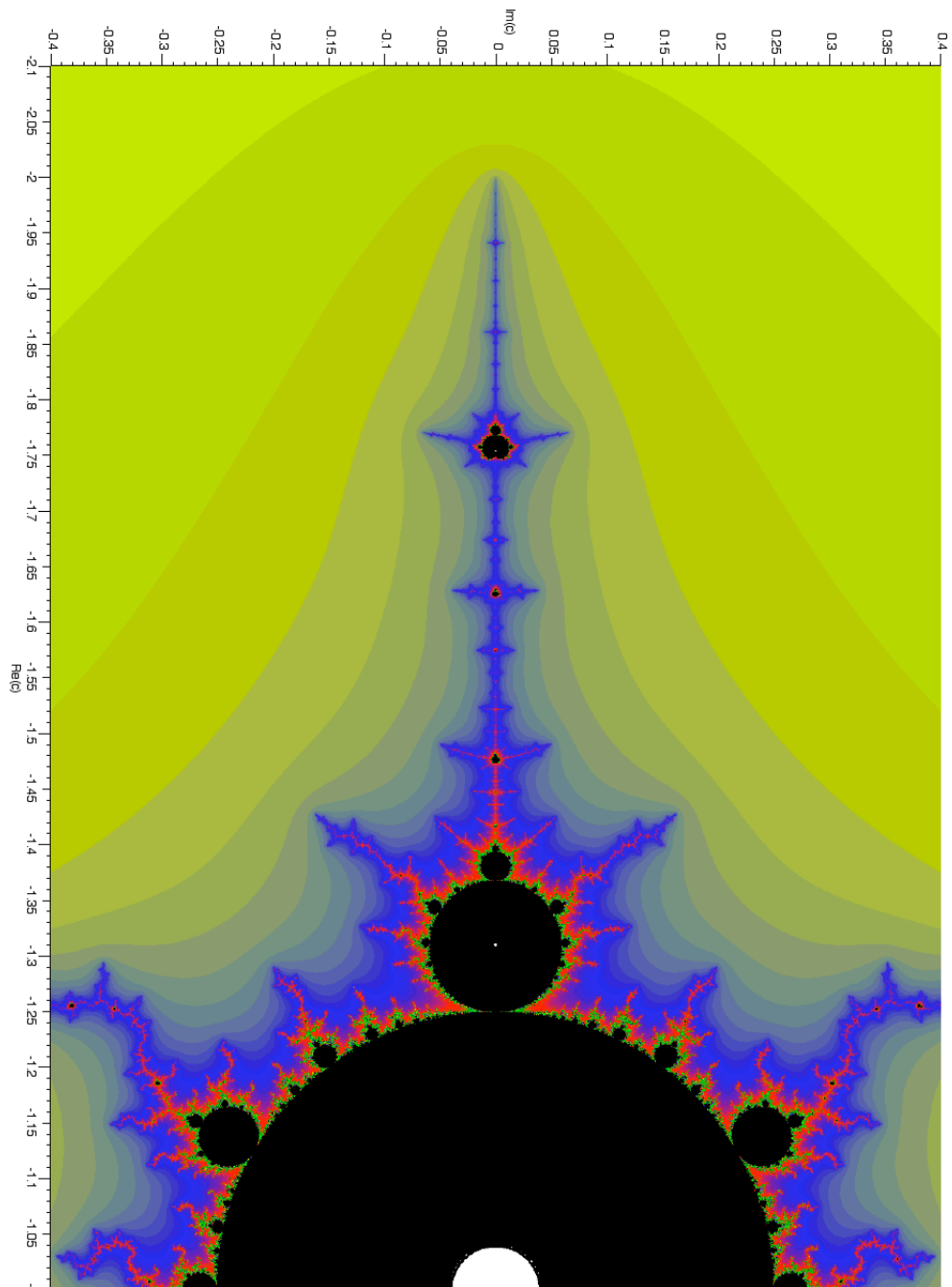


Figure 9.1: Parameter slice with $b = 0$

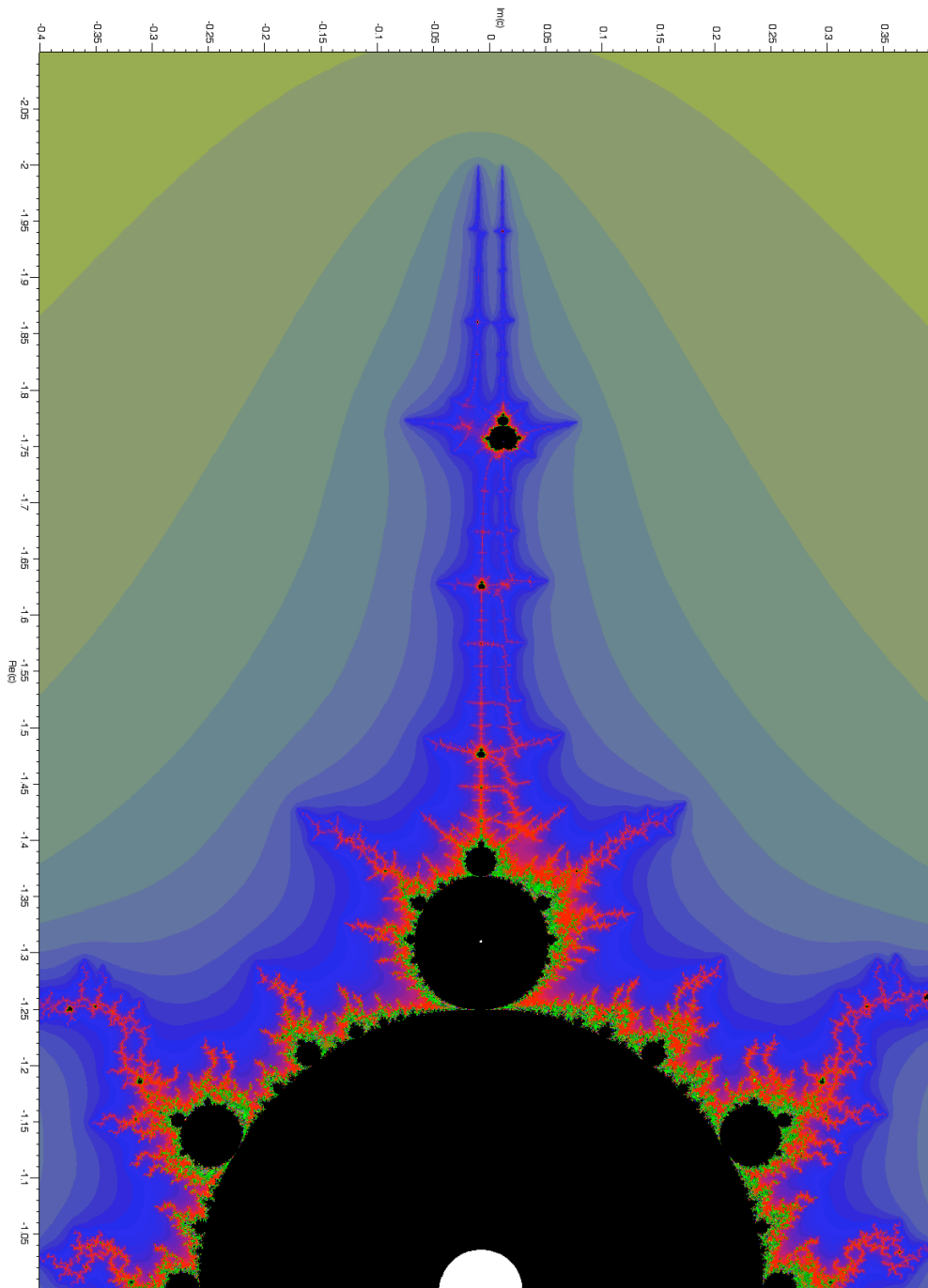


Figure 9.2: Parameter slice with $b = 0.005i$

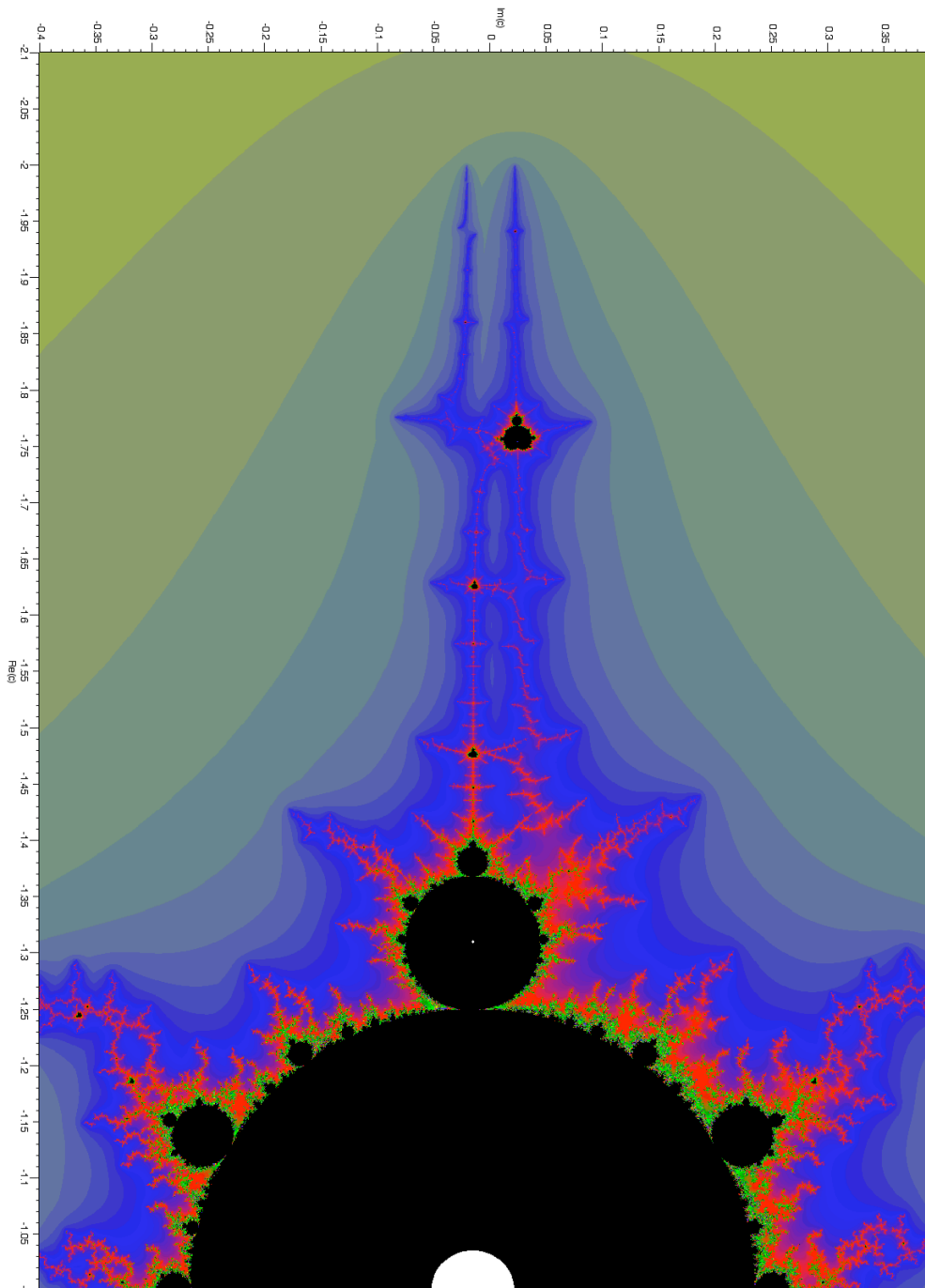


Figure 9.3: Parameter slice with $b = 0.01i$

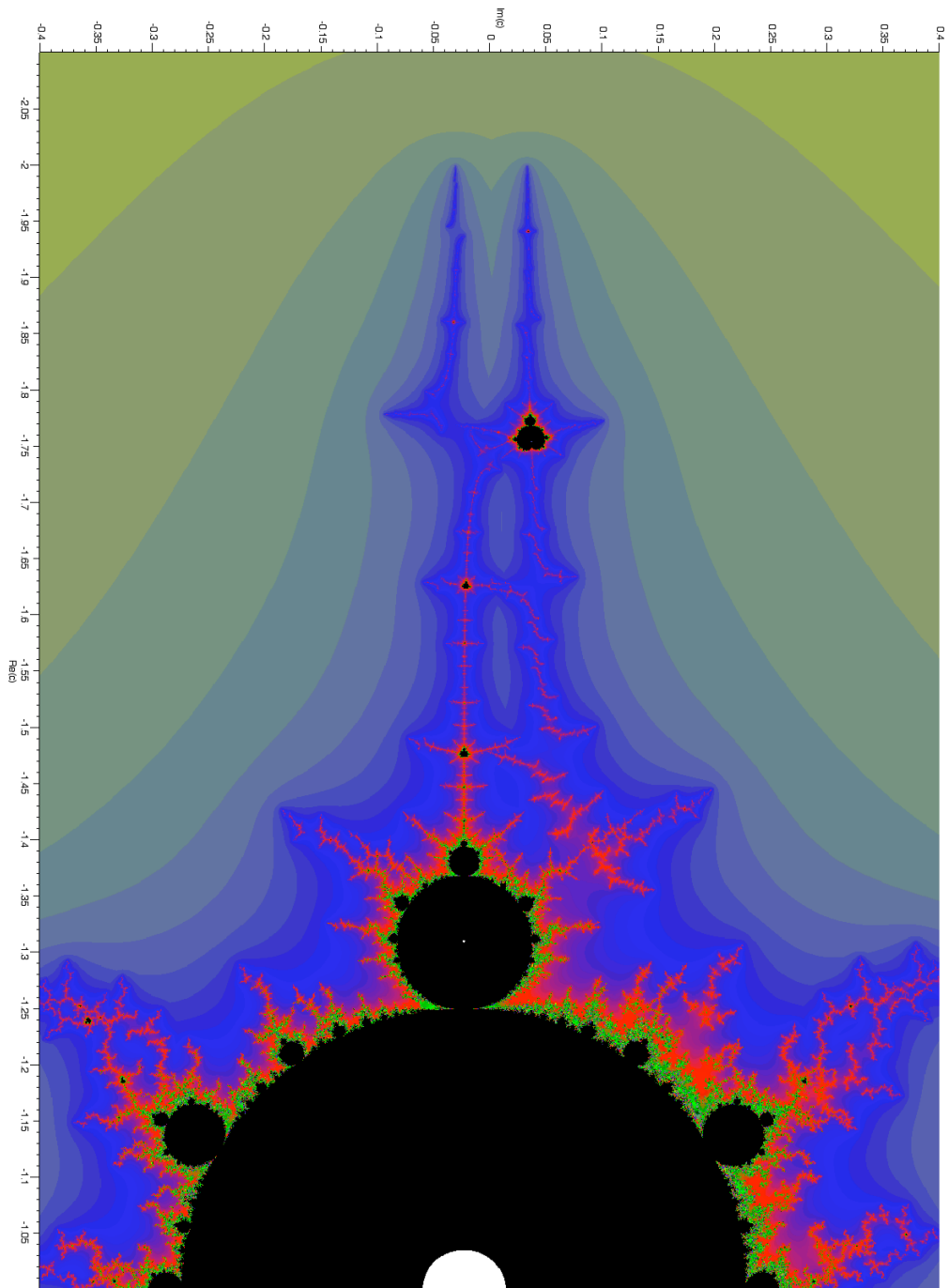


Figure 9.4: Parameter slice with $b = 0.015i$

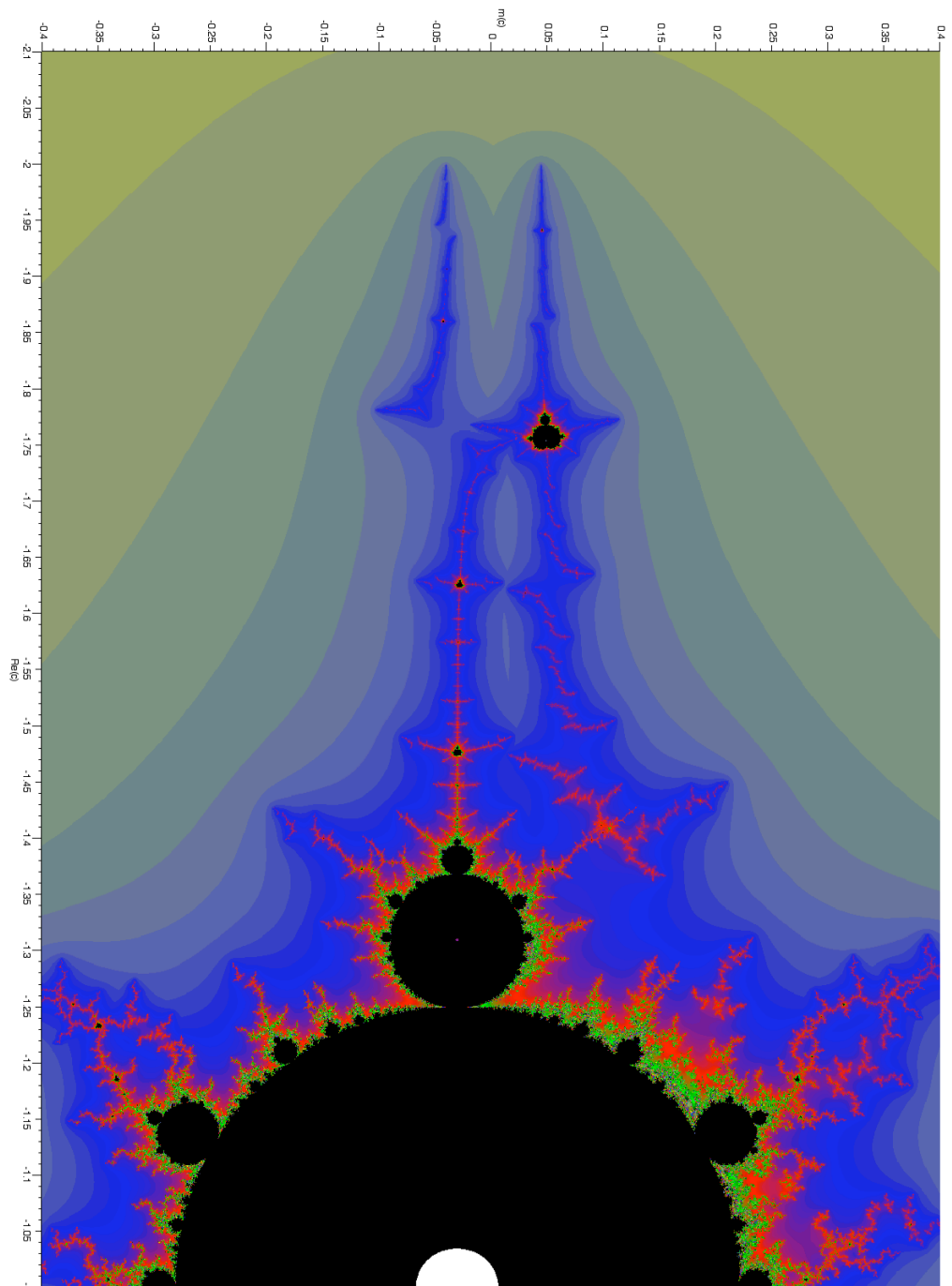


Figure 9.5: Parameter slice with $b = 0.02i$

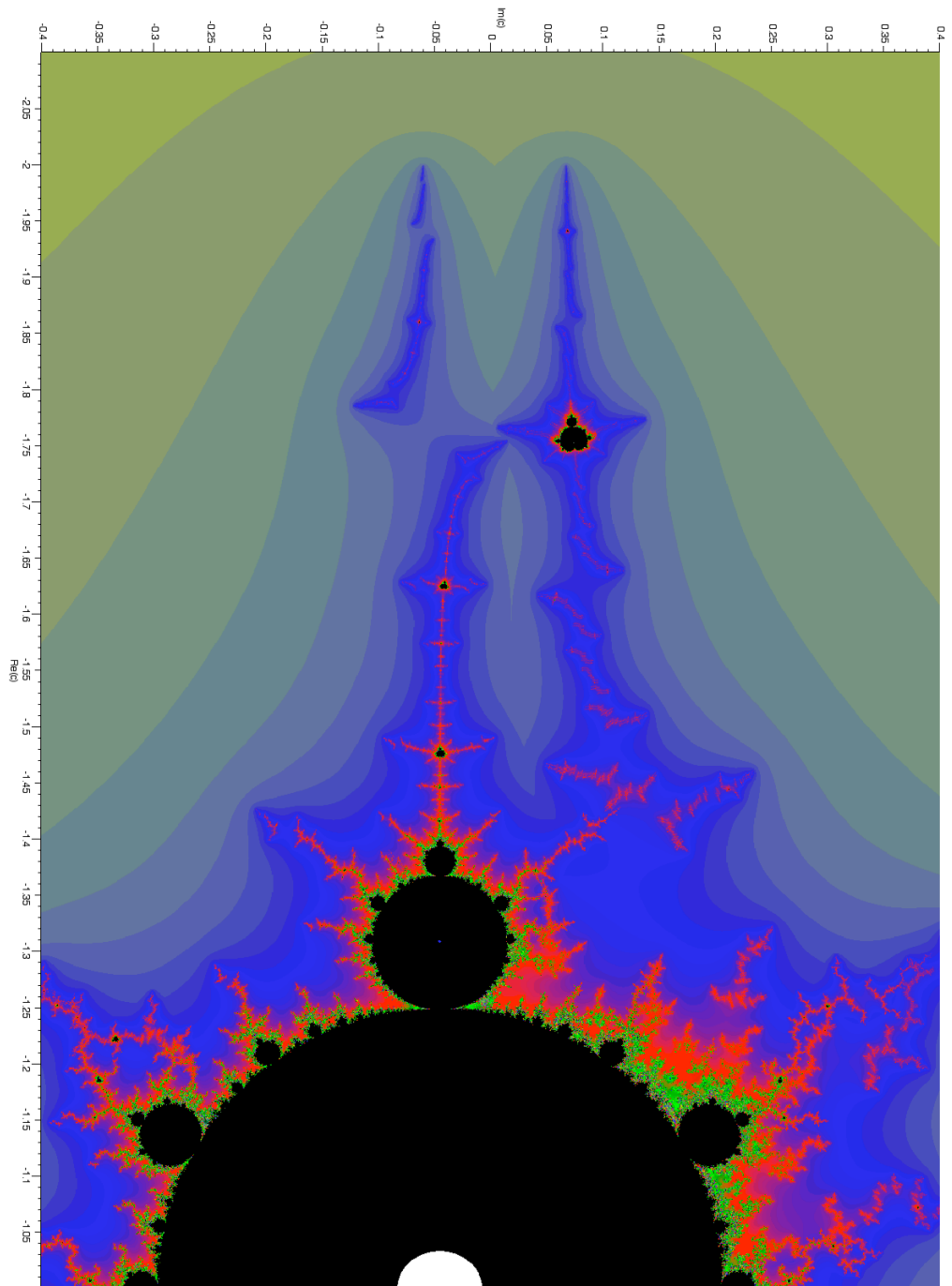


Figure 9.6: Parameter slice with $b = 0.03i$

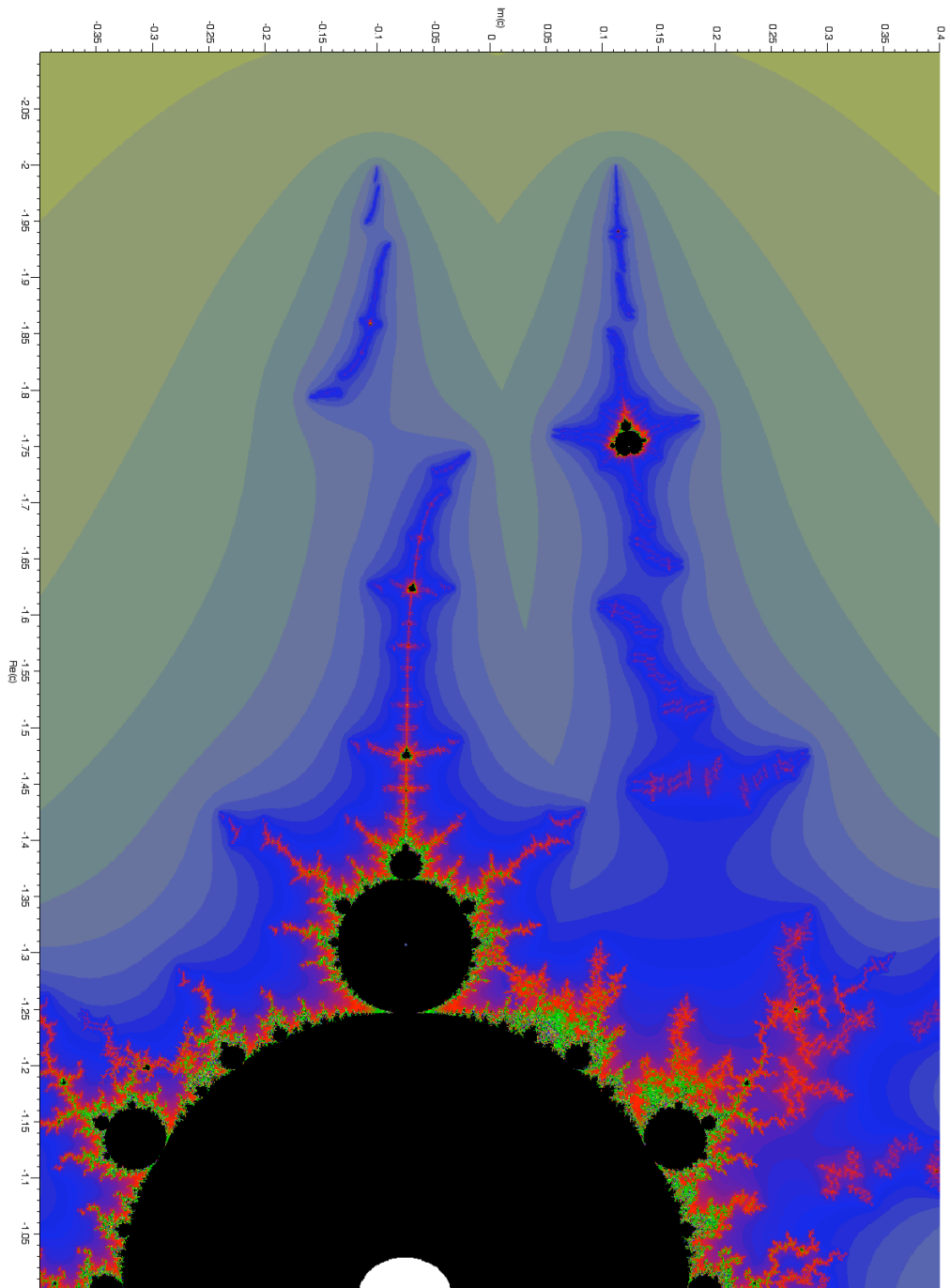


Figure 9.7: Parameter slice with $b = 0.05i$

Let \mathcal{W}_{air} be the one-dimensional parameter wake with boundary rays at angles $3/7$ and $4/7$ and which is associated with the airplane polynomial. The only wake conspicuous to \mathcal{W}_{air} is itself, and $K(\mathcal{W}_{\text{air}}) = BAA$. There is a gap in the bottom herd left by the airplane because the airplane traveled with the top herd. Every polynomial in \mathcal{W}_{air} (except for the airplane component itself) has an initial kneading sequence BAA , and this region is where the herd we loop around comes from. The airplane follows the A -herd, because its kneading sequence is $\star BA$, which ends in A , so the herd we are looping around is the B herd. Conjecture 8.3 implies that the monodromy action around the loop in Figure 9.8 is $B \star BAA$.

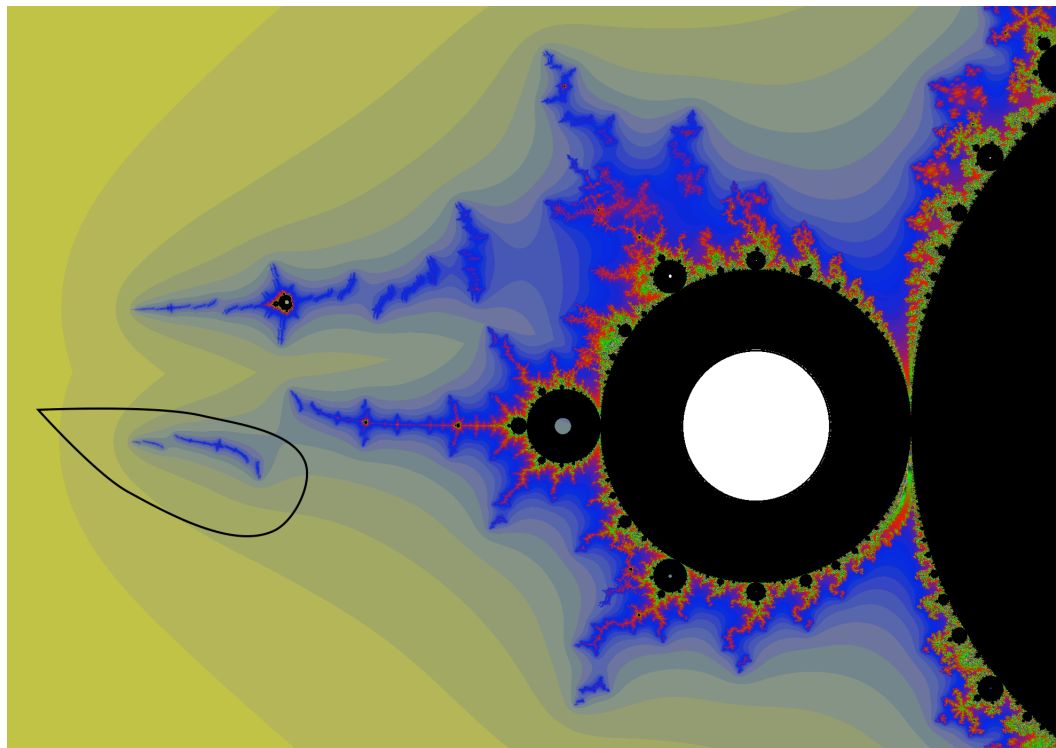


Figure 9.8: Loop around B herd of \mathcal{W}_{air} with $b = 0.05i$

The black loop in Figure 9.1 is not in $\mathcal{U}^{\mathcal{W}_{\text{air}}}$, but if this loop is homotopic to a loop in $\mathcal{U}^{\mathcal{W}_{\text{air}}}$, then by Theorem 7.5, the monodromy action of this loop would have to be trivial on every sequence which did not include the substring BAA . This is a necessary

condition for the monodromy action of this loop to be $B \star BAA$.

9.2 $BB \star BAA$ and $AB \star BAA$

The B -herd is composed of the AB - and the BB -herds. As we perturb b farther, the BB and the AB herds split up. In the Figure 9.9, we can also see the AB and the BB herds splitting further into the AAB , BAB , ABB and BBB herds.

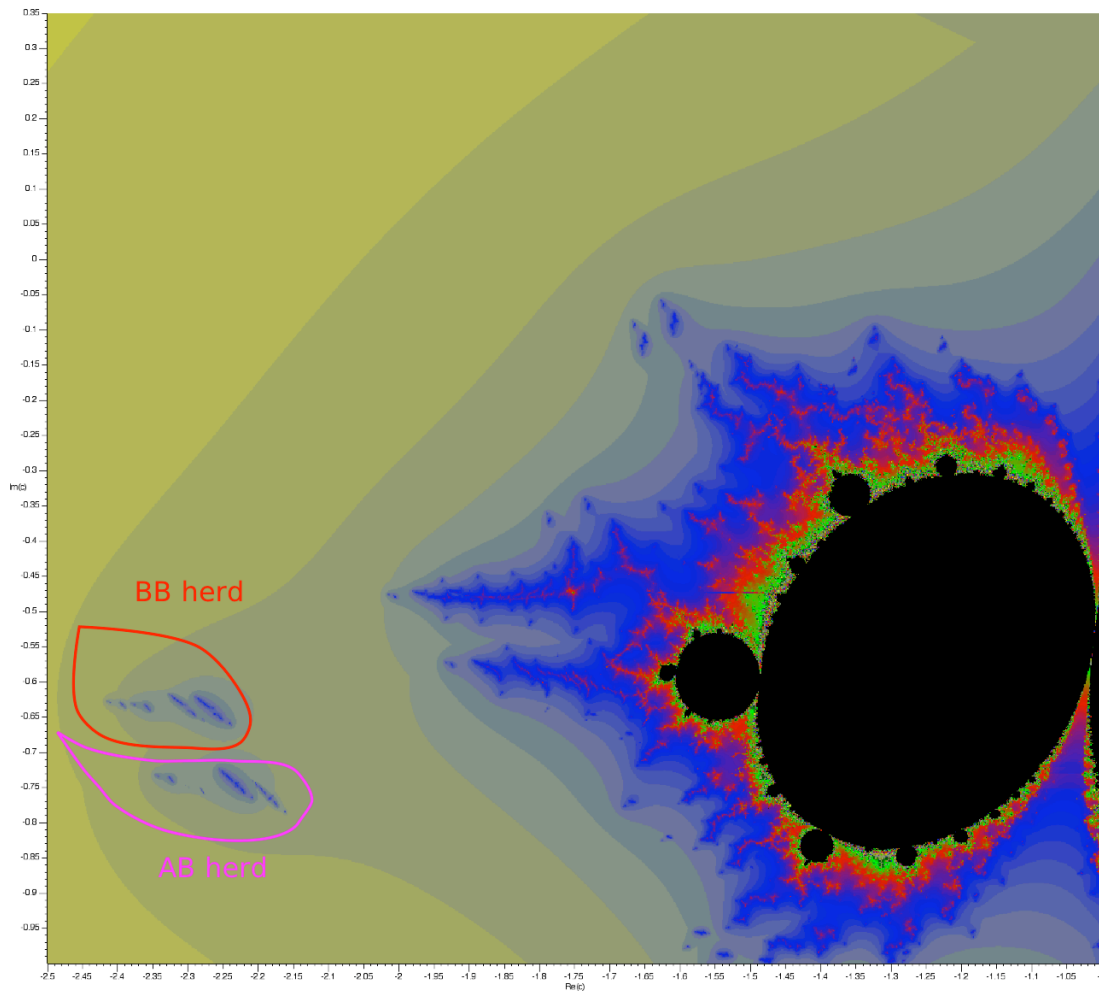


Figure 9.9: Loops around BB and AB herds of \mathcal{W}_{air} with $b = 0.2 + 0.3i$

The automorphism $B \star BAA$ is the composition of $AB \star BAA$ with $BB \star BAA$, and

these two automorphisms commute. Conjecture 8.3 implies that the monodromy action of the purple loop around the AB herd of \mathcal{W}_{air} is $AB \star BAA$ and that the monodromy action of the red loop around the BB herd of \mathcal{W}_{air} is $BB \star BAA$.

9.3 $A \star BAA$

Lemma 9.3. $A \star BAA$ is not an automorphism of the full 2-shift.

Proof. $A \star BAA$ maps both of the sequences \overline{BAA} and \overline{BAB} to the sequence \overline{BAB} , so this endomorphism is not injective. \square

The author is unable to find a loop in the horseshoe locus that travels only around the A -herd of \mathcal{W}_{air} (see Figure 9.7). There is no obvious gap to go through, because the airplane travels with the A -herd. Conjecture 8.4 implies that such a loop does not exist in the Horseshoe locus.

To find a loop that goes around the A -herd of \mathcal{W}_{air} , the computer experimentation suggests that one must find a gap created by some other hyperbolic component which travels in the other direction.

9.4 $A \star BAA, A \star BABBA$

There is a period 5 renormalized Mandelbrot set on the real axis of the Mandelbrot set to the right of the airplane at the landing point of the 13/31 and 18/31 parameter rays whose kneading sequence is $\overline{BABB\star}$. Call the parameter wake associated with this component \mathcal{W}_{BABBA} . The only two wakes conspicuous to \mathcal{W}_{BABBA} are itself and \mathcal{W}_{air} , and

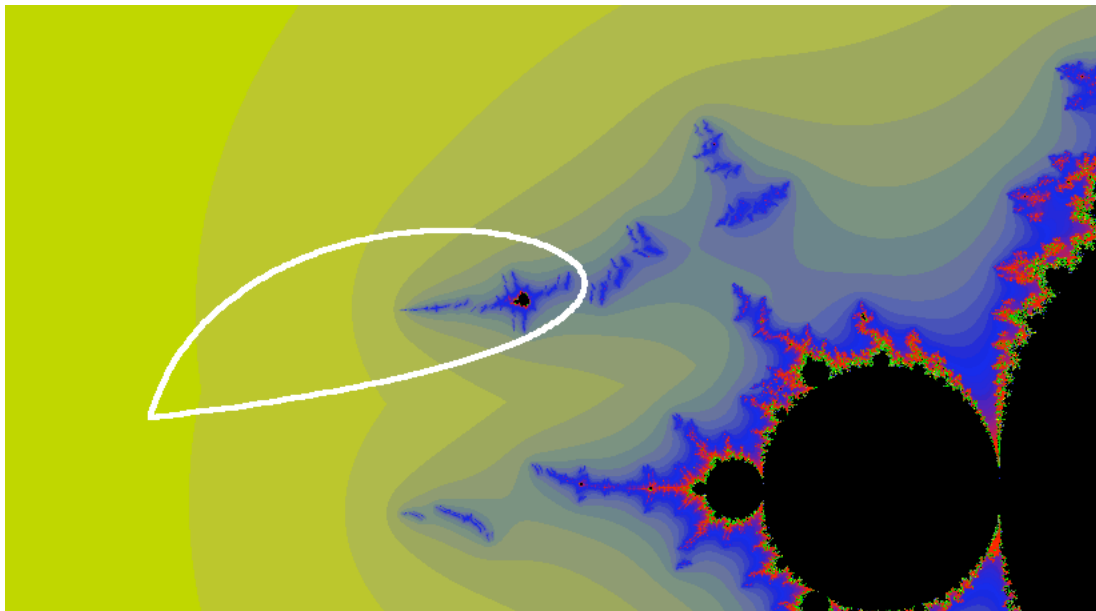


Figure 9.10: Loop around A herd of \mathcal{W}_{BABB}

$K(\mathcal{W}_{BABB}) = BABBA$. The loop in Figure 9.10 goes through the A herd corresponding to where this period 5 component left a gap.

The polynomials in \mathcal{M} between this period 5 component and the airplane all have an initial kneading sequence of $BABBA$. So this loop goes around the A herd of polynomials in the Mandelbrot set with initial kneading sequences of either BAA or $BABBA$.

Lemma 9.4. *The two-string compound marker endomorphism $A \star BAA$, $A \star BABBA$ is a compound marker automorphism.*

Proof. We will say that a marker string matches at a particular position when that position is where the \star matches.

Let ϕ be the compound marker endomorphism $A \star BAA$, $A \star BABBA$. It is clear that ϕ is continuous and commutes with the shift. We will show that ϕ is bijective by showing that ϕ is an involution. Choose any $x = (x_i) \in \{A, B\}^{\mathbb{Z}}$. Let $y = (y_i) = \phi(x)$ and $z = (z_i) = \phi(y)$. We will show that $z = x$ by showing that x and y differ at an index if and

only if y and z differ at the same place.

Suppose x and y differ at index 0. Then $x_{-1} = x_2 = A$ and $x_1 = B$. Also either $x_3 = A$ (case 1) or $x_3 = x_4 = B$ and $x_5 = A$ (case 2).

Let us consider case 1 first. In this case, neither $A \star BAA$ nor $A \star BABBA$ can match x at position -1 , 1 , or 2 , so $y_{-1} = x_{-1} = A$, $y_1 = x_1 = B$, and $y_2 = x_2 = A$. Either string could potentially match x at position 3. Let 1a be the case where there is no match and let 1b be the case where one of the two marker strings matches x at position 3.

Let us consider case 1a. Then, in addition to the information we have for case 1, we know that $y_3 = x_3 = A$. Hence the marker string $A \star BAA$ matches y at index 0. Thus, $z_0 \neq y_0$.

Let us consider case 1b. We know that $y_3 = B$. We also know that no matter which string matches x at index 3, $x_4 = B$ and $x_5 = A$. Neither marker string can match x at index 4 or 5, so $y_4 = x_4 = B$ and $y_5 = x_5 = A$. This forces the string $B \star BABBA$ to match y at index 0, and we see that $z_0 \neq y_0$.

Now let us consider case 2. Neither marker string can match x at index -1 , 1 , 2 , 4 , or 5 , so $y_1 = x_1 = B$, $y_2 = x_2 = A$, $y_4 = x_4 = B$, and $y_5 = x_5 = A$. However, either marker string can match x at index 3, so y_3 may be either A or B . If $y_3 = A$, then y matches the marker string $A \star BAA$ at index 0. If $y_3 = B$, then y matches $A \star BABBA$ at index 0. Either way, $z_0 \neq y_0$.

We have proven that if $x_0 \neq y_0$, then $y_0 \neq z_0$. Now, let us assume that $y_0 \neq z_0$. Then either y matches $B \star BAA$ at index 0 (case 3) or y matches $B \star BABBA$ at index zero (case 4).

Let us consider case 3. Suppose that $x_{-1} = B \neq A = y_{-1}$. Then x must match one of

the marker strings at index -1 . This implies that $x_0 = B$ and $x_1 = A \neq y_1$. So x must match a marker string at index 1 as well, but $x_0 = B$ contradicts this. So we know that $x_{-1} = A$. Now suppose that $x_1 = A$. Then because $x_1 \neq y_1$, then one of the marker strings must match x at index 1, so $x_2 = B$ and $x_3 = A$. Because $x_2 \neq y_2$, then a string must match x at index 2 as well, which implies that $x_3 = B$, a contradiction. Thus, $x_1 = B$. Since $x_1 = B$, then neither string can match at index 2, so $y_2 = x_2 = A$. Let 3a be the case that $x_3 = A$ and let 3b be the case that $x_3 = B$.

Let us consider case 3a. In this case, x matches the marker string $B \star BAA$ at index 0, so $x_0 \neq y_0$.

Let us consider case 3b. In this case, since $x_3 \neq y_3$, then we know that $x_4 = B$ and $x_5 = A$. Hence x matches the string $A \star BABBA$ at index 0, and $x_0 \neq y_0$.

Let us consider case 4. Suppose that $x_5 = B$. Because $x_5 \neq y_5$, then a marker string must match x at index 5, so $x_4 = A$. Because $x_4 \neq y_4$, then a marker string must match x at index 4, so $x_3 = A$. Because $x_3 \neq y_3$, then a marker string must match x at index 3, so $x_4 = B$, a contradiction. Hence we know that $x_5 = A$. Neither string can now match x at index 4, so $x_4 = y_4 = B$. Similarly, the fact that $x_4 = B$ keeps either marker string from matching x at index 2, so $x_2 = y_2 = A$. Neither string can match x at index 1 because $x_2 = A$, so $x_1 = y_1 = B$. Because $x_1 = B$, then neither string can match x at index -1 , so $x_{-1} = y_{-1} = A$. If $x_3 = A$, then x matches $A \star BAA$ at index 0, and $x_0 \neq y_0$. On the other hand, if $x_3 = B$, then x matches $A \star BABBA$ at index 0, and $x_0 \neq y_0$.

Thus, we see that in all cases, $z_0 \neq y_0$ implies that $x_0 \neq y_0$. So $x_0 = y_0$ if and only if $y_0 = z_0$. In either case, $x_0 = z_0$. Marker endomorphisms commute with the shift, so $x = z = \phi(\phi(x))$ for any $x \in \Sigma_2$. ϕ is its own inverse and is an automorphism. \square

As mentioned earlier $A \star BAA$ by itself is not an automorphism. However, $A \star BAA$,

$A \star BABBA$ is in fact a compound marker automorphism, and Conjecture 8.3 implies that this automorphism describes the monodromy action of the loop in Figure 9.10.

9.5 $A \star BAA, A \star BABBA, B \star BAA$

If we could move the two gaps from the loop that generated $A \star BAA, A \star BABBA$ and the loop that generated $B \star BAA$ on top of each other, then we might expect given Conjecture 8.3 that a loop going through the combined gap to generate the compound marker endomorphism $A \star BAA, A \star BABBA, B \star BAA$. However, this action fails to be an automorphism (Lemma 9.6). Figures 9.11, 9.12, and 9.13 show an attempt to move these gaps on top of each other.

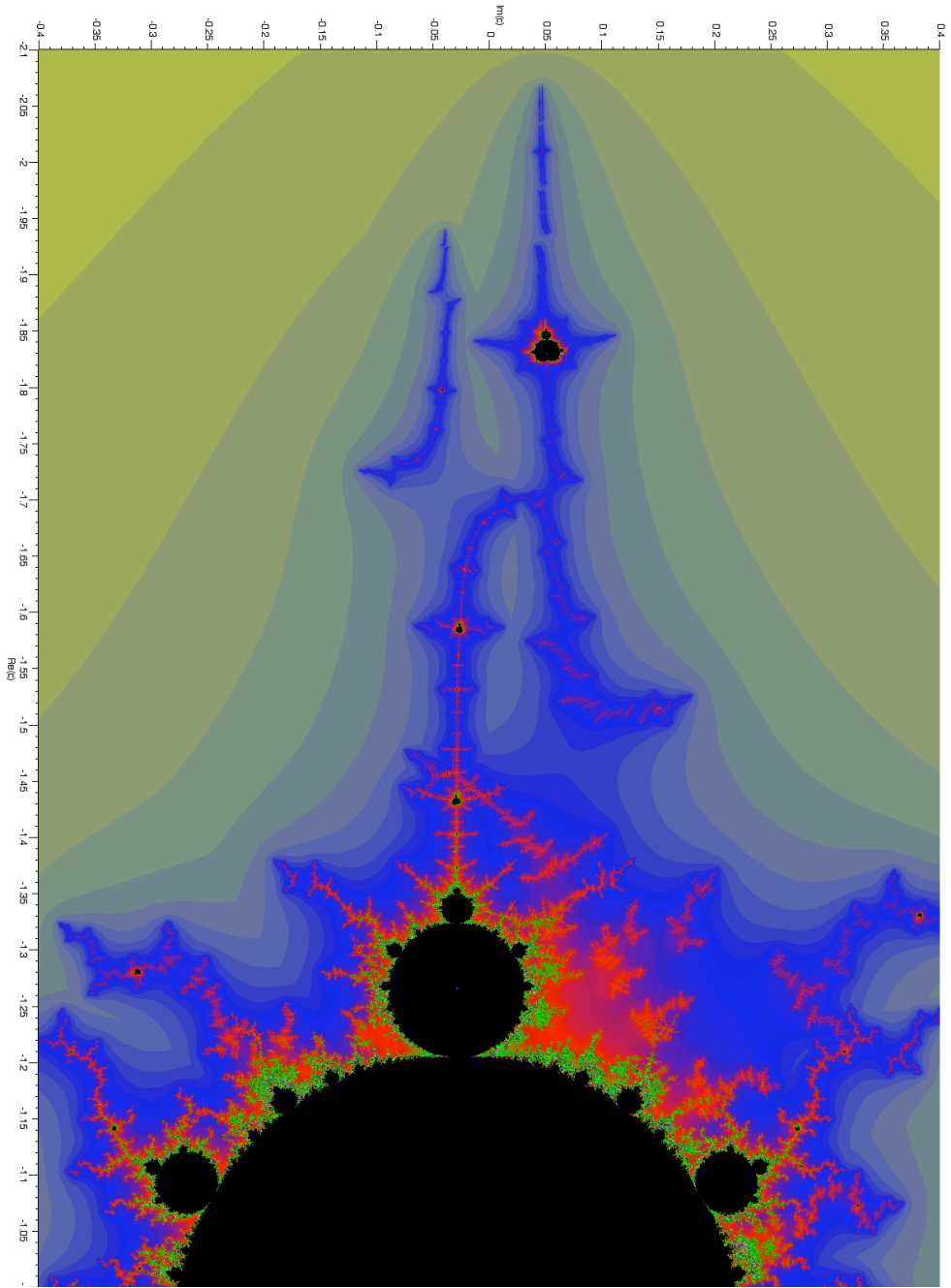


Figure 9.11: Parameter slice with $b = -0.03 + 0.02i$

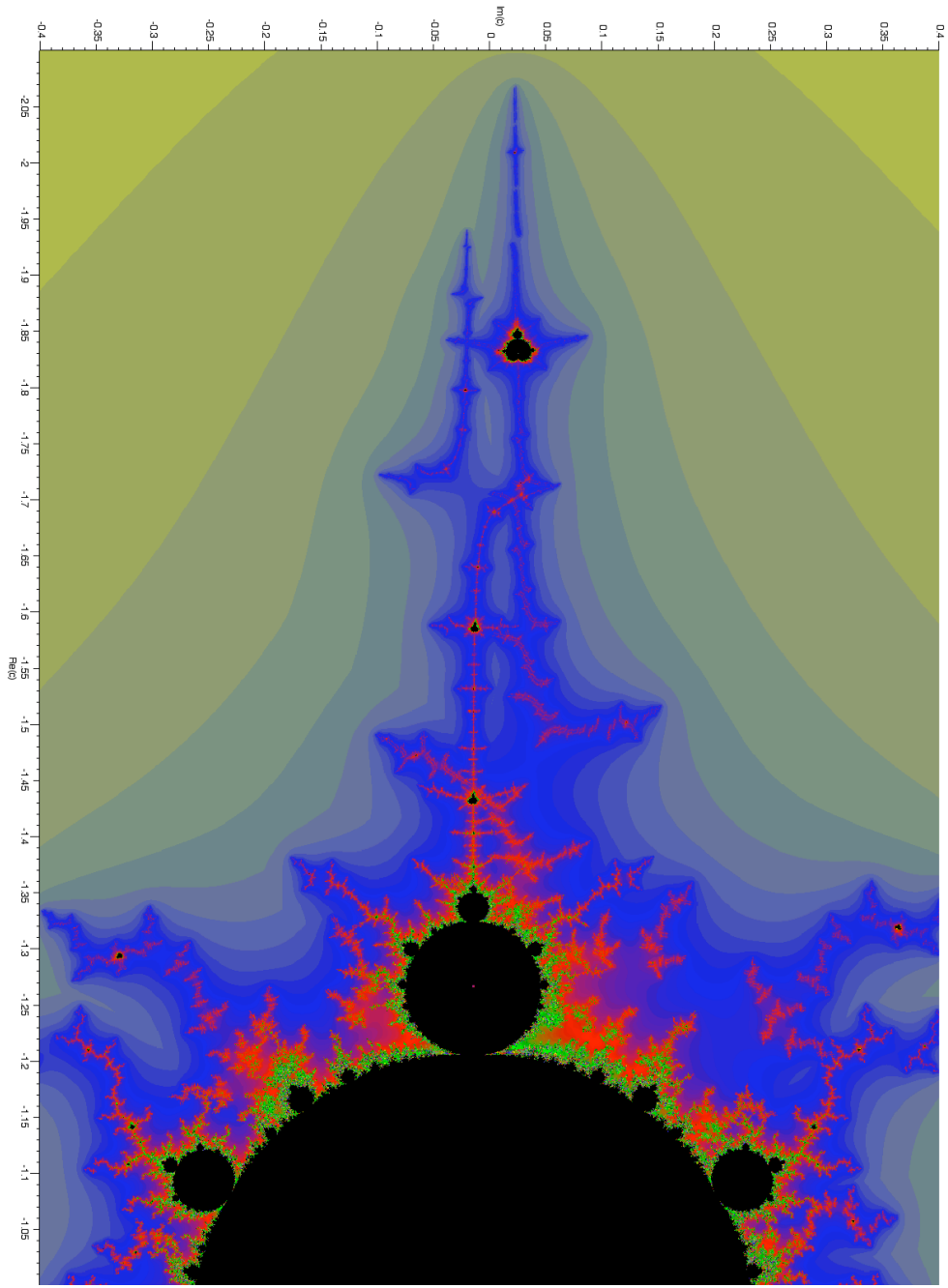


Figure 9.12: Parameter slice with $b = -0.03 + 0.01i$

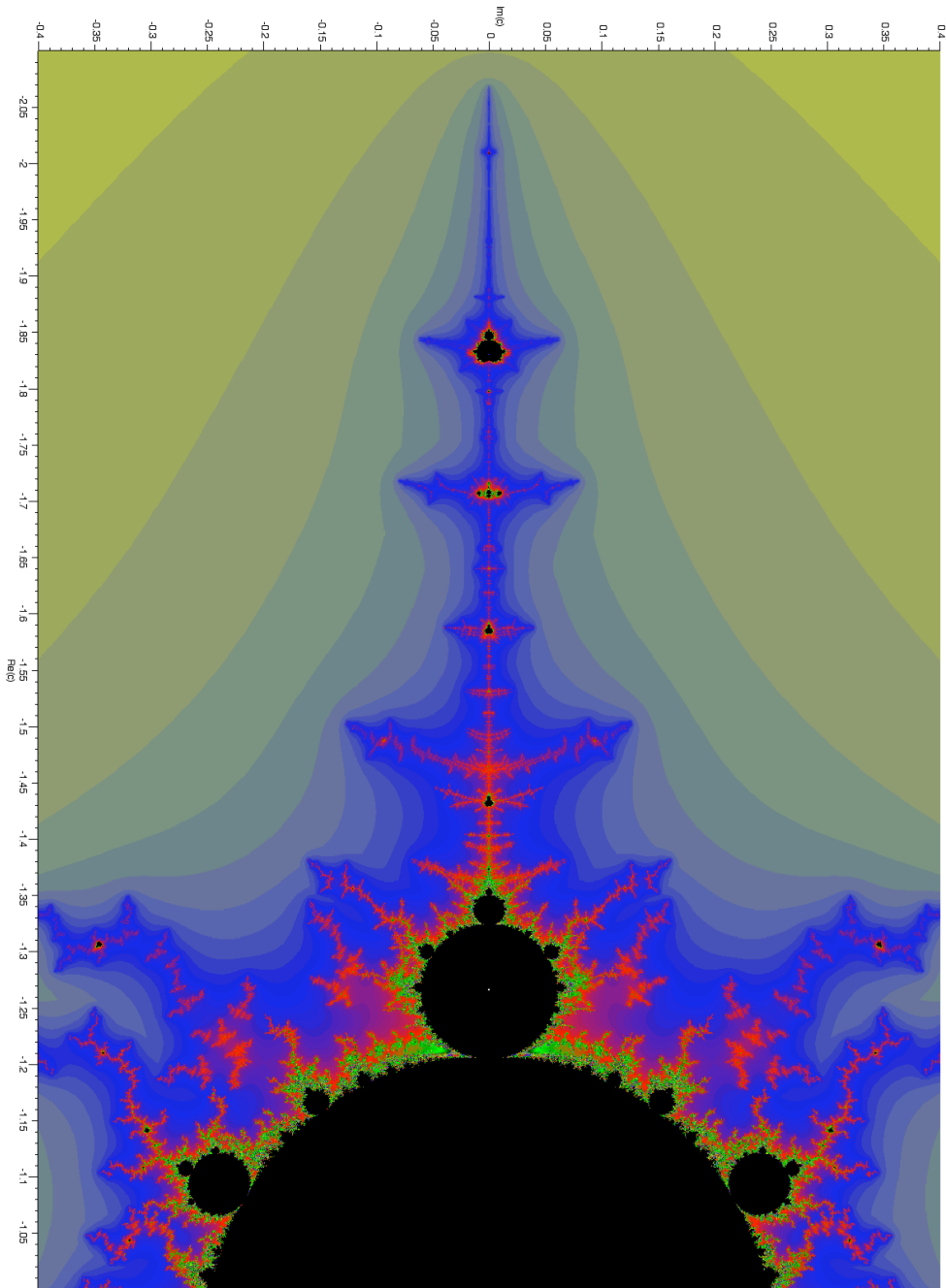


Figure 9.13: Parameter slice with $b = -0.03$

This is not to say that there are not loops that go through both gaps.

The monodromy action on such loops would be the two-string compound marker automorphism $A \star BAA$, $A \star BABBA$ composed with the simple marker automorphism $B \star BAA$, which would be an automorphism. This loop could be contained in the $b = -0.03 + 0.02i$ slice of parameter space, as is illustrated in Figure 9.11.

Complex conjugacy is a symmetry of parameter space. If it were possible to homotope such a loop to a real Jacobian, then it would therefore also be possible to homotope that same loop to the $b = -0.03 - 0.02i$ slice of parameter space. Conjecture 8.3 would then imply that the monodromy action of this loop would simultaneously have to be $A \star BAA$, $A \star BABBA$ post-composed with $B \star BAA$ as well as $B \star BAA$ post-composed with $A \star BAA$, $A \star BABBA$. However, the action $A \star BAA$, $A \star BABBA$ does not commute with $B \star BAA$ (Lemma 9.5). Therefore, if Conjecture 8.3 is correct, then it is not possible to move these two gaps on top of each other.

Lemma 9.5. *The two-string compound marker automorphism $A \star BAA$, $A \star BABBA$ does not commute with the one-string simple marker automorphism $B \star BAA$.*

Proof. Let ψ be the action of the compound marker string $A \star BAA$, $A \star BABBA$, and let φ be the action of the compound marker string $B \star BAA$. Let x be the bi-finite string $\overline{AABABBABA}$. Then:

$$\psi(x) = \overline{ABBABBABA}$$

$$\varphi(\psi(x)) = \overline{ABBABBBBA}$$

And we also see that:

$$\varphi(x) = \overline{AABABBBBA}$$

$$\psi(\varphi(x)) = \overline{AABABBABA}$$

Hence we see that $\psi \circ \varphi \neq \varphi \circ \psi$, because they disagree on x . □

Lemma 9.6. *The three-string compound marker endomorphism $A \star BAA$, $A \star BABBA$, $B \star BAA$ is not an automorphism.*

Proof. This compound marker endomorphism maps both of the bi-infinite sequences $\overline{BAABABBA}$ and $\overline{BABBABBB}$ to $\overline{BABBABBB}$, so it cannot be injective. \square

9.6 $ABAAB \star BAA$ and $BBAAB \star BAA$

Figure 9.14 shows the $ABAAB$ and the $BBAAB$ herds of \mathcal{W}_{air} . Here the Jacobian is $-0.1 + 0.9i$.

$ABAAB \star BAA$ and $BBAAB \star BAA$ are compound marker endomorphisms that are not compound marker automorphisms.

When b is large enough to separate the $BBAAB$ herd from the $ABAAB$ herd of \mathcal{W}_{air} , other nonhyperbolic components come in between them from other parts of the Mandelbrot set.

Figure 9.15 shows the same region of parameter space, but following different critical points.

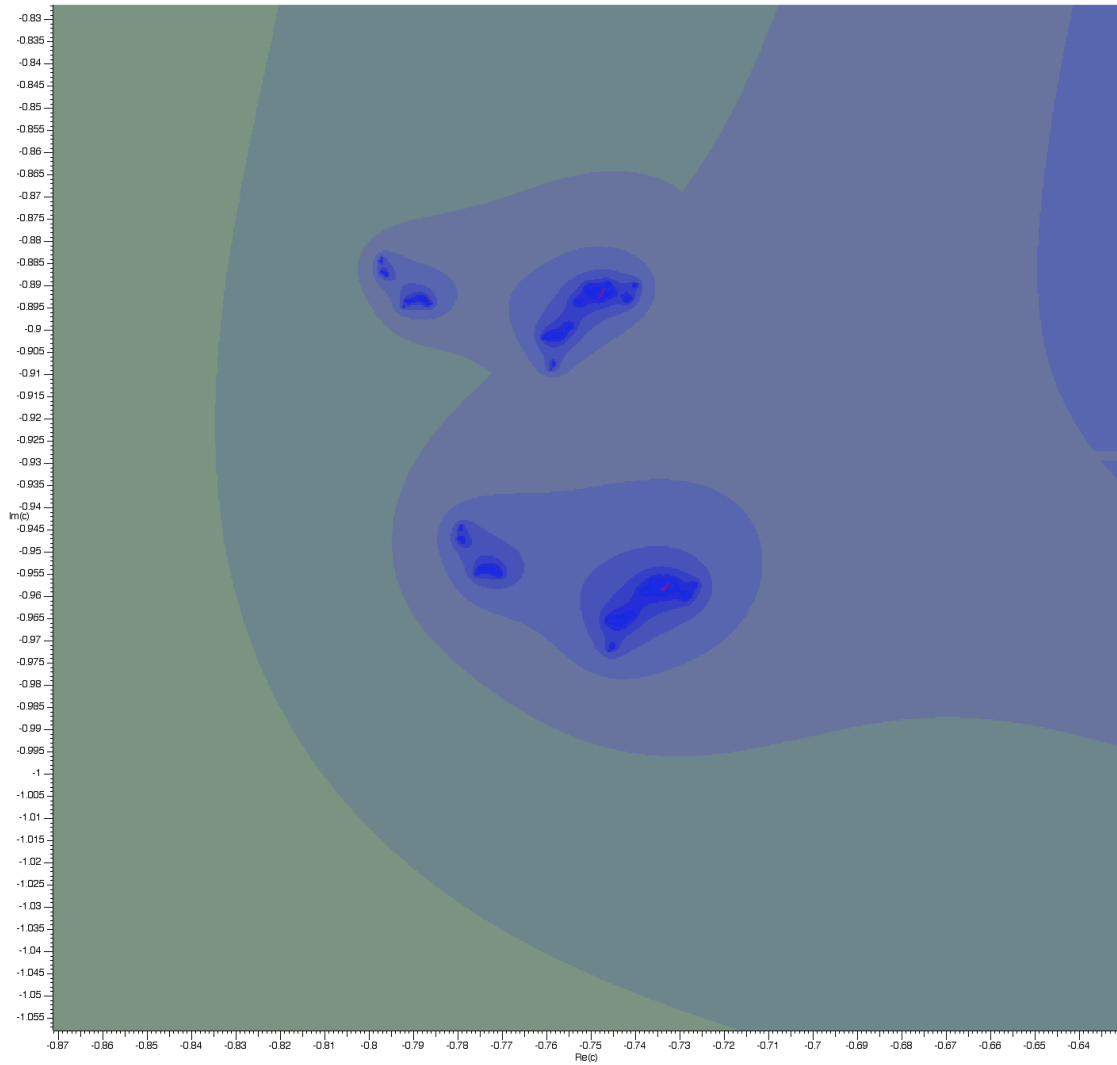


Figure 9.14: *ABAAB* and *BBAAB* herds of \mathcal{W}_{air} with $b = -0.1 + 0.9i$

Overlaying Figures 9.14 and 9.15 yields Figure 9.16.

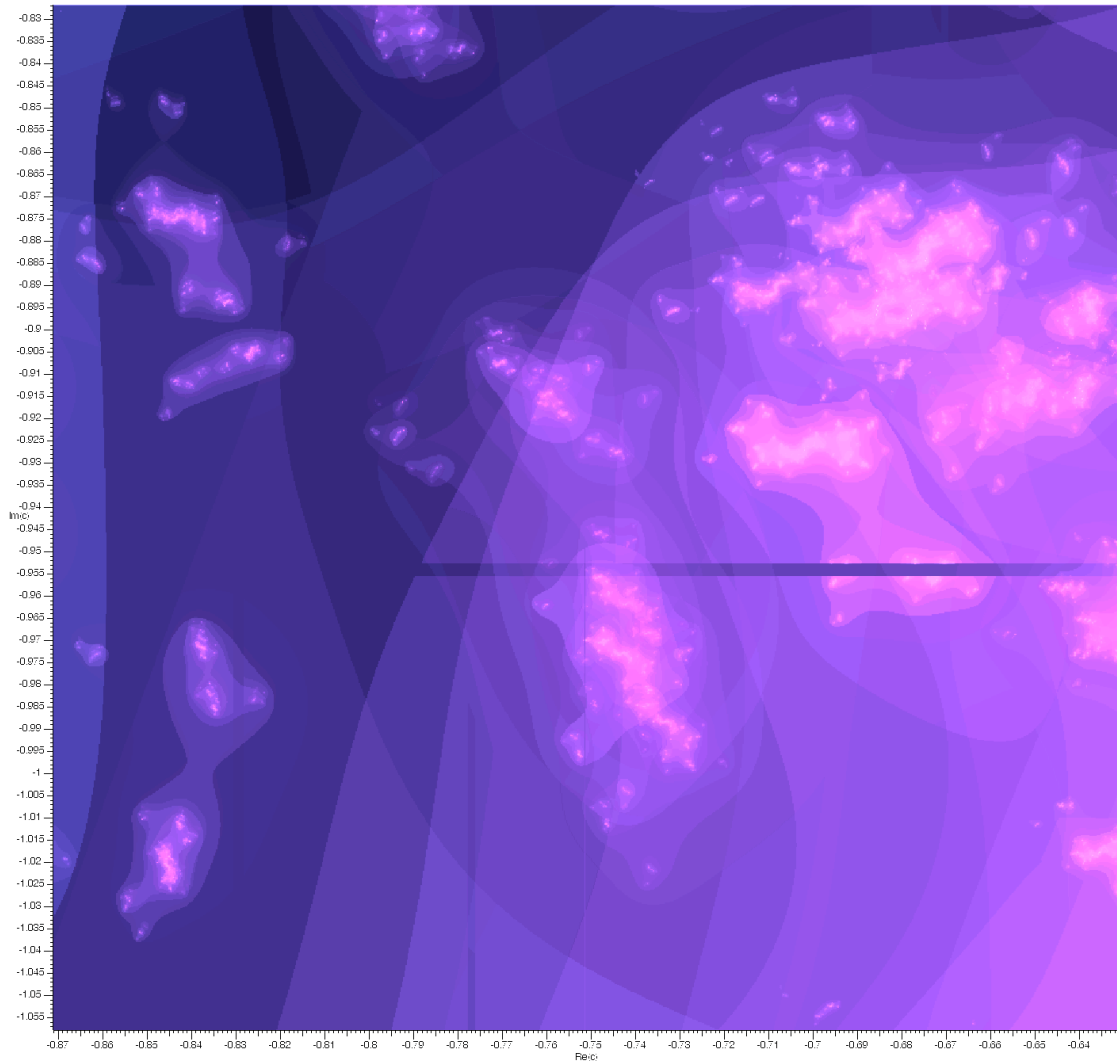


Figure 9.15: Other herds near the $ABAAB$ and $BBAAB$ herds of \mathcal{W}_{air} with $b = -0.1 + 0.9i$

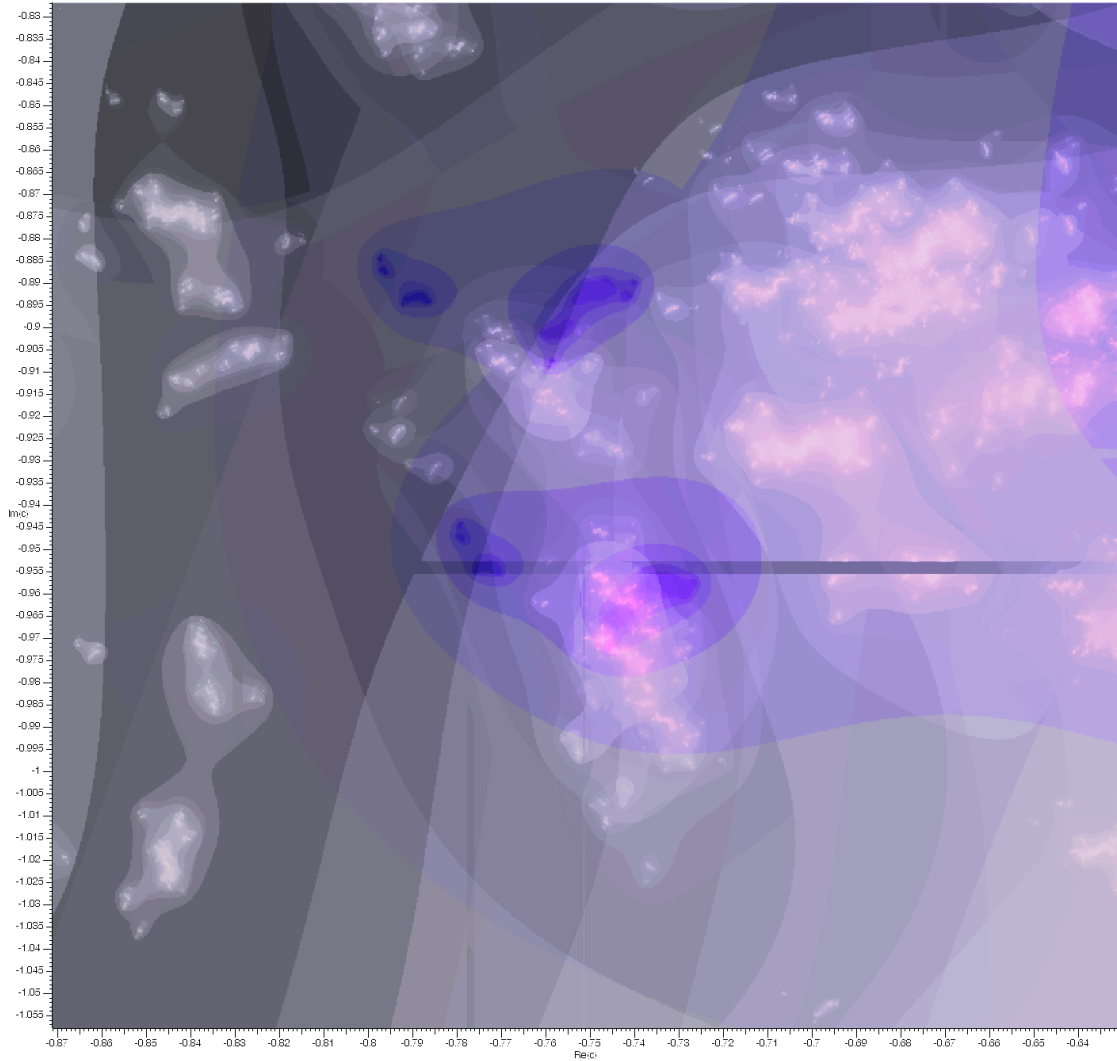


Figure 9.16: Other herds obstructing loops around $ABAAB$ and $BBAAB$ herds of \mathcal{W}_{air} with $b = -0.1 + 0.9i$

The author is unable to find a loop inside the horseshoe locus that loops only around the $BBAAB$ herd of \mathcal{W}_{air} . Conjecture 8.4 claims that such a loop does not exist.

APPENDIX A
MONODROMIES OF INVERSE LIMIT SYSTEMS

A.1 Inverse Limit System Setup

This chapter will show some results that relate monodromy actions of inverse limit systems with those of the base dynamical system.

Let S_X and S_Y be locally trivial fiber bundles with totally disconnected fibers over base spaces X and Y , respectively with natural projections $\tau_X : S_X \rightarrow X$ and $\tau_Y : S_Y \rightarrow Y$, each of which takes a fibre to its basepoint. For every $x \in X$, let $s_x \subset S_X$ be the fiber over the point x . For every $y \in Y$, let $s_y \subset S_Y$ be the fiber over the point y . We let $\pi : X \rightarrow Y$ be a continuous map and $\tilde{\pi} : S_X \rightarrow S_Y$ also be continuous, so that the following diagram commutes:

$$\begin{array}{ccc} S_x & \xrightarrow{\tau_X} & X \\ \downarrow \tilde{\pi} & & \downarrow \pi \\ S_y & \xrightarrow{\tau_Y} & Y \end{array}$$

$\tilde{\pi}$ maps fibres to fibres. In particular it maps a point $z \in S_X$ in the fibre above $x \in X$ to a point in S_Y in the fibre above $\pi(x)$.

Also, for any $y \in Y$, we have some dynamical system $g_y : s_y \rightarrow s_y$, defined continuously with respect to $y \in Y$. We also assume that $g_y : s_y \rightarrow s_y$ is surjective for all y . We insist that there is a dynamical system $f_x : S_x \rightarrow S_x$ which is the inverse limit of $g_{\pi(x)}$. $(S_x, f_x) = \varprojlim (S_{\pi(x)}, g_{\pi(x)})$. In particular S_x is isomorphic to $\{(\dots, z_{-1}, z_0, z_1, \dots) \mid \forall i \in \mathbb{Z}, z_i \in S_{\pi(x)} \text{ and } g_{\pi(x)}(z_i) = z_{i+1}\}$. Define $\hat{\pi} : S_x \rightarrow S_{\pi(x)}$ be the natural projection associated with the inverse limit construction that takes $(\dots, z_{-1}, z_0, z_1, \dots)$ to z_0 .

For every $x \in X$ and $y = \pi(x)$, We have the following commutative diagram:

$$\begin{array}{ccc} S_x & \xrightarrow{f_x} & S_x \\ \downarrow \tilde{\pi} & & \downarrow \tilde{\pi} \\ S_y & \xrightarrow{g_y} & S_y \end{array}$$

Define $f : S_X \rightarrow S_X$ by $f(z) = f_{\tau_X(z)}(z)$. Similarly define $g : S_Y \rightarrow S_Y$ by $g(z) = g_{\tau_Y(z)}(z)$. f and g are dynamical systems on S_X and S_Y , respectively, for which every fibre is invariant. So we also have:

$$\begin{array}{ccc} S_X & \xrightarrow{f} & S_X \\ \downarrow \tilde{\pi} & & \downarrow \tilde{\pi} \\ S_Y & \xrightarrow{g} & S_Y \end{array}$$

This setup describes a situation where we have an inverse limit of a hyperbolic dynamical system. Y should be thought of as the parameter space for the hyperbolic dynamical system, and X should be thought of as the parameter space for the inverse limit system. S_x and S_y are the dynamical spaces for our maps with respective parameter values x and y .

A.2 Coding Setup

Fix any basepoint $x_0 \in X$ and let $y_0 = \pi(x_0) \in Y$. Let $(\Delta_1, \dots, \Delta_d)$ be a partition of S_{y_0} . The pull-back by $\tilde{\pi}$ induces a partition $(\Theta_1, \dots, \Theta_d)$ on S_{x_0} . $\Theta_i = \{z \in S_{x_0} | \pi(z) \in \Delta_i\}$.

We do not insist that these partitions have the Markov property.

Points in S_{x_0} and S_{y_0} have itineraries relative to these partitions under the actions of

f_{x_0} and g_{y_0} . For $z \in S_{x_0}$, let $\mathcal{I}(z)$ be the two-sided itinerary of z . For $x \in S_{y_0}$, let $\mathcal{I}(z)$ be the one-sided itinerary of z . For any $z \in S_{x_0}$, the right-infinite tail of $\mathcal{I}(z)$ starting at index 0 is identical to $\mathcal{I}(\pi(z))$.

A.3 Monodromy Actions

In each of the spaces X and Y , the fact that we have locally trivial fiber bundles which are completely disconnected implies by the path-lifting property that we have monodromy actions on the fibre above any basepoint, in particular x_0 and y_0 . Let $\rho_x : \Pi_1(X, x_0) \rightarrow \text{Aut}(S_{x_0}, f_{x_0})$ and $\rho_y : \Pi_1(Y, y_0) \rightarrow \text{Aut}(S_{y_0}, g_{y_0})$ be these monodromy actions. Here $\text{Aut}(S_{x_0}, f_{x_0})$ and $\text{Aut}(S_{y_0}, g_{y_0})$ represent the group of continuous automorphisms on S_{x_0} and S_{y_0} that commute with f_{x_0} and g_{y_0} , respectively. Every loop in X projects to a loop in Y under π , so there is a homomorphism from $\Pi_1(X, x_0)$ to $\Pi_1(Y, y_0)$, which we will also denote by π . (This map is a homomorphism when we consider a composition of loops such as $(\gamma_1 \circ \gamma_2)$ to mean first going around γ_2 and then going around γ_1 , as will be the convention here. The map is an anti-homomorphism if one makes the alternate choice.)

Fix some particular loop $\gamma \in \Pi_1(X, x_0)$ for the remainder of this appendix. Iterating a point of S_{x_0} under the dynamical system f_{x_0} and then computing its monodromy action by γ is the same as finding the monodromy of the point and then iterating it under the dynamics. This is because if a particular path ω through S_X (which projects to a loop γ in X based at x_0) connects w with z , then $f(\omega)$ must connect $f_x(w)$ with $f_x(z)$. The same argument also shows that the monodromy action of a loop in Y commutes with g_{y_0}

$$\begin{array}{ccc}
S_{x_0} & \xrightarrow{\rho_x(\gamma)} & S_{x_0} \\
\downarrow f_{x_0} & & \downarrow f_{x_0} \\
S_{x_0} & \xrightarrow{\rho_x(\gamma)} & S_{x_0}
\end{array}
\qquad
\begin{array}{ccc}
S_{y_0} & \xrightarrow{\rho_y(\gamma)} & S_{y_0} \\
\downarrow g_{y_0} & & \downarrow g_{y_0} \\
S_{y_0} & \xrightarrow{\rho_y(\gamma)} & S_{y_0}
\end{array}$$

Similarly, it does not make a difference if we compute the monodromy of a loop γ acting on $z \in S_{x_0}$ in the top space, and then project $\rho_x(\gamma)(z)$ down by $\tilde{\pi}$ or if we first project down both z and γ and compute the monodromy action of $\pi(\gamma)$ on $\pi(z) \in S_{y_0}$. This is because if some path ω in S_X connects z to $\rho_x(\gamma)(z)$, then $\pi(\omega)$ in S_Y connects $\pi(z)$ with $\rho_y(\pi(\gamma))(\pi(z))$. We have the following commutative diagram:

$$\begin{array}{ccc}
S_{x_0} & \xrightarrow{\rho_x(\gamma)} & S_{x_0} \\
\downarrow \tilde{\pi} & & \downarrow \tilde{\pi} \\
S_{y_0} & \xrightarrow{\rho_y(\pi(\gamma))} & S_{y_0}
\end{array}$$

Putting these commutative diagrams together gives:

$$\begin{array}{ccccc}
S_{x_0} & \xrightarrow{\rho_x(\gamma)} & S_{x_0} & & S_{x_0} \\
\downarrow f_{x_0} & & \downarrow f_{x_0} & & \downarrow f_{x_0} \\
S_{x_0} & \xrightarrow{\rho_x(\gamma)} & S_{x_0} & & S_{x_0} \\
\downarrow \tilde{\pi} & & \downarrow \tilde{\pi} & & \downarrow \tilde{\pi} \\
S_{y_0} & \xrightarrow{\rho_y(\pi(\gamma))} & S_{y_0} & & S_{y_0} \\
\downarrow g_{y_0} & & \downarrow g_{y_0} & & \downarrow g_{y_0} \\
S_{y_0} & \xrightarrow{\rho_y(\pi(\gamma))} & S_{y_0} & & S_{y_0}
\end{array}$$

Theorem A.1. $\rho_y(\pi(\gamma)) = 1$ if and only if $\rho_x(\gamma) = 1$.

Proof. (\implies) Suppose that $\rho_y(\pi(\gamma)) = 1$ and $\rho_x(\gamma) \neq 1$. Then there is some $z \in S_{x_0}$ with

$\rho_x(\gamma)(z) = w \neq z$. Since S_{x_0} is an inverse limit system of S_{y_0} , there is some $n \in \mathbb{Z}$ such that $\tilde{\pi}(f_x^n(z)) \neq \tilde{\pi}(f_x^n(w))$.

Since $\rho_y(\pi(\gamma)) = 1$, then $\rho_y(\pi(\gamma))(\tilde{\pi}(f_x^n(z))) = \tilde{\pi}(f_x^n(z))$, but

$$\rho_y(\pi(\gamma))(\tilde{\pi}(f_x^n(z))) = \tilde{\pi}(\rho_x(\gamma)(f_x^n(z))) = \tilde{\pi}(f_x^n(\rho_x(\gamma)(z))) = \tilde{\pi}(f_x^n(w))$$

These equations together imply that $\tilde{\pi}(f_x^n(z)) = \tilde{\pi}(f_x^n(w))$, a contradiction, so the assumption that $\rho_x(\gamma) \neq 1$ must have been mistaken.

(\Leftarrow) Suppose that $\rho_x(\gamma) = 1$, but that $\rho_y(\pi(\gamma)) \neq 1$. So there is a $z \in S_{y_0}$ so that $\rho_{y_0}(\pi(\gamma))(z) = w \neq z$. Because the dynamical system (S_{y_0}, g_{y_0}) is surjective, then the inverse limit system of it, (S_{x_0}, f_{x_0}) , must surjectively map to it by $\tilde{\pi}$. Hence, there must be a point $u \in S_{x_0}$ so that $\tilde{\pi}(u) = z$. Since $\rho_x(\gamma) = 1$, then $\rho_x(\gamma)(u) = u$, and we get:

$$w = \rho_{y_0}(\pi(\gamma))(z) = \rho_{y_0}(\pi(\gamma))(\tilde{\pi}(u)) = \tilde{\pi}(\rho_x(\gamma)(u)) = \tilde{\pi}(u) = z$$

This contradicts $w \neq z$. □

Lemma A.2. *Every itinerary realized by S_{y_0} is the right-infinite tail of some itinerary realized by a point of S_{x_0} .*

Proof. $g_{y_0} : S_{y_0} \rightarrow S_{y_0}$ is surjective, so given any point $z_0 \in S_{y_0}$, we can construct a bi-infinite sequence $(\dots, z_{-1}, z_0, z_1, \dots)$ so that $z_i \in S_{y_0}$ and $g_{y_0}(z_i) = z_{i+1}$. This bi-infinite sequence can be considered as an element of S_{x_0} and right-infinite tail of its itinerary is the same as that of the arbitrarily chosen z_0 . □

Lemma A.3. *The right-infinite tail of any itinerary of S_{x_0} is realized by some point of S_{y_0}*

Proof. Given any bi-itinerary realized by some $z \in S_{x_0}$, it is clear that its right-infinite tail is the same as the itinerary of $\tilde{\pi}(z) \in S_{y_0}$. □

Corollary A.4. *The itineraries of points in S_{x_0} and S_{y_0} have the same allowed and forbidden finite strings as well as right-infinite sequences.*

Proof. By Lemmas A.2 and A.3, given any finite string or right-infinite sequence, if it is realized as the itinerary of any point of either S_{x_0} or S_{y_0} , then it must be realized by a point from the other. \square

Theorem A.5. *$\rho_y(\pi(\gamma))$ acts on itineraries by some index-wise permutation if and only if $\rho_x(\gamma)$ acts on itineraries by the same permutation.*

Proof. Let δ be any permutation on the set $\{1, \dots, d\}$.

(\Leftarrow)

Suppose that $\rho_x(\gamma)$ acts on itineraries by δ , that is to say that $\rho_x(\gamma)$ sends points with itineraries $(\dots, \Theta_{e_{-1}}, \Theta_{e_0}, \Theta_{e_1}, \dots)$ to points with itineraries $(\dots, \Theta_{\delta(e_{-1})}, \Theta_{\delta(e_0)}, \Theta_{\delta(e_1)}, \dots)$. For every i , $\rho_x(\gamma)$ gives a bijection from Θ_i to $\Theta_{\delta(i)}$. $\tilde{\pi}(\Theta_i) = \Delta_i$, so

$$\rho_y(\pi(\gamma))(\Delta_i) = \rho_y(\pi(\gamma))(\tilde{\pi}(\Theta_i)) = \tilde{\pi}(\rho_x(\gamma)(\Theta_i)) = \tilde{\pi}(\Theta_{\delta(i)}) = \Delta_{\delta(i)}$$

Hence a point in S_{y_0} with itinerary $(\Delta_{f_0}, \Delta_{f_1}, \dots)$ will be sent to a point with itinerary $(\Delta_{\delta(f_0)}, \Delta_{\delta(f_1)}, \dots)$.

(\Rightarrow)

Suppose that $\rho_y(\pi(\gamma))$ acts on itineraries by δ . For every i , $\rho_y(\pi(\gamma))$ gives a bijection from Δ_i to $\Delta_{\delta(i)}$. Then a point in Θ_i must be sent to a point in $\Theta_{\delta(i)}$ by the action of $\rho_x(\gamma)$, and we see that $\rho_x(\gamma)$ must induce the permutation δ on the itineraries of points in S_{x_0} . \square

Definition A.6. *A one-sided marker string on d symbols is a finite string on d symbols,*

except for the left-most index, which will be considered as an element of the symmetric group on d symbols.¹

One-sided marker strings on d symbols act on one-sided and two-sided sequences on d symbols by implementing their permutation on a particular index of a particular sequence when the rest of the string matches the sequence to the right of that index.

Definition A.7. *A one-sided marker string is called a one-sided marker automorphism if the action it induces on one-sided sequences is an automorphism and it commutes with the shift operator.*

Theorem A.8. *$\rho_y(\pi(\gamma))$ is a one-sided marker automorphism if and only if $\rho_x(\gamma)$ is the same one-sided marker automorphism.*

Proof. Suppose $\rho_y(\pi(\gamma))$ is a one-sided marker automorphism of length n . Let us consider a new partition of S_{y_0} indexed by $\{1, \dots, d\}^n$ constructed as follows:

$$\Delta^{(e_0, \dots, e_{n-1})} = \bigcap_{i=0}^{n-1} g_{y_0}^{\circ -i}(\Delta_{e_i})$$

Again, we can lift this partition to get a partition $\{\Theta^{(e_0, \dots, e_{n-1})}\}$.

Whether or not a symbol in the original itinerary is permuted depends only on that symbol and the next $n - 1$ symbols in the itinerary, so $\rho_y(\pi(\gamma))$ acts as a permutation on the itineraries under the new partition. By Theorem A.5, $\rho_x(\pi(\gamma))$ acts as a permutation under its new partition, so under the original partition, it must induce the same one-sided marker automorphism as $\rho_y(\pi(\gamma))$. The same argument works in the other direction. \square

At first glance, since the identity is a one-sided marker automorphism, it may seem that Theorem A.8 is a strictly stronger statement than Theorem A.1, but the former is

¹It is possible to extend this definition to one-sided compound marker strings parallel to Definition 8.1, and the resulting theorems go through without difficulty.

valid even without a partition of dynamical space or an action that respects a partition in any meaningful way.

BIBLIOGRAPHY

- [Ara08] Zin Arai. On loops in the hyperbolic locus of the complex Hénon map and their monodromies. preprint, 2008.
- [BDK91] Paul Blanchard, Robert L. Devaney, and Linda Keen. The dynamics of complex polynomials and automorphisms of the shift. *Inventiones Mathematicae*, 104(1):545–580, December 1991.
- [BFK90] Mike Boyle, John Franks, and Bruce Kitchens. Automorphisms of one-sided subshifts of finite type. *Ergodic Theory and Dynamical Systems*, 10:421–449, September 1990.
- [BLR88] Mike Boyle, Douglas Lind, and Daniel Rudolph. The automorphism group of a shift of finite type. *Transactions of the American Mathematical Society*, 306(1):71–114, March 1988.
- [BS06] Eric Bedford and John Smillie. The Hénon family: The complex horseshoe locus and real parameter values. *Contemporary Mathematics*, 396:21–36, 2006.
- [DH82] Adrien Douady and John Hubbard. Itération des polynômes quadratiques complexes. *Comptes Rendus des Séances de l'Académie des Sciences*, 294(3):123–126, 1982.
- [DH84] Adrien Douady and John Hubbard. Etude dynamique des polynômes complexes. *Publications Math. d'Orsay*, 1984.
- [DH85] Adrien Douady and John Hubbard. On the dynamics of polynomial-like mappings. *Annales Scientifiques de l'Ecole Normale Supérieure*, 18(2):287–343, 1985.
- [Hén76] Michel Hénon. A two-dimensional mapping with a strange attractor. *Communications in Mathematical Physics*, 50:69–77, 1976.
- [HOV94a] John H. Hubbard and Ralph W. Oberste-Vorth. Hénon mappings in the complex domain I: The global topology of dynamical space. *Publications Mathématiques de l'I.H.É.S.*, 79:5–46, 1994.
- [HOV94b] John H. Hubbard and Ralph W. Oberste-Vorth. Hénon mappings in the complex domain II: Projective and inductive limits of polynomials. *Publications Mathématiques de l'I.H.É.S.*, 79:5–46, 1994.

- [HP00] John Hubbard and Karl Papadantonakis. Exploring the parameter space for Hénon mappings. preprint, 2000.
- [Hub86] John Hubbard. *The Hénon Mappings in the Complex Domain*, pages 101–111. Academic Press, 1986.
- [Koc05] Sarah Koch. Moving in herds: Critical points of the Hénon map, September 2005. Cornell University Dynamics Seminar.
- [Koc07] Sarah Koch, 2004-2007. Conversations.
- [Lor63] Edward Lorenz. Deterministic nonperiodic flow. *Journal of the Atmospheric Sciences*, 20:130–141, 1963.
- [Mil00] John Milnor. Periodic orbits, external rays and the Mandelbrot set: An expository account. *Geometrie Complexe et Systemes Dynamiques*, 261:277–333, 2000.
- [OV87] Ralph Oberste-Vorth. *Complex Horseshoes and the Dynamics of Mappings of Two Complex Variables*. PhD thesis, Cornell University, 1987.
- [Sch94] Dierk Sebastian Schleicher. *Internal Addresses in the Mandelbrot Set and Irreducibility of Polynomials*. PhD thesis, Cornell University, August 1994.
- [Sch00] Dierk Schleicher. Rational parameter rays of the mandelbrot set. *Astrisque*, 261:409–447, 2000.
- [Sch04] Dierk Schleicher. On fibers and local connectivity of Mandelbrot and multi-brot sets. *Proceedings of the Symposium on Pure Mathematics*, 72:477, 2004.